# Reactive distillation for cosmetic ingredients : an alternative for the production of isopropyl myristate?

# Reactive Distillation for Cosmetic Ingredients

An alternative for the production of isopropyl myristate?

**Promotiecommissie**

| | | |
|---|---|---|
| Voorzitter | prof.dr. P.J. Lemstra | Technische Universiteit Eindhoven |
| Promotor | prof.dr.ir. A.B. de Haan | Technische Universiteit Eindhoven |
| Copromotor | dr.ir. E. Zondervan | Technische Universiteit Eindhoven |
| Leden | prof.ir. G.J. Harmsen | Rijksuniversiteit Groningen |
| | dr.ir. P. Bongers | Technische Universiteit Eindhoven |
| | prof.dr.ing. E. Brunazzi | Università di Pisa |
| | prof.dr. G. Rothenberg | Universiteit van Amsterdam |
| Adviseur | dr. H. Roessler | Cognis GmbH |

The research described in this thesis was carried out in the Separation Technology group at the University of Twente and in the Process Systems Engineering group at the Eindhoven University of Technology. It was funded by the Netherlands Organisation for Scientific Research (NWO), project #06256 and supported by Sulzer Chemtech Ltd, BASF Nederland B.V., Uniqema Nederland B.V., Oleon NV and Cognis GmbH.

Reactive Distillation for Cosmetic Ingredients
An alternative for the production of isopropyl myristate?

M.C. de Jong

A catalogue record is available from the Eindhoven University of Technology library

ISBN: 978-90-386-2238-5

Cover design by Iris Rutten



Printed by Gildeprint Drukkerijen B.V. in Enschede

# Reactive Distillation for Cosmetic Ingredients

An alternative for the production of isopropyl myristate?

PROEFSCHRIFT

ter verkrijging van de graad van doctor aan de
Technische Universiteit Eindhoven, op gezag van de
rector magnificus, prof.dr.ir. C.J. van Duijn, voor een
commissie aangewezen door het College voor
Promoties in het openbaar te verdedigen
op donderdag 17 juni 2010 om 16.00 uur

door

Marjette Christine de Jong

geboren te Amsterdam

Dit proefschrift is goedgekeurd door de promotor:

prof.dr.ir. A.B. de Haan

Copromotor:
dr.ir. E. Zondervan

# Contents

# Summary


## Reactive Distillation for Cosmetic Ingredients

### An alternative for the production of isopropyl myristate?

This thesis starts with a brief overview of the current production processes for fatty acid esters. Because these processes have several drawbacks, a new technology is proposed: Entrainer-based Reactive Distillation. In Entrainer-based Reactive Distillation, in situ separation is used to improve the yield of reaction, whereas an entrainer feed is added to overcome the alcohol-water azeotrope, by selectively increasing the relative volatility of water. The objective of this research is the development of a multi-product Entrainer-based Reactive Distillation process for the synthesis of fatty acid esters using a heterogeneous catalyst, and evaluate its attractiveness compared to the current technologies.

In Chapter 2 it is demonstrated that, due to the similarities between Entrainer-based Reactive Distillation and azeotropic distillation, the same selection rules can be applied to select a suitable entrainer. From a list of suitable entrainers for the azeotropic distillation of isopropanol and water, cyclohexane and isopropyl acetate are chosen. Residue curve maps, simulations of the distillation section of the column, and simulations of the total Entrainer-based Reactive Distillation concept show that both can be used as an entrainer in Entrainer-based Reactive Distillation. Whether Entrainer-based Reactive Distillation will be feasible, strongly depends on the kinetics of the reaction.

For this reason Chapter 3 discusses the reaction kinetics of the esterification of myristic acid with isopropanol and with *n*-propanol, using sulphated zirconia (SZ) and *p*-toluene sulphonic acid (*p*TSA) as catalysts, for a temperature range of 343-403K. SZ appeared to be an unsuitable catalyst for the esterification of myristic acid with isopropanol since it did not increase the reaction rate of the uncatalysed reaction. For the reactions with *p*TSA the reaction rates are determined. The reactions follow first order kinetics in all components. The kinetic model corresponds with the results for the esterification of myristic acid with isopropanol and the results for the esterification of palmitic acid from literature. As expected, the reaction rate increases with increasing amount of catalyst and with increasing temperature. The reaction rate and equilibrium conversion increases with an increasing alcohol to myristic acid feed ratio. The reaction with *n*-propanol is considerably faster (at 373K about 3.8 times) than the reaction with isopropanol.

On the basis of the entrainer selection and kinetics studies Chapter 4 will discuss the gains that can be obtained using Entrainer-based Reactive Distillation with regard to conventional Reactive Distillation. Five process configurations for the esterification of myristic acid with isopropanol and *n*-propanol using a homogeneous catalyst, are compared, by simulation in Aspen Plus. In the esterification with isopropanol at 1 bar, the addition of the entrainer has no positive influence on the conversion, because the amount required for water removal causes a temperature decrease in the column. This temperature decrease has a negative influence on the conversion, because the high activation energy of the reaction cannot be overcome. However, in the esterification with isopropanol at 5 and 10 bar and in the esterification with *n*-propanol (either 1, 5 or 10 bar), the addition of the entrainer has a positive influence on the conversion. More entrainer leads to a higher conversion. Surprising is the observation that the conventional Reactive Distillation configuration (RD1) reaches the desired purity and conversion. Because of its polarity, water is pressed out of the liquid phase, in which the reaction takes place, so the reaction can reach nearly complete conversion. Because the decrease of the reaction volume due to the addition of the entrainer is rather small and the

energy consumption is comparable, conventional Reactive Distillation (RD1) is the preferable configuration for the esterification of myristic acid with either isopropanol or *n*-propanol.

Subsequently, the Aspen Plus process for the Reactive Distillation is validated through pilot plant experiments in Chapter 5. A detailed model of the pilot plant is created for different operating conditions. Experiments with a pilot column are performed to verify the model. The conducted experiments correspond well with the predicted values; the model can be used in the construction of a conceptual design. However, not all the intended validation experiments could be performed, because of the practical difficulties that arise when negligible liquid level in the column has to be ensured. Also the break down of the pumps due to clogging appeared a limiting factor in the experiments.

Finally, the process model from Chapter 5 is used to construct a conceptual design for the esterification of myristic acid with isopropanol through Reactive Distillation (packed, tray and bubble column). A parameter optimisation study is performed to investigate the influence of the different process parameters. Finally all results are integrated in conceptual designs for the industrial scale processes, which are evaluated against the batch process based on required reaction volumes. The required reaction volume can be decreased with 27 or 79%, allowing a maximum temperature of respectively 170 and 220°C, using a packed Reactive Distillation column. Using a tray Reactive Distillation column and a maximum temperature of 220°C, the required reaction volume can be decreased with 93%. Due to the less favourable mass transfer characteristics, in the Bubble Column the required reaction volume can only be decreased with 78%. It is further noted that, at a temperature of 220°C, the tray Reactive Distillation is the preferable process for the esterification of myristic acid isopropanol, based on the required reaction volumes. The influence of the maximum column temperature and the influence of a larger liquid hold-up per stage as a result of a different column configuration are of equal importance for the required reaction volume.

This thesis shows that Reactive Distillation can be used for the produc-

tion of isopropyl myristate, which results in an enormous decrease in reaction volume compared to the batch process. Therefore, it can be concluded that Reactive Distillation has the potential to become an economically attractive alternative, not only for fatty acid esters based on methanol and primary alcohol which is already known, but also for the production of isopropyl myristate.

# Samenvatting

## Reactieve Destillatie voor Cosmetische Ingrediënten

### Een alternatief voor de productie van isopropyl myristaat?

Dit proefschrift start met een kort overzicht van de huidige productie processen voor vetzure esters. Omdat deze processen verscheidene nadelen hebben, wordt er een nieuwe technologie voorgesteld: Entrainer-gebaseerde Reactieve Destillatie. In Entrainer-gebaseerde Reactieve Destillatie, wordt in situ scheiding gebruikt om de opbrengst van de reactie te verbeteren, terwijl de entrainer voeding wordt toegevoegd om de alcohol-water azeotroop te overwinnen, door de selectieve verhoging van de relatieve vluchtigheid van water. Het doel van dit onderzoek is de ontwikkeling van een multi-product Entrainer-gebaseerde Reactieve Destillatie proces voor de synthese van vetzure esters, gebruikmakend van een heterogene katalysator. Daarnaast zal het nieuwe proces vergeleken worden met de huidige technologieën.

In Hoofdstuk 2 wordt aangetoond dat, vanwege overeenkomstigheden tussen Entrainer-gebaseerde Reactieve Destillatie en azeotropische destillatie, dezelfde selectieregels kunnen worden toegepast voor het selecteren van een entrainer. Uit een lijst met geschikte entrainers voor de azeotropische destillatie van isopropanol en water zijn cyclohexaan en isopropyl acetaat gekozen. Residue curve maps, simulaties van de destillatiesectie van de kolom en simulaties van

het totale Entrainer-gebaseerde Reactieve Destillatie concept laten zijn dat beide als entrainer gebruikt kunnen worden in Entrainer-gebaseerde Reactieve Destillatie. Of Entrainer-gebaseerde Reactieve Destillatie praktisch uitvoerbaar zal zijn, hangt sterk af van de kinetiek van de reactie.

Om deze reden wordt de reactiekinetiek van de esterificatie van myristinezuur met isopropanol en met *n*-propanol, met gesulfoneerd zirconia (SZ) and *p*-tolueen sulfonzuur (*p*TSA) als katalysatoren, voor een temperatuur range van 343-403K in Hoofdstuk 3 behandelt. SZ bleek een ongeschikte katalysator te zijn voor de esterificatie van myristinezuur met isopropanol, aangezien het de reactiesnelheid van de ongekatalyseerde reactie niet verhoogde. Voor de reacties met *p*TSA zijn de reactiesnelheden bepaald. De reacties volgen eerste orde kinetiek in alle componenten. Het kinetisch model komt overeen met de resultaten voor de esterificatie van myristinezuur met isopropanol en de resultaten uit de literatuur voor de esterificatie van palmitinezuur. Zoals verwacht neemt de reactiesnelheid toe met toenemende hoeveelheid katalysator en met toenemende temperatuur. De reactie snelheid en evenwichtsconversie nemen toe met een toenemende alcohol tot myristinezuur voedingsratio. De reactie met *n*-propanol is aanzienlijk sneller (bij 373K omstreeks 3.8 maal) dan de reactie met isopropanol.

Op basis van de entrainer selectie en de kinetiek studies zal in Hoofdstuk 4 de winst die verkregen kan worden bij het gebruik van Entrainer-gebaseerde Reactieve Destillatie, ten aanzien van conventionele Reactieve Destillatie besproken worden. Vijf procesconfiguraties voor de esterificatie van myristinezuur met isopropanol en *n*-propanol, waarbij een homogene katalysator wordt gebruikt, worden met elkaar vergeleken door simulaties in Aspen Plus. In de esterificatie met isopropanol bij 1 bar, heeft het toevoegen van de entrainer geen positieve invloed op de conversie omdat de vereiste hoeveelheid voor de waterverwijdering zorgt voor een temperatuursdaling in de kolom. Deze temperatuursdaling heeft een negatieve invloed op de conversie, omdat de hoge activeringsenergie van de reactie niet overwonnen kan worden. Echter, in de esterificatie met isopropanol bij 5 en 10 bar en in de esterificatie met *n*-propanol (1, 5 of 10 bar) heeft het toevoegen van de entrainer een positieve

invloed op de conversie. Meer entrainer leidt to een hogere conversie. Verrassend is de observatie dat in de conventionele Reactieve Distillatie configuratie (RD1) de gewenste zuiverheid en conversie wordt bereikt. Vanwege zijn polariteit wordt water uit de vloeistoffase, waar de reactie plaatsvindt, geduwd, zodat the reactie bijna volledige conversie kan bereiken. Omdat de afname van het reactievolume, vanwege de toevoeging van de entrainer, nogal klein is en, de energieconsumptie vergelijkbaar, heeft conventionele Reactieve Destillatie (RD1) configuratie de voorkeur voor de esterificatie van myristinezuur met zowel isopropanol als *n*-propanol.

Vervolgens wordt het Aspen Plus proces voor de Reactieve Destillatie gevalideerd door middel van pilot plant experimenten in Hoofdstuk 5. Er is een gedetailleerd model van de pilot plant gemaakt voor verschillende operationele condities. Experimenten met een pilot kolom zijn uitgevoerd om het model te verifiëren. De uitgevoerde experimenten komen goed overeen met de voorspelde waarden; het model kan worden gebruikt voor de constructie van een conceptueel ontwerp. Echter, vanwege praktische moeilijkheden die ontstaan wanneer een verwaarloosbaar vloeistof niveau in de kolom moet worden gewaarborgd, konden niet alle voorgenomen validatie experimenten worden uitgevoerd. Ook het begeven van de pompen wegens verstopping bleek een limiterende factor in de experimenten.

Tot slot wordt het procesmodel uit Hoofdstuk 5 gebruikt voor het construeren van een conceptueel ontwerp voor de esterificatie van myristinezuur met isopropanol door middel van Reactieve Destillatie (gepakte, schotel en bellenkolom). Er is een parameteroptimalisatiestudie gedaan om de invloed van verschillende procesparameters te bestuderen. Uiteindelijk zijn alle resultaten gentegreerd in conceptuele ontwerpen voor de processen op industriële schaal, welke zijn vergeleken met het batchproces op basis van de vereiste reactievolumes. Wanneer een gepakte Reactieve Destillatiekolom wordt gebruikt kan het vereiste reactievolume worden verlaagd met 27 of 29%, voor een toegestane maximum temperatuur van respectievelijk 170 en 220°C,. Bij gebruik van een schotelkolom en een maximum toegestane temperatuur van 220°C, kan het vereiste reactievolume worden verlaagd met 93%. Vanwege de minder gunstige

stoftransportkarakteristieken in de Bellenkolom, kan het vereiste reactievolume hierin verlaagd worden met maar 78%. Verder moet worden opgemerkt dat bij een temperatuur van 220°C, op basis van de vereiste reactievolumes, de voorkeur wordt gegeven vaan de Reactieve Destillatie schotelkolom voor de esterificatie van myristinezuur met isopropanol. De invloed van de maximum kolomtemperatuur en de invloed van een grotere vloeistof hold-up per stage als resultaat van een andere kolomconfiguraties zijn even belangrijk voor het vereiste reactievolume.

Dit proefschrift laat zien dat Reactieve Destillatie gebruikt kan worden voor de productie van isopropyl myristaat, resulterend in een enorme afname van het reactievolume vergeleken met het batch proces. Daarom kan worden geconcludeerd dat Reactieve Destillatie de potentie heeft om een economisch aantrekkelijk alternatief te worden, voor niet alleen vetzure esters gebaseerd op methanol en primaire alcohol, wat al bekend is, maar ook voor de productie van isopropyl myristaat.

# Chapter 1

# Introduction

*In this chapter a brief overview of the current production processes for fatty acid esters is given. Because those processes have several drawbacks, a new technology is proposed: Entrainer-based Reactive Distillation. In Entrainer-based Reactive Distillation, in situ separation is used to improve the yield of reaction, whereas an entrainer feed is added to overcome the alcohol-water azeotrope, by selectively increasing the relative volatility of water. The objective of this research is the development of a multi-product Entrainer-based Reactive Distillation process for the synthesis of fatty acid esters using a heterogeneous catalyst, and evaluate its attractiveness compared to the current technologies.*

## 1.1 Background

Fatty acid esters are (natural-based) chemicals used in a broad range of different fields of application, such as the cosmetic industry, the food industry, solvents and plasticisers, the coating industry, lubricants, biodiesel et cetera [1, 2]. The fatty acid esters include methyl esters, partial glycerides, wax esters (esters of fatty acids with long-chain fatty alcohols), and ester oils (esters of fatty acids with poly alcohols). The second largest sector in where fatty acid esters are applied is, after solvents and plasticisers, the formulation and man-

ufacture of perfumes, flavours, cosmetics, soap and soap products. The main part of this thesis focuses on isopropyl myristate, which is used in cosmetics as the oil component and is one of the most common used fatty acid esters. [1–3]

## 1.2 Current production processes

### 1.2.1 Esterification

The synthesis of fatty acid esters is analogous to that of monocarboxylic esters. The most common way to produce esters is by a condensation reaction of a carboxylic acid and an alcohol, with the simultaneous elimination of water [4, 5]:

$$R_1{-}COOH + R_2{-}OH \rightleftharpoons R_1{-}COO{-}R_2 + H_2O \tag{1.1}$$

Besides the desired esterification reaction also an etherification reaction takes place:

$$R_1{-}OH + HO{-}R_2 \rightleftharpoons R_1{-}O{-}R_2 + H_2O \tag{1.2}$$

In the synthesis of fatty acid esters the carboxylic acid is a fatty acid. Fatty acids are all aliphatic carboxylic acids with a carbon chain length of $C_6$-$C_{24}$. They are often obtained from animal and vegetable fats through splitting of the triglycerides (fats) into glycerol and fatty acids. [1]

The esterification is an acid catalysed reaction. Commonly used catalysts are strong mineral acids such as sulfuric and hydrochloric acids. Lewis acids such as boron trifluoride, tin and zinc salts, aluminum halides, and organo-titanates have been used as well. Heterogeneous catalysts like cation-exchange resins and zeolites are also applied. They can be preferable in continuous operation, because of the ability to be used in a fixed-bed reactor. [5, 6]

The esterification reaction is an equilibrium reaction, therefore a yield of 100% cannot be reached. To improve the yield, a large excess of one of the reactants, usually the alcohol, is applied. To force the equilibrium to the side of the products it is also possible to remove one of the products, usually water,

from the reaction mixture. The way the conversion is optimised, depends on the volatility of the ester, which for this purpose is classified into three groups [5, 6]:

1. In the case of esters of high volatility, such as methyl formate, methyl acetate and ethyl formate, which have lower boiling points than those of the corresponding alcohols, the esters can be easily removed from the reaction mixture by distillation.

2. Esters of medium volatility, such as propyl, butyl, and amyl formates, ethyl, propyl, butyl and amyl acetates and the methyl and ethyl esters of propionic, butyric and valeric acids, are capable of removing the water from the reaction mixture (self-entraining). In some cases, ternary azeotropic mixtures of alcohol, ester and water are formed. In these cases there are two possibilities: the ester is completely removed as a vapour mixture with alcohol and part of the water, while the residual water accumulates in the system, or all of the water is removed as a vapour mixture with part of the ester and alcohol while the residual ester accumulates as a high boiler in the system. The first possibility occurs in the case of ethyl acetate, the second in case of butyl acetate.

3. In the case of esters of low volatility there are several possibilities. When dealing with esters of butyl and amyl alcohols, water is removed as a binary azeotropic mixture with the alcohol. To produce esters of the lower alcohols (methyl, ethyl, propyl) it may be necessary to add a hydrocarbon such as benzene or toluene to increase the amount of distilled water (entrainer). With high boiling alcohols, such as benzyl, furfuryl and $\beta$-phenylethyl, addition of an entrainer is required to eliminate the water by distillation.

Because fatty acid esters are very low boiling, they can be grouped under the third category. The industrial production of esters is carried out by batch and continuous methods. Both methods are described below.

### 1.2.2 Batch process

Batch production processes involve costly separations, large energy consumption and production of polluting by-products. Because of equilibrium limitations, high conversions can be only obtained by using a large excess of alcohol. In the batch method the reactants are charged into a still pot of appropriate capacity which is fitted with an efficient fractionating column, usually of the bubble-cap or packed type. The proportions of the reactants vary with the nature of the acid and alcohol. [6]

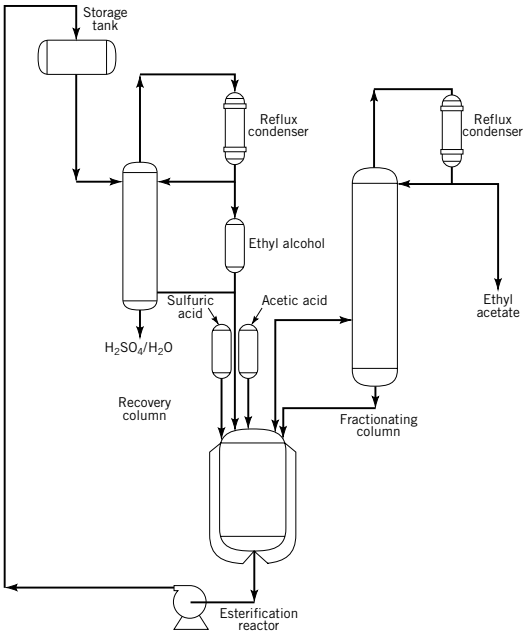


Figure 1.1: Batch ethyl acetate process [5]

In Figure 1.1 the synthesis of ethyl acetate in a batch process is shown. The reaction takes places in a heated still pot or tank which is filled with acetic acid, 95% ethanol and sulfuric acid. The vapour, which is generated

due to heating, is fed into the fractionating column. The temperature at the top of this column is approximately 70°C, such that the top product is the ternary azeotropic mixture of 83% ethyl acetate, 9% alcohol and 8% water. The bottom product of the column is recycled to the reaction tank. The esterification takes place until all the acetic acid has reacted. The alcohol, sulfuric acid and water from the reaction tank will be separated in a recovery column. The condensated top product of the fractionating column is the ethyl acetate product. This ternary mixture is production-grade ethyl acetate, which is satisfactory for most applications. For a pure product, further purification is necessary. [5, 7]

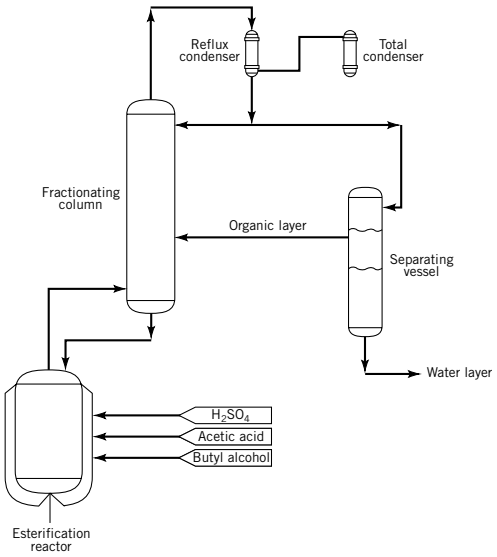


Figure 1.2: Batch *n*-butyl acetate process [5]

In Figure 1.2 the synthesis of *n*-butyl acetate in a batch process is shown. The esterification reactor is filled with glacial acetic acid, an excess of butyl alcohol and sulfuric acid. After several hours of heating, the slow rectifica-

tion takes places to remove the (already) formed water. The distillate of the fractionating column will form two liquid phases, an aqueous phase and an organic phase, consisting of butyl acetate and butanol. The organic phase is recycled continuously to the column to improve the water removal. Esterification continuous until no more water can be removed. The acid remaining in the reactor is neutralised with a sodium hydroxide solution. The organic phase is washed with water and distilled to obtain butyl acetate of 75-85% purity. [5, 7]

Little has been published on the production of alkyl esters of fatty acids. They can be prepared by direct esterification, but for higher fatty acid esters (oleates and stearates) alcoholysis of an appropriate neutral fat is a more common way to produce them, in which the glycerol part of triglyceride is replaced by three alcohol molecules. [6]

### 1.2.3 Reactive Distillation

For a more competitive process it is preferable to produce fatty esters in a continuous way, at higher yields. Continuous esterifications have been carried out on a relatively large scale since 1921, when the first patents covering these processes appeared. [6]

In many chemical manufacturing processes, separation steps are necessary to obtain the pure products. Usually reaction and separation stages are carried out in individual equipment units, for this reason equipment and energy costs are higher in comparison to an integrated process. Reactive separation processes, a combination of separation and reaction inside a single unit, is an increasingly used technology. Reactants are converted to products with simultaneous separation of the products and recycle of unused reactants. Reactive separation can be efficient, both in size and in cost of capital equipment as well as in energy. [8]

Reaction can be used to improve separation or separation can be used to improve reaction. In the first case a reactive entrainer is added. This entrainer reacts with one of the components in the mixture that has to be

separated, making the separation easier. In the second case the products are separated from the reaction mixture by shifting the chemical equilibrium. Reactive Distillation has several advantages [8, 9]:

- Increased yield by shifting the chemical and thermodynamic equilibrium through continuous removal or reactants or products from the reaction mixture.
- Improved selectivity through suppression of undesired side reactions by removing one of the products from the reaction mixture.
- Reduced energy consumption via direct heat integration in case of exothermic reactions.
- Avoidance of hot spots by simultaneous liquid evaporation.
- Avoidance of azeotropes and separation of close boiling components using a reactive entrainer.
- A multi-functional reactor design can be applied, such as several catalyst zones in one Reactive Distillation column to allow more than one reaction.

These advantages can result in reduced capital investment and lower operating costs because the amount of hardware would be reduced by using Reactive Distillation compared to conventional processes. In some processes the improvements by using Reactive Distillation are significant. It is expected that many more processes are suitable for Reactive Distillation. [10] However, Reactive Distillation is not always advantageous, there are also some constraints [8, 9]:

- Common operation range (temperature and pressure) for distillation and reaction is required.
- Proper boiling point sequence: the key component should be a top or a bottom product, undesired side or consecutive products should be medium boiling components.

- Difficulties in providing proper residence time characteristics.
- High flow rates can give problems due to liquid distribution problems.

Among suitable Reactive Distillation processes are etherifications, nitrations, esterifications, transesterifications, condensations and alkylations [8, 11]. One of the best known Reactive Distillation processes is the Eastman Chemical Company's methyl acetate process. By making methyl acetate through Reactive Distillation instead of the conventional process, eleven major units plus peripherals are replaced by one single unit. The old technology was complicated and expensive because the products form azeotropes with each other. To obtain pure products these azeotropes have to be broken. In the Reactive Distillation process the azeotrope is broken because one of the reactants works as an extractant and the products are separated immediately. [10, 12, 13]

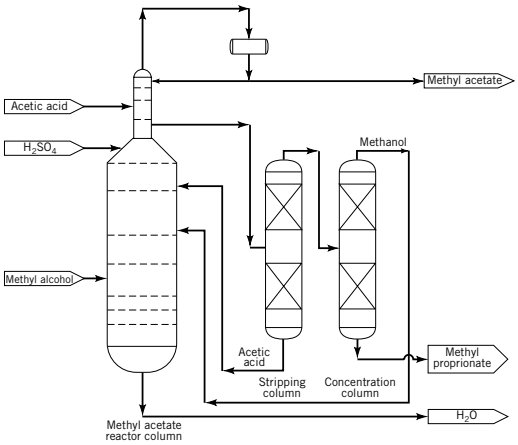


Figure 1.3: Continuous methyl acetate process [5]

In Figure 1.3 the continuous methyl acetate process is shown. The esterification reaction catalysed by sulfuric acid takes place in the middle section (reactive section) of the reactive column. Acetic acid is fed to the top section (rectification section) of column, and the methanol to the lower section of

the column. Between the acetic acid feed and the reactive section, the acetic acid acts as an entrainer and extracts water and some methanol from methyl acetate. The acetic acid and methyl acetate are then separated in the rectification section giving high purity methyl acetate (at least 99.5 wt%) as the top product. The catalyst and impurities (primarily methyl propionate and isopropyl acetate) are removed from the reactor section by a sidedraw. The impurities are further concentrated and removed from the process in two distillation columns. The catalyst and acetic acid are being recycled back into the Reactive Distillation column. In the bottom section of the column, the unreacted methanol and acetic acid are stripped from from the water, resulting in water as the bottom product. [5, 9]

Besides methyl acetate, also the esterification of other alcohols has been extensively investigated, however information on the esterification of long chain carboxylic acids such as fatty acids by Reactive Distillation is scarce. A few processes with various fatty esters and alcohols are described [14–16]. All refer to a homogeneous catalyst which causes pollution of the product. Steinigeweg and Gmehling [17] described a process using a heterogeneous catalyst. They investigated the esterification of decanoic acid with methanol. However, the problem of this process is that the ester is not obtained in pure form and requires further purification. Besides that, the alcohol, except for methanol, forms an azeotrope with water which is a disadvantage for realising higher yields. Omota et al. [18, 19] studied the feasibility of a single column process using a heterogeneous catalyst for the esterification of lauric acid with 2-ethylhexanol and methanol. They found that it is possible to obtain pure fatty acid ester in a single column process. Both esters can be produced in the same set-up, but under different operating conditions. However, problems may occur because the product purity is highly sensitive to changes in the reflux ratio. The optimal reflux ratio is very low, which could give control problems.

The major part of the research projects are about methanol and primary alcohols. However, for the cosmetics industry the main fatty acid esters of interest are based on isopropanol, of which the typical reaction rates are 10-100 times lower compared to methanol and primary alcohols, requiring excessive

reaction volumes. Chin et al. [20] and Bhatia et al. [21, 22] reported that Reactive Distillation can be successfully applied for the for the esterification of palmitic acid with isopropanol through Reactive Distillation with an zinc acetate catalyst supported on silica gel. However, Chin et al. [20] also report a low reflux ratio. As already mentioned, this could result in control problems.

## 1.3 Entrainer-based Reactive Distillation

Among new technologies, Entrainer-based Reactive Distillation based on solid catalysts is a promising way eliminate the drawbacks of the current continuous production processes. [23]

In Entrainer-based Reactive Distillation, in situ separation is used to improve the yield of reaction, whereas an entrainer feed is added to make the separation feasible by selectively increasing the relative volatility of one of the products. Entrainer-based Reactive Distillation promises to be advantageous for the synthesis of fatty acid esters. The entrainer increases the relative volatility of water (by-product) compared to the alcohol (reactant), such that during the reaction the water can be continuously removed by distillation. In this way the chemical equilibrium is shifted such that higher conversions can be obtained. Preferably different esters should be produced in the same set-up (multi-product design), possibly using the same entrainer which will

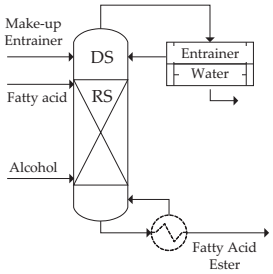


Figure 1.4: Entrainer-based Reactive Distillation

be beneficial towards the investment costs. In Figure 1.4 the flowsheet of the desired process is given, in which RS stands for Reactive Section and DS for Distillation Section.

## 1.4 Objective and outline

The main objective of this thesis is the development of a multi-product Entrainer-based Reactive Distillation process for the synthesis of fatty acid esters using a heterogeneous catalyst, and evaluate it attractiveness compared to the current technologies.

The development of a proper heterogeneous catalyst should have resulted from a research study, conducted at the University of Amsterdam, within the framework of the same research project. The goal of that research study was the development of an active, selective and multi-substrate catalyst for fatty acid esterification. The research concentrated on Sulphated Zirconia catalyst because it showed high activity and selectivity for the esterification of lauric acid with a variety of primary alcohols ranging from 2-ethylhexanol to methanol [24, 25]. Unfortunately, eventually no sufficiently active Sulphated Zirconia catalyst for the esterification with isopropanol was obtained.

With a theoretical study, Dimian et al. [23] have demonstrated, that the Entrainer-based Reactive Distillation process has high potential for the esterification of lauric acid with *n*-propanol. However, this preliminary study was mainly based on computer simulations. To quantify the advantages of Entrainer-based Reactive Distillation more in detail, a thorough study regarding kinetics, thermodynamics, hydrodynamics and mass transfer is necessary, and computer simulations have to be supported by experimental results.

In order to obtain the required experimental data and achieve the overall objective, this thesis is structured as schematically depicted in Figure 1.5. The following topics are included:

- The entrainer is a crucial part of the Entrainer-based Reactive Distillation process. A suitable entrainer will be selected in Chapter 2, based

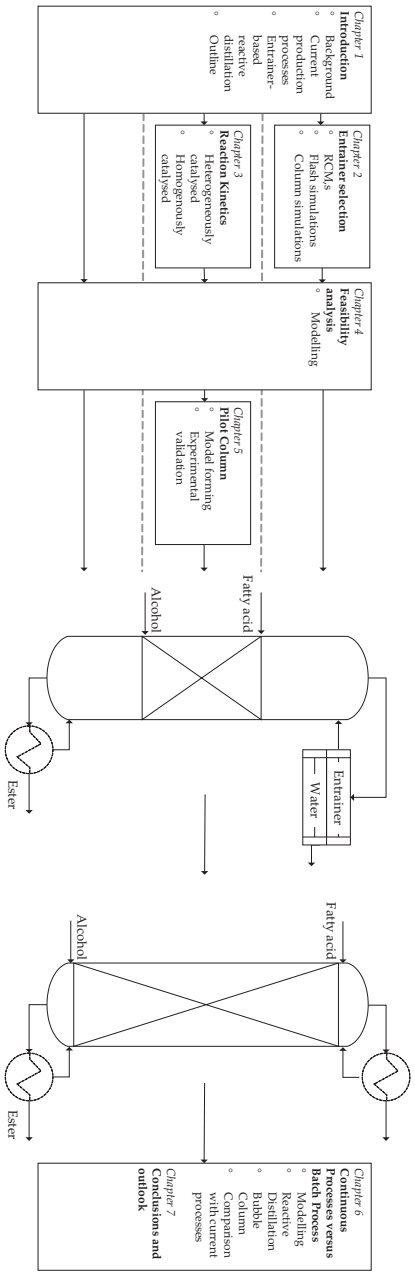


Figure 1.5: Thesis content

on residue curve maps, flash simulations and column simulations.

- In Chapter 3 the necessary reaction kinetics are determined through batch characterisation. Because no suitable heterogeneous catalyst was found it was decided to continue with a homogeneous catalyst.

- Based on the results from both previous chapters a technical feasibility analysis of the process is performed in Chapter 4. It is investigated what gains can be obtained by using Entrainer-based Reactive Distillation compared to conventional Reactive Distillation and other Reactive Distillation configurations. Because conventional Reactive Distillation was the preferred configuration, this was applied in the conceptual design instead of the Entrainer-based Reactive Distillation.

- The model used in Chapter 4 is applied on the pilot column in Chapter 5. This includes the determination of the hydrodynamic parameters of the column packing, while in Chapter 4 the hydrodynamics of the system were assumed to be ideal. Experiments are performed to validate this model.

- In Chapter 6, a conceptual design, based on the model from Chapter 5, for an industrial scale Reactive Distillation process as well as a Bubble Column is discussed. In order to investigate the attractiveness of the continuous processes the conceptual designs are compared to the current technologies.

- Finally, Chapter 7 presents the conclusions of this thesis and recommendations for future work

# References

[1] Brockmann, R.; Demmering, G.; Kreutzer, U.; Lindemann, M.; Plachenka, J.; Steinberner, U. Fatty acids. In *Ullmann's Encyclopedia of Industrial Chemistry*; John Wiley & Sons, Inc.: 2005.

[2] Kalish, J. Fatty Acids in Cosmetics. In *Fatty Acids and Their Industrial Applications*; Pattison, E., Ed.; Marcel Dekker, Inc.: New York, 1968.

[3] Gervajio, G. Fatty Acids and Derivatives from Coconut Oil. In *Bailey's Industrial Oil and Fat Products*, Vol. 6, Sixth ed.; Shahidi, F., Ed.; Wiley-Interscience: 2005.

[4] Sakamuri, R. Esters, Organic. In *Kirk-Othmer Encyclopedia of Chemical Technology*, Vol. 10; John Wiley & Sons, Inc.: 2003.

[5] Aslam, M.; Torrence, G.; Zey, E. Esterification. In *Kirk-Othmer Encyclopedia of Chemical Technology*, Vol. 10; John Wiley & Sons, Inc.: 1994.

[6] Markley, K. S. Esters and Esterification. In *Fatty acids*; Markley, K. S., Ed.; Interscience publishers, Inc., New York: 1961.

[7] Keyes, D. *Ind. Eng. Chem.* **1932,** *24,* 1096-1103.

[8] Noeres, C.; Kenig, E.; Górak, A. *Chem. Eng. Process.* **2003,** *42,* 157-178.

[9] Towler, G. P.; Frey, S. J. Reactive distillation. In *Reactive Separation Process*; Kulprathipanja, S., Ed.; Taylor & Francis: 2002.

[10] Doherty, M. F.; Malone, M. F. *Conceptual design of distillation systems;* McGraw-Hill: Boston, 2001.

[11] Harmsen, G. *Chem. Eng. Process.* **2007,** *46,* 774-780.

[12] Agreda, V. H.; Partin, L.; Heise, W. *Chem. Eng. Prog.* **1990,** *February,* 40-46.

[13] Sharma, M.; Mahajani, S. Industrial Applications of Reactive Distillation. In *Reactive Distillation*; Sundmacher, K.; Kienle, A., Eds.; 2003.

[14] Bock, H.; Wozny, G.; Gutsche, B. *Chem. Eng. Process.* **1997,** *36,* 101-109.

[15] Jeromin, L. M.; Bremus, N.; Peukert, E. *Fette, Seifen, Anstrichmittel* **1981,** *83,* 493-504.

[16] Schleper, B.; Gutsche, B.; Wnuck, J.; Jeromin, L. *Chem. Ing. Tech.* **1990,** *62,* 226-227.

[17] Steinigeweg, S.; Gmehling, J. *Ind. Eng. Chem. Res.* **2003,** *42,* 3612-3619.

[18] Omota, F.; Dimian, A.; Bliek, A. *Chem. Eng. Sc.* **2003,** *58,* 3159-3174.

[19] Omota, F.; Dimian, A.; Bliek, A. *Chem. Eng. Sc.* **2003,** *58,* 3175-3185.

[20] Chin, S.; Ahmad, A.; Mohamed, A.; Bhatia, S. *International Journal of Chemical Reactor Engineering* **2006,** *4,* 1-17.

[21] Bhatia, S.; Ahmad, A.; Mohamed, A.; Chin, S. *Chem. Eng Sc.* **2006,** *61,* 7436-7447.

[22] Bhatia, S.; Mohamed, A.; Ahmad, A.; Chin, S. *Comp. Chem. Eng.* **2007,** *31,* 1187-1198.

[23] Dimian, A. C.; Omota, F.; Bliek, A. *Chem. Eng. Process.* **2004,** *43,* 411-420.

[24] Kiss, A.; Dimian, A.; Rothenberg, G. *Adv. Synth. Catal.* **2006,** *348,* 75-81.

[25] Kiss, A.; Omota, F.; Dimian, A.; Rothenberg, G. *Topics in Catalysis* **2006,** *40,* 141-150.

# Chapter 2

# Entrainer selection

*In this chapter it is demonstrated that, due to the similarities between Entrainer-based Reactive Distillation and azeotropic distillation, the same selection rules can be applied to select a suitable entrainer. From a list of suitable entrainers for the azeotropic distillation of isopropanol and water, cyclohexane and isopropyl acetate are chosen. Residue curve maps, simulations of the distillation section of the column, and simulations of the total Entrainer-based Reactive Distillation concept show that both can be used as an entrainer in Entrainer-based Reactive Distillation. Whether Entrainer-based Reactive Distillation will be feasible, strongly depends on the kinetics of the reaction.*

## 2.1 Introduction

In the distillation section of the Entrainer-based Reactive Distillation process an entrainer enhances the removal of water from a water-alcohol mixture. The water-alcohol mixture from the reactive section enters the distillation section at the bottom as a vapour while the entrainer is fed at the top. Because of the azeotropic nature of a water-alcohol mixture, the separation shows similarities with azeotropic distillation. The main difference is that in azeotropic distillation the feed is not necessarily introduced at the bottom and the separation

takes place in the whole column instead of a column section. Because of these similarities, the guidelines for entrainer selection in azeotropic distillation are used as starting point for the entrainer selection in Entrainer-based Reactive Distillation. Therefore the theory of the entrainer selection will be discussed first in this chapter before discussing how this can be applied to Entrainer-based Reactive Distillation entrainer selection. From the entrainers used in the azeotropic distillation of water and isopropanol an entrainer will be selected for the esterification of myristic acid with isopropanol and with *n*-propanol through the Entrainer-based Reactive Distillation process. With the aid of residue curve maps, simulations of the distillation section and simulations of the total concept it will be investigated whether this entrainer is also suitable for the Entrainer-based Reactive Distillation process.

## 2.2 Theory

### 2.2.1 Azeotropic distillation

The term azeotropic distillation has been used for different distillation techniques in which the specific azeotropic behaviour is used to effect a separation. In other words, every method to make the separation of an azeotropic mixture feasible can be called azeotropic distillation. [1] Most of these methods, except pressure-swing distillation, make use of the addition of a "mass separating agent" or so called entrainer. This entrainer enhances the relative volatilities of the components and causes an easy separation of the original components. Entrainers can be divided into distinct classes that define the principal distillation techniques. There are four types of entrainers [2, 3]:

1. Liquid entrainers that do not induce liquid-phase separation are used in homogeneous azeotropic distillation. Classical extractive distillation is a special case in this category.

2. Liquid entrainers that do induce liquid-phase separation are used in heterogeneous azeotropic distillation.

3. Reactive entrainers that react with one of the components such that the product can be easily separated from the non-reacting components. This is Reactive Distillation in which the reaction is used to improve the separation.

4. Entrainers that ionically dissociate and change the composition of the azeotrope are used in salt-effect distillation, which is a variation of extractive distillation.

The term azeotropic distillation often refers only to heterogeneous azeotropic distillation, because this is the most used form of azeotropic distillation [2, 3]. Because the Entrainer-based Reactive Distillation process corresponds the most with homo- and heterogeneous azeotropic distillation, the entrainer is a non-reactive solvent, only the first two possibilities will be described more in detail.

The feasibility of a given entrainer depends on the phase equilibrium behaviour of the resulting ternary or multi-component mixture. This can be studied through residue curve maps. [1] These residue curve maps represent the simple distillation of a mixture. In simple distillation, a mixture is boiled and the vapour phase is removed continuously. Because the vapour phase is always richer in the more volatile components than the liquid phase, the composition of the liquid will change continuously with time. The trajectory of this liquid composition is called a simple distillation residue curve or a residue curve. The collection of all such curves for a given mixture is called a residue curve map. Residue curve maps can be determined experimentally or calculated with vapour-liquid-liquid equilibrium computation techniques.

Residue curves can only start at, end at, or be deflected by the pure components and azeotropes in a mixture. They always start in an unstable node and end in a stable node. The components and azeotropes that deflect residue curves are saddles.

In Figure 2.1*a* the residue curve map for a nonazeotropic ternary mixture is shown. All ternary mixtures without azeotrope are represented by this map. All the residue curves originate at the light component, move toward the in-

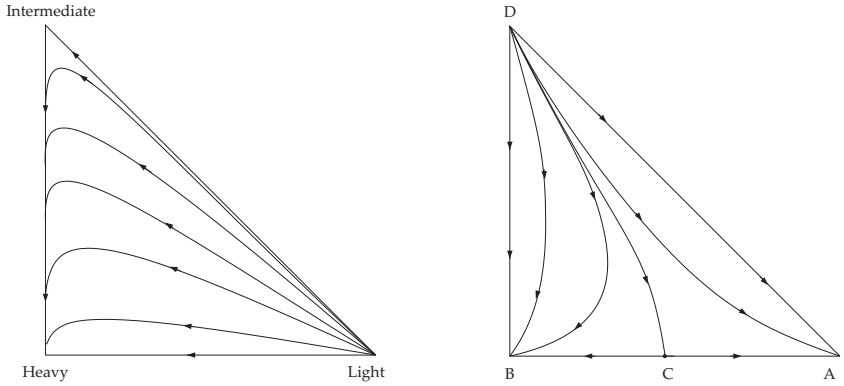


Figure 2.1: Residue curve maps

termediate boiling component and end at the heavy component. Following a residue curve the boiling temperature of the mixture continuously increases along the curve. Therefore, for Figure 2.1*a* it can be stated: the light component is an unstable node; the intermediate component, which deflects the residue curves, is a saddle; and the heavy component is a stable node.

When azeotropes are present, many different residue curve maps are possible. In Figure 2.1*b* an example is given. In this residue curve map a minimum boiling binary azeotrope ($C$) is formed by the intermediate $A$) and heavy component ($B$), this azeotrope is a saddle. Pure component $D$ is an unstable node, pure components $A$ and $B$ are stable node, and the boiling point order from low to high is $D \rightarrow C \rightarrow A$ or $B$.

When a residue curve ends in a saddle, like the residue curve connecting component $D$ to the azeotrope $C$, it has the special property that it divides the composition triangle into two separate distillation regions. This kind of residue curves are called distillation boundaries, which cannot be crossed. Any initial mixture with a composition lying to the left of the distillation boundary will result in a final residue of pure $B$ and any initial mixture with a composition lying into the right of the distillation boundary will result in a final residue of

pure $A$. Each distillation region must contain a stable node, an unstable node and at least one saddle. Different distillation regions can have some saddles and nodes in common. For a feasible separation, the bottom and distillate compositions should lie in the same distillation region.

The steady-state composition profile in a packed column at total reflux is identical to a residue curve in simple distillation. But in the case of a finite reflux or a staged column, the composition profile can be slightly different. Nevertheless the simple distillation boundaries remain a good approximation of the finite-reflux distillation bounderies. Simple distillation boundaries can in theory be crossed by the profiles in a continuous column, but this is often not the case, in other words residue curve maps can be used as a starting point for feasibility studies. [2–4]

### Homogeneous azeotropic distillation

As stated in the previous paragraph, a feasible distillation sequence for separating a homogeneous azeotropic mixture can be identified by determining whether or not the desired products lie in the same distillation region. For homogeneous azeotropic distillation there are several possibilities. In Figure 2.2 the seven most favourable maps for breaking minimum boiling binary azeotropes, which is the case with a water-alcohol mixture, can be seen with their corresponding column configurations. Any solvent forming a residue curve map similar to one of these will be a feasible entrainer for separating the azeotropic mixture. [2–4]

When the entrainer is intermediate-boiling (Figure 2.2$a$) and does not introduce a new azeotrope, the heavier component ($B$) will be the bottom product of the first column and the top mixture of $A$, and $E$ will be separated into pure components in the second column. This can be seen in the residue curve map because all residue curves end in $B$ and with only $A$ and $E$ present they end in $E$.

In the case of classical extractive distillation with a heavy entrainer that does not form any new azeotropes (Figure 2.2$b$), the lighter component ($A$) will

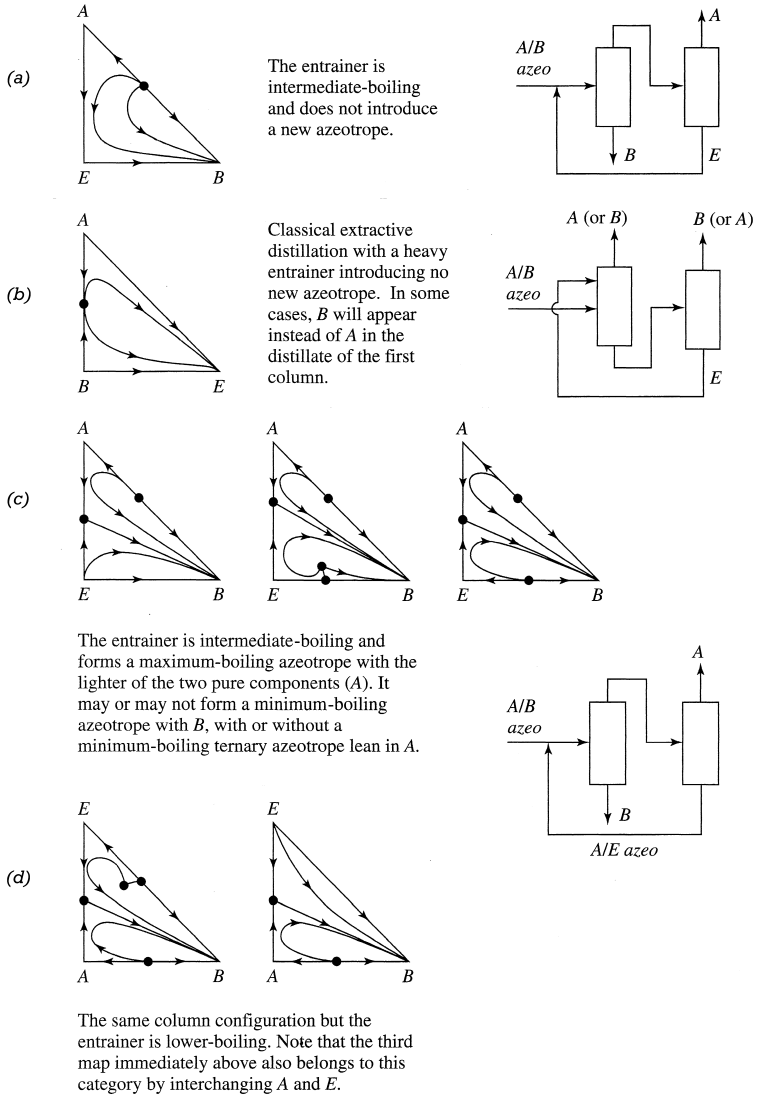


Figure 2.2: Favourable residue curve maps for breaking the A-B azeotrope using entrainer E by homogeneous azeotropic distillation [2, 4]

be the distillate product of the first column column and the heavier component ($B$) the one of the second column. In the residue curve map this can be observed because the residue curve is pointing away from $A$ (unstable node) and all end in $E$.

When the entrainer is intermediate-boiling (Figure 2.2$c$) and forms a maximum-boiling azeotrope with the lighter component($A$), the heavier component ($B$) will be the bottom product of the first column. The top mixture of $A$ and $E$ will be separated into pure $A$ and an azeotropic mixture of $A$ and $E$. This can be seen in the residue curve map because all residue curves end in $B$ and with only $A$ and $E$ present, they end in the $A$-$E$ azeotrope. This is also the case when the entrainer is low-boiling (Figure 2.2$d$).

Industrial applications based on homogeneous azeotropic distillation, other than extractive distillation are not common, because the requirement that $A$ and $B$ must lie in the same distillation region in the residue curve map with the entrainer is difficult to meet. An intermediate-boiling component that does not form an azeotrope while the other two components form a minimum-boiling azeotrope (Figure 2.2$a$) is an uncommon system and maximum-boiling azeotropes are far less common than minimum-boiling azeotropes. An alternative technique is heterogeneous azeotropic distillation. [1]

#### Heterogeneous azeotropic distillation

As in homogeneous systems, residue curves cannot cross heterogeneous distillation boundaries. However, the key feature of a feasible heterogeneous entrainer is that it generates a liquid-liquid immiscibility with one of the pure components such that a point on a residue curve in the heterogeneous region splits into two equilibrium liquid phases that can lie in two different distillation regions. In this way the distillation boundary is crossed by a liquid-liquid phase separation.

Any entrainer that induces a liquid-phase heterogeneity over a portion of the composition triangle, which does not divide the distillate and residue products to be separated into different distillation regions is automatically

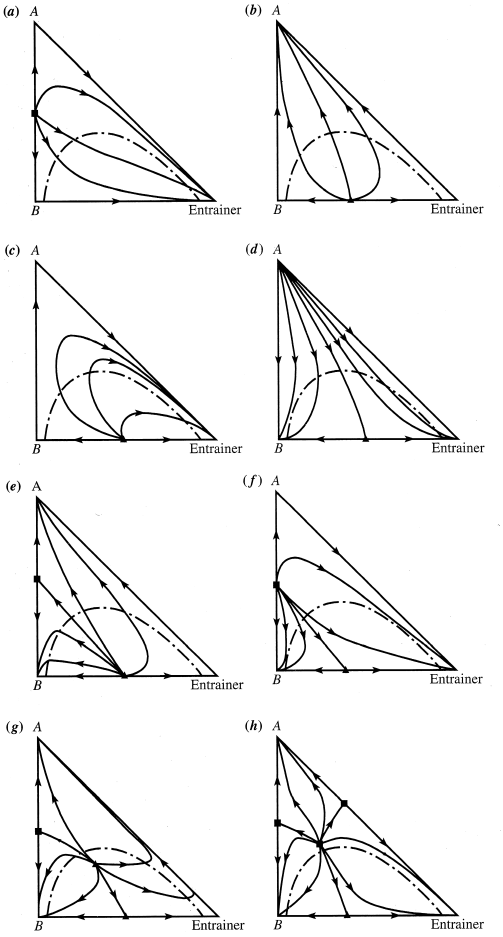


Figure 2.3: Selection of residue curve maps for the entrainer selection in heterogeneous azeotropic distillation [2]

a feasible entrainer. Although entrainers that are responsible for obtaining almost pure products would be of course more favourable.

The entrainer cannot introduce a new azeotrope or it forms a maximum-boiling azeotrope with one of the two pure components (with or without a ternary homogeneous or heterogeneous azeotrope). In Figure 2.3 some possible examples of the numerous possibilities can be seen. [2, 5, 6]

In both Figures 2.3*a* and *f* the *A*-*B* azeotrope is the unstable node and therefore the distillate product. Depending on the feed composition and column specifications, the bottom product lays in the heterogeneous regions and can be separated by decantation into two phases: a phase rich in *E* and a phase rich in *B*.

In Figures 2.3*b*, *c* and *e* the *E*-*B* azeotrope is the unstable node and therefore the distillate product. Because this azeotrope lies in the heterogeneous region, it can be separated by decantation into two phases: a phase rich in *E* and a phase rich in *B*. In 2.3*b*, component *A* will be the bottom product of the distillation column, because all the residue curves end in *A*. In *c* and *e* the bottom product depends on the feed composition and column specifications. In *a* it will be a mixture containing *A* and *E* and for *e* it can be component *A*.

In Figure 2.3*d* a binary heterogeneous azeotrope is formed with component *B*. Component *A* will be the distillate product of the distillation column, because all the residue curves start in *A*. Depending on the feed composition and column specifications the bottom product lays in the heterogeneous regions and can be separated by decantation into two phases: a phase rich in *E* and a phase rich in *B*.

In Figures 2.3*g* and *h* a binary heterogeneous azeotrope is formed with component *B*, a binary homogeneous azeotrope is formed with component *A* and a ternary azeotrope is formed. The ternary azeotrope is the unstable node for all distillation regions and will be therefore the distillate product in all cases. When the ternary azeotrope lays in the heterogeneous region (Figure 2.3*g*) it can be separated by decantation into two phases: a phase rich in *E* and a phase rich in *B*. The bottom product depends on the feed composition

and column specifications.

### 2.2.2 Entrainer-based Reactive Distillation

The purpose of the entrainer in Entrainer-based Reactive Distillation is to enhance water removal instead of alcohol by distillation such that the reaction equilibrium is shifted and a higher conversion is obtained. In order to do so, the entrainer should fulfill the following criteria:

1. Increase the relative volatility of water compared to alcohol, such that water can be removed over the top.
2. Have an immiscibility region with water, such that the distillate can be separated in two immiscible liquid phases by decanting.
3. Have a low solubility of the entrainer in water, such that no further purification is necessary.
4. Have a low solubility of water in the entrainer, such that the entrainer can be used as a recycle.
5. Be acceptable as impurity in products.

It should be remarked that the liquid-liquid split mentioned in criterium (2) is only desired in the decanter. Phase splitting in the distillation column should be avoided. These criteria are similar to the heterogeneous azeotropic distillation of a water-alcohol mixture in which the water is removed over the top together with the entrainer and the alcohol leaves the column at the bottom. From the guidelines for entrainer selection by heterogeneous azeotropic distillation, specific features that the desired distillation line map, which can be seen in Figure 2.4, should have can be stated:

- The entrainer should form a minimum boiling ternary azeotrope with alcohol and water (or a binary heterogeneous azeotrope with water in the most preferable case) to create a distillation region which contains both products: an entrainer-water mixture (composition near ternary azeotrope) as top vapour and alcohol as bottom product.

- This ternary azeotrope should lie in the heterogeneous region (ternary heterogeneous azeotrope) such that the mixture can be split into two liquid phases.

- This heterogeneous region must be wide and the tie-lines should point to the water vertex in order to get a water rich and an entrainer rich phase after condensation and decantation.

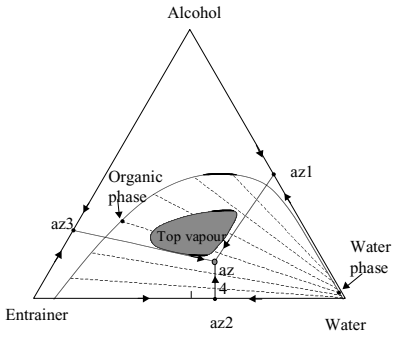


Figure 2.4: Desired residue curve map for entrainer selection in Entrainer-based Reactive Distillation for fatty acid esterification [7]

Note that this is a distillation line map. Distillation lines represent the liquid composition profiles in a trayed distillation columns operating at total reflux instead of residue curves. For practical purpose there is little difference between the two types of curves. Following a distillation line the temperature decreases, in case of a residue curve this is the other way around. [3]

Stéger et al. [8] reported that for a distillation column existing of different sections, the residue curve map theory cannot be used. In this research, batch extractive distillation was studied, in which an extractive and a rectifying section were used. Because there are two sections in the column, the composition profile consists of two parts and thus a residue curve map is not sufficient for evaluating the feasibility. Besides the evaluation of residue curve maps, also

column simulations should be included in the entrainer selection procedure to verify the results obtained from the residue curve maps.

## 2.3 Methods

### 2.3.1 Entrainer selection

Starting point for the entrainer selection is the selection of entrainers used in the azeotropic distillation of water and isopropanol. The Dortmund Data Bank Software Package has been used to perform an entrainer search, based on equilibrium data. For the separation of water and isopropanol at atmospheric pressure this resulted in the following entrainers:

| | |
|---|---|
| Benzene | Octane |
| 1-Chloro-2-methylpropane | 1-Octene |
| Chloroform | Tetrachloromethane |
| Cyclohexane | Toluene |
| Cyclohexene | Trichloroethylene |
| 1,2-Dichloroethane | Acrylonitrile |
| Hexane | Thiophene |
| Heptane | Acetic acid isopropyl ester |
| 2-Methylbutane | 1-Heptene |
| Diisopropyl ether | Propyl bromide |
| 2,2,4-Trimethylpentane | 1,3-Cyclohexadiene |
| 1-Hexene | Bromodichloromethane [R20B1] |

From this list, non-polar solvents, such as benzene, toluene, hexane, cyclohexane, et cetera, are well known as entrainer for the separation of water and alcohols. [2, 9, 10] However, not all of these are suitable because of toxicity and odour. Cyclohexane is assumed the most non-polar solvent, which is acceptable as impurity in the product. As an alternative also isopropyl acetate will be investigated, because an acetate sharing the same alcohol with the fatty ester has been reported to be a suitable entrainer [7]. Isopropyl acetate, which is expected to have a lower capability for the removal of water

than cyclohexane. Due to its more polar nature isopropyl acetate will have a stronger affinity with water.

Residue curve maps, simulations of the distillation section and simulations of the total concept are used to verify that cyclohexane and isopropyl acetate are suitable entrainers for the Entrainer-based Reactive Distillation process.

### 2.3.2 Thermodynamic model

For the simulations in Aspen Plus a property model has to be selected. Parameters based on vapour-liquid equilibrium data do not give good predictions for the liquid-liquid equilibria and vice versa. [11] Therefore a combination will be used: NRTL parameters based on vapour-liquid equilibrium data will be used for the interaction between isopropanol and water and isopropanol and cyclohexane, and NRTL parameters based on liquid-liquid equilibrium data will be used for the interaction between water and cyclohexane. Vapour-liquid equilibrium data and liquid-liquid equilibrium data from literature [12–16] of several water-isopropanol systems including a third component, are compared to the different available parameter sets in Aspen. Only the comparison of water-isopropanol-cyclohexane [12] and water-isopropanol-isopropyl acetate [15, 16] will be shown as example.

The set of NRTL parameters developed by Aspen Tech based on data from the Dortmund Data Bank was found to correspond well with the most of the experimental vapour-liquid equilibria literature data and is used further. The binary coefficients used in the simulations can be found in Table 4.2.

In Figure 2.5 the vapour compositions and boiling temperatures for the isopropanol-water-cyclohexane system reported by Verhoeye [12] and for the isopropanol-water-isopropyl acetate system reported by Teodorescu [15], are compared with the values calculated by Aspen Plus. In Figure 2.6*a* the liquid-liquid equilibria at 25°C are given for the literature system [12] and the system calculated by Aspen Plus. The size of the liquid-liquid envelope is well described but it can be seen that the tie-lines do not correspond, especially at the side of the entrainer rich phase. In Figure 2.6*b* the liquid-liquid equi-

| Component i | Water | Water | Isopropanol | Water |
|---|---|---|---|---|
| Component j | Isopropanol | Cyclohexane | Cyclohexane | Isopropyl acetate |
| Source | VLE-IG | LLE-ASPEN | VLE-IG | LLE-ASPEN |
| aij | 6.8284 | 13.1428 | 0 | 26.9 |
| aji | -1.3115 | -10.4585 | 0 | -1.4234 |
| bij | -1483.46 | -1066.98 | 105.7733 | -6530.3008 |
| bji | 426.3978 | 4954.897 | 689.9346 | 618.5185 |
| cij | 0.3 | 0.2 | 0.3 | 0.2 |
| | | | | |
| Component i | Isopropanol | Water | Cyclohexane | n-propanol |
| Component j | Isopropyl acetate | n-propanol | n-propanol | Isopropyl acetate |
| Source | VLE-IG | VLE-IG | VLE-IG | R-PCES |
| aij | 0 | 5.4486 | 6.8277 | 0 |
| aji | 0 | -1.7411 | -4.1888 | 0 |
| bij | 110.5442 | -861.179 | -1548.27 | 191.351326 |
| bji | 100.1164 | 576.4458 | 1490.146 | 157.849157 |
| cij | 0.3 | 0.3 | 0.3 | 0.3 |

Table 2.1: The binary coefficients of the NRTL model used in the simulations

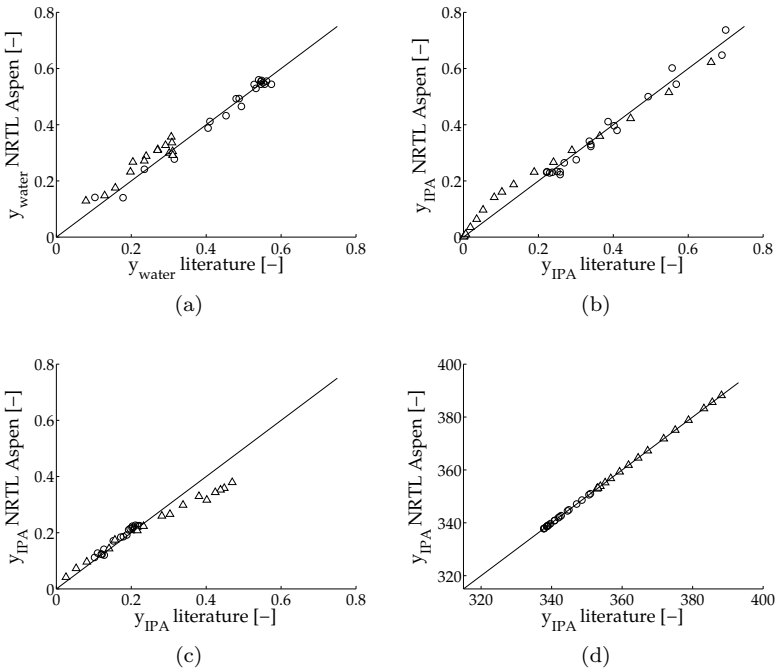


Figure 2.5: Vapour composition of (a) water, (b) isopropanol and (c) entrainer and (d) boiling temperatures for water-isopropanol-cyclohexane (○) and water-isopropanol-isopropyl acetate (△) calculated by Aspen Plus versus literature [12, 15]

libria for water-isopropanol-isopropyl acetate at 50°C reported by Hong [16] and calculated by Aspen Plus are given. The tie-lines are directed the same way but the sizes of the liquid-liquid envelopes do not correspond. Aspen Plus predicts the entrainer rich phase to contain more entrainer and alcohol and less water than is reported in literature.

The decanter should be simulated with a separate set of NRTL parameters obtained from liquid-liquid equilibrium data. Because insufficient experimental data is available, it is decided to use the current NRTL parameters. As result, the amount of entrainer predicted by simulation is somewhat overestimated.

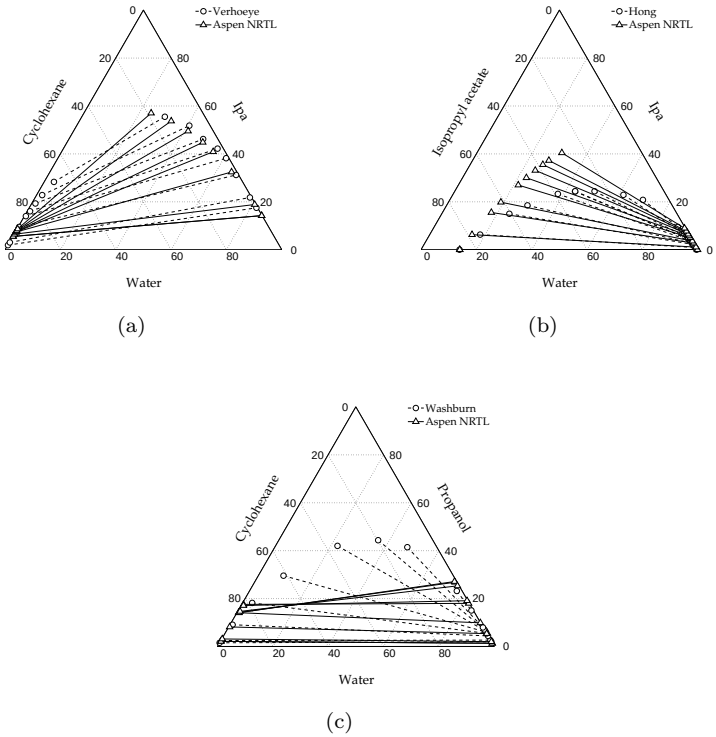


Figure 2.6: Liquid-liquid equilibria for (a) water-isopropanol-cyclohexane and (b) water-isopropanol-isopropyl acetate and (c) water-propanol-cyclohexane calculated by Aspen Plus versus literature [12, 16, 17]

In the case of *n*-propanol, only liquid-liquid equilibrium data is available for the water-*n*-propanol-cyclohexane system [17]. The data does not correspond with each other. However, around the heterogeneous azeotrope (0.26 water, 0.15 *n*-propanol, 0.59 cyclohexane), which approximately will be the composition of the stream to the decanter, the differences are relatively small.

In Table 2.2 and 2.3 the computed azeotropic mixtures are compared to those reported in literature [18]. For the *n*-propanol-isopropyl acetate and

| Temperature [°C] | Water [-] | Isopropanol [-] | Cyclohexane [-] | $(\sum \Delta x)/n_c$ [-] |
|---|---|---|---|---|
| **69.25** | **0.00** | **0.39** | **0.61** | |
| 69.35 | 0.00 | 0.40 | 0.60 | 0.01 |
| 69.42 | 0.00 | 0.39 | 0.61 | 0.00 |
| **69.49** | **0.30** | **0.00** | **0.70** | |
| 69.40 | 0.30 | 0.00 | 0.70 | 0.00 |
| **80.37** | **0.33** | **0.67** | **0.00** | |
| 80.37 | 0.31 | 0.69 | 0.00 | 0.02 |
| 80.55 | 0.33 | 0.67 | 0.00 | 0.00 |
| **64.12** | **0.22** | **0.23** | **0.54** | |
| 64.30 | 0.21 | 0.22 | 0.57 | 0.02 |
| Temperature [°C] | Water [-] | Isopropanol [-] | Isopropyl acetate [-] | $(\sum \Delta x)/n_c$ [-] |
| **77.46** | **0.42** | **0.00** | **0.58** | |
| 75.90 | 0.41 | 0.00 | 0.59 | 0.01 |
| 76.60 | 0.40 | 0.00 | 0.60 | 0.02 |
| **80.37** | **0.33** | **0.67** | **0.00** | |
| 80.37 | 0.31 | 0.69 | 0.00 | 0.02 |
| 80.55 | 0.33 | 0.67 | 0.00 | 0.00 |
| **80.76** | **0.00** | **0.67** | **0.33** | |
| 80.10 | 0.00 | 0.66 | 0.34 | 0.01 |
| 80.90 | 0.00 | 0.69 | 0.31 | 0.02 |
| **75.83** | **0.38** | **0.23** | **0.39** | |
| 75.50 | 0.39 | 0.14 | 0.47 | 0.06 |

Table 2.2: Azeotropes predicted by the used NRTL model (**bold values**) versus literature data [18] for the water-isopropanol-cyclohexane and water-isopropanol-isopropyl acetate

| Temperature [°C] | Water [-] | $n$-propanol [-] | Cyclohexane [-] | $(\sum \Delta x)/n_c$ [-] |
|---|---|---|---|---|
| **69.49** | **0.30** | **0.00** | **0.70** | |
| 69.40 | 0.30 | 0.00 | 0.70 | 0.00 |
| **74.66** | **0.00** | **0.24** | **0.76** | |
| 74.69 | 0.00 | 0.24 | 0.76 | 0.00 |
| 74.70 | 0.00 | 0.26 | 0.74 | 0.02 |
| **87.67** | **0.60** | **0.40** | **0.00** | |
| 87.66 | 0.57 | 0.43 | 0.00 | 0.03 |
| 87.76 | 0.58 | 0.42 | 0.00 | 0.02 |
| **66.83** | **0.26** | **0.15** | **0.59** | |
| 65.90 | 0.27 | 0.12 | 0.61 | 0.02 |
| Temperature [°C] | Water [-] | $n$-propanol [-] | Isopropyl acetate [-] | $(\sum \Delta x)/n_c$ [-] |
| **77.46** | **0.42** | **0.00** | **0.58** | |
| 75.90 | 0.41 | 0.00 | 0.59 | 0.01 |
| 76.60 | 0.40 | 0.00 | 0.60 | 0.02 |
| **86.01** | **0.00** | **0.30** | **0.70** | |
| **87.67** | **0.60** | **0.40** | **0.00** | |
| 87.66 | 0.57 | 0.43 | 0.00 | 0.03 |
| 87.76 | 0.58 | 0.42 | 0.00 | 0.02 |
| **77.14** | **0.41** | **0.09** | **0.50** | |

Table 2.3: Azeotropes predicted by the used NRTL model (**bold values**) versus literature data [18] for the water-$n$-propanol-cyclohexane and water-$n$-propanol-isopropyl acetate

the water-*n*-propanol-isopropyl acetate azeotrope no literature data is available. The computed composition of the water-isopropanol-isopropyl acetate azeotrope has an average deviation from the literature composition of 0.06. For the water-isopropyl acetate azeotrope the computed boiling temperature deviates around one degree from the literature temperature. For all the other azeotropes the model data corresponds well with the literature data. Therefore, it can be concluded that the thermodynamic model may be less accurate for the isopropyl acetate systems.

In the simulations in which also the reactive system is present, the same property model is used. The unknown interaction parameters are estimated using UNIFAC. UNIFAC predicts an azeotrope between myristic acid and isopropyl myristate. It is unlikely that this will occur, because the components have similar polarity. Therefore the interaction between those components is set to zero manually.

## 2.4 Results and discussion

### 2.4.1 Residue curve maps

In Figure 2.7*a* and *b* the residue curve maps for the water-isopropanol-cyclohexane and water-isopropanol-isopropyl acetate mixtures are shown. Both residue curve maps show an immiscibility region and a heterogeneous ternary azeotrope. The heterogeneous ternary azeotrope is for all distillation regions the unstable node because all distillation curves start in this point, thus the distillate vapour is close to the ternary azeotrope. When operating in the correct distillation region, the residue product is isopropanol because it is a stable node (residue curves only end here). The distillate vapour will split into two liquid phases after condensation according to the liquid tie-lines. The immiscibility region of cyclohexane is situated close to the entrainer vertex, meaning that the entrainer phase contains little water. However, the orientation of the tie-lines seems to indicate that the aqueous phase would contain some alcohol and entrainer. In contrast, the tie-lines in the isopropyl acetate residue

curve map do point to the water vertex but the immiscibility region is not situated close to the entrainer vertex, thus the entrainer phase will contain a significant amount of water. Because both residue curve maps look like the desired residue curve map discussed before, it can be concluded that both solvents are suitable. However, it should be noted that the tielines in the water-isopropanol-cyclohexane residue curve map show inaccurate behaviour due to the crossing among them. Column simulations should point out the quantitative effects.

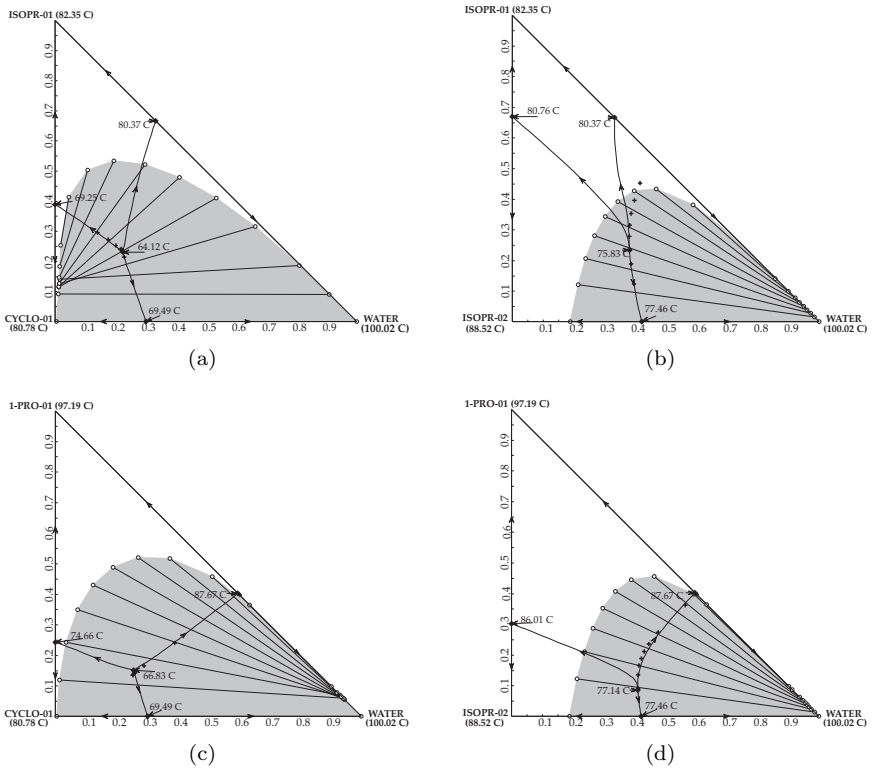


Figure 2.7: Residue curve maps for the separation of water and isopropanol: (a) cyclohexane, (b) isopropyl acetate, and for the separation of water and *n*-propanol (+ = vapour line): (c) cyclohexane, (d) isopropyl acetate

In Figure 2.7*c* and *d* the residue curve maps for the water-*n*-propanol-cyclohexane and water-*n*-propanol-isopropyl acetate mixture are shown. They are similar to those with isopropanol. Therefore, when the entrainers are suitable for the separation of water and isopropanol, they also will be suitable for the separation of water and *n*-propanol. Only in the case of cyclohexane, the tie-lines are different. While using *n*-propanol they are more directed to the water vertex than when using isopropanol. This means that after phase separation, the aqueous phase contains less alcohol and entrainer to be recovered.

### 2.4.2 Column simulations distillation section

In Aspen Plus, a distillation section of 10 stages was simulated in a column without reboiler, see Figure 2.8. The isopropanol-water mixture enters the column at the bottom as a vapour. The entrainer enters at the top as a liquid, with a temperature of just below its boiling point. The operating pressure is 1 bar. The effect of adding different amounts of entrainers was simulated while the alcohol-water feed was held constant at 1000 mol $hr^{-1}$. Two isopropanol-water mixtures were evaluated: 0.10 mole fraction of water, 0.90 mole fraction of isopropanol and 0.32 mole fraction of water, 0.68 mole fraction of isopropanol (azeotropic composition). To distinguish between the effect on the separation by distillation and the separation by condensation and decantation, the reflux was not closed. The temperature of the decanter is 60°C.

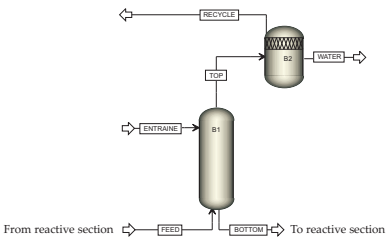


Figure 2.8: Flowsheet of the distillation section (DS)

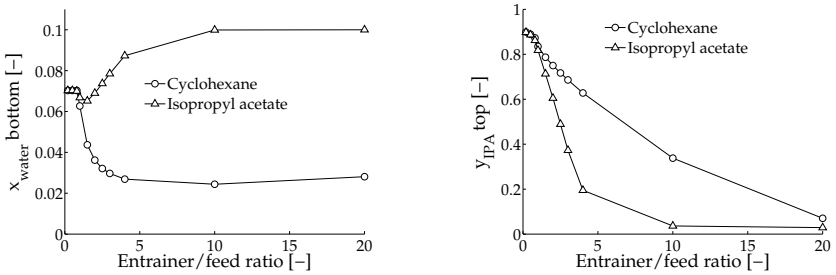


(a) (b)

Figure 2.9: (a) Mole fraction of water in bottom and (b) mole fraction of isopropanol in top for different amounts of entrainer in a pseudo-binary mixture simulation of the distillation section (DS) with a feed of 0.10 mole fraction of water and 0.90 mole fraction of isopropanol

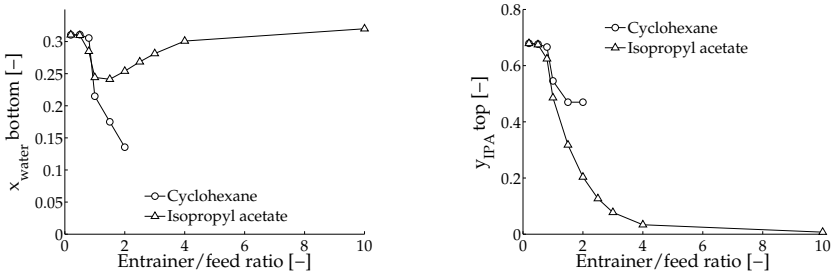


(a) (b)

Figure 2.10: (a) Mole fraction of water in bottom and (b) mole fraction of isopropanol in top for different amounts of entrainer in a pseudo-binary mixture simulation of the distillation section (DS) with a feed of 0.32 mole fraction of water and 0.68 mole fraction of isopropanol

In Figures 2.9 and 2.10 the compositions of isopropanol and water as a pseudo-binary mixture (in calculating the compositions, the entrainer is not considered) are given for different amounts of entrainer added. It can be seen in Figure 2.9*a* that for low entrainer ratios the mole fraction of water (pseudo-

binary mixture) in the bottom is 0.07, which is the liquid composition that is in equilibrium with the 0.10 water, 0.90 isopropanol vapour feed. As long as this is the bottom composition the entrainer does not function because no water has been removed. When a certain entrainer ratio (1.0 for cyclohexane and 0.8 for isopropyl acetate) is reached, the water mole fraction in the bottom of the pseudo-binary mixture decreases. Due to its higher affinity with water, isopropyl acetate has a lower value for the entrainer ratio where the entrainer starts to have effect than cyclohexane. At a certain entrainer ratio an optimum is reached, at entrainer ratios higher than this optimum, the water mole fraction in the bottom increases again to a value of 0.10. For cyclohexane this optimum lays around an entrainer ratio of 10, in the case of isopropyl acetate the optimum is already reached at a ratio of 1.5.

Similar effects can be observed for an azeotropic feed mixture in Figure 2.10*a*. As long as the bottom contains a mole fraction of 0.32 water, the entrainer does not function because no water is removed. The entrainer ratios where the entrainer starts to have effect are lower than in the case of the 0.1-0.9 feed (0.8 for cyclohexane and 0.5 for isopropyl acetate. In the case of cyclohexane no optimum is reached because above an entrainer to feed ratio of 2, two liquid phases are obtained in the column which is not desirable.

For a feed of 0.10 mole fraction water and 0.90 mole fraction isopropanol, it can be seen in Figure 2.9*b*, that in the range of entrainer ratios where the entrainer is effective (cyclohexane: 1.0-10, isopropyl acetate: 0.8-1.5) the amount of isopropanol in the top stream is decreased. This corresponds with the water removal from the bottom stream: the lower the mole fraction of water in the bottom, the lower the isopropanol fraction in the top. Despite the lower water removal by isopropyl acetate in the bottom, the top stream contains less alcohol than in the case of cyclohexane. The same effect is obtained for the azeotropic feed mixture in Figure 2.10*b*.

In Figures 2.11 and 2.12 the compositions of *n*-propanol and water as a pseudo-binary mixture (in calculating the compositions, the entrainer is not considered) are given for different amounts of entrainer added. For cyclohexane as entrainer, similar effects as in the isopropanol system are found. However,

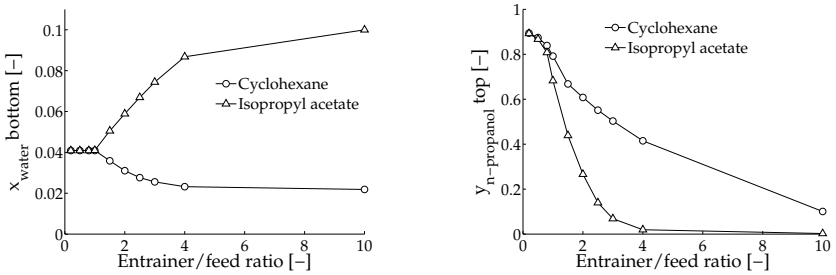


(a) (b)

Figure 2.11: (a) Mole fraction of water in bottom and (b) mole fraction of *n*-propanol in top for different amounts of entrainer in a pseudo-binary mixture simulation of the distillation section (DS) with a feed of 0.10 mole fraction of water and 0.90 mole fraction of *n*-propanol

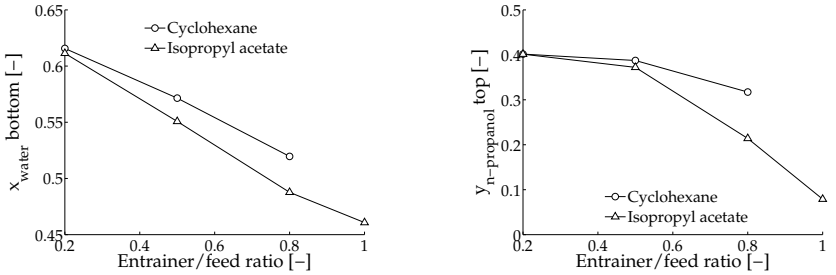


(a) (b)

Figure 2.12: (a) Mole fraction of water in bottom and (b) mole fraction of *n*-propanol in top for different amounts of entrainer in a pseudo-binary mixture simulation of the distillation section (DS) with a feed of 0.60 mole fraction of water and 0.40 mole fraction of *n*-propanol

in the case of isopropyl acetate as entrainer, the mole fraction of water in the bottom will not decrease at a feed of 0.10 mole fraction of water and 0.90 mole fraction of *n*-propanol. This can be seen in Figure 2.11*a*. The major part of both the water and the *n*-propanol is pushed to the bottom. The top consists mainly of entrainer. For an azeotropic feed mixture, it can be seen in Figure

2.12 that the mole fraction of water in the bottom decreases.

In Figure 2.13, the flow profiles along the column are given for an entrainer to feed ratio of 0.5, 1.5, 2.5 and 4.0 for respectively cyclohexane and isopropyl acetate, while using a feed mixture of 0.10 mole fraction water and 0.90 mole fraction isopropanol. It can be noticed that the entrainer is more present in the liquid phase than in the vapour phase. The amount of cyclohexane is more gradually spread through the column than isopropyl acetate. The cyclohexane penetrates more deeply into the distillation section, the isopropyl acetate is more present in the top of the distillation section. The effect of the entrainer is best seen in the isopropanol being pushed into the bottom part of the column. In both cases, the more entrainer is added, the more isopropanol is found in the bottom liquid phase. It seems that isopropyl acetate is a better entrainer because initially it pushes more isopropanol to the bottom than cyclohexane. However, at an isopropyl acetate to feed ratios of 2.5 and 4.0, the amount of water in the bottom liquid is increasing again. When using cyclohexane, lower water contents can be achieved.

In Figure 2.14 and 2.15 the flow profiles along the column are represented in a ternary diagram for an entrainer to feed ratio of 0.5 and 2.5 for cyclohexane and isopropyl acetate, while using respectively a feed mixture of 0.10 mole fraction water and 0.90 mole fraction isopropanol or 0.90 mole fraction *n*-propanol respectively. It should be noted that distillation boundaries cannot be crossed during distillation. However, in this case no reboiler is present, which explains the crossings. At an entrainer to feed ratio of 0.5 this distillation takes place in the upper distillation region. In order to get a top vapour consisting of entrainer and water and hardly any isopropanol, sufficient entrainer has to be added such that the distillation takes place in the left distillation region. For both entrainers it can be seen that this happens with an entrainer to feed ratio of 2.5.

However, when too much entrainer is added, the top vapour consists of mostly entrainer and water is not drawn off at the top. In Figure 2.14*b* and 2.15*b* it can be seen that this happens for an isopropyl acetate to feed ratio of 2.5. From the location of the distillation boundaries it can bee seen that

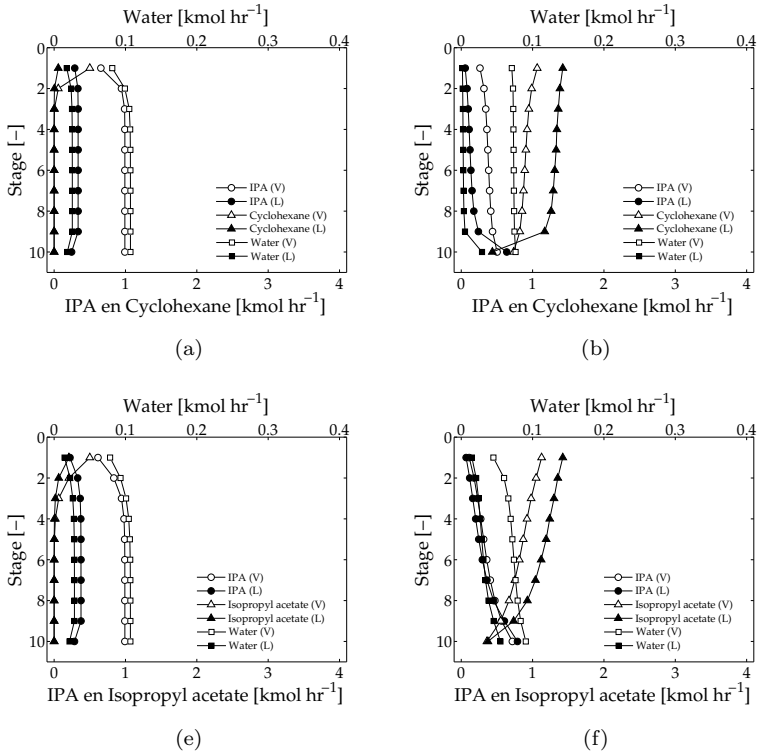


Figure 2.13: Vapour and liquid phase profiles in the distillation section simulation for a cyclohexane/feed ratio = (a) 0.5 (b) 1.5 (c) 2.5 (d) 4.0 and an isopropyl acetate/feed ratio = (e) 0.5 (f) 1.5 (g) 2.5 (h) 4.0

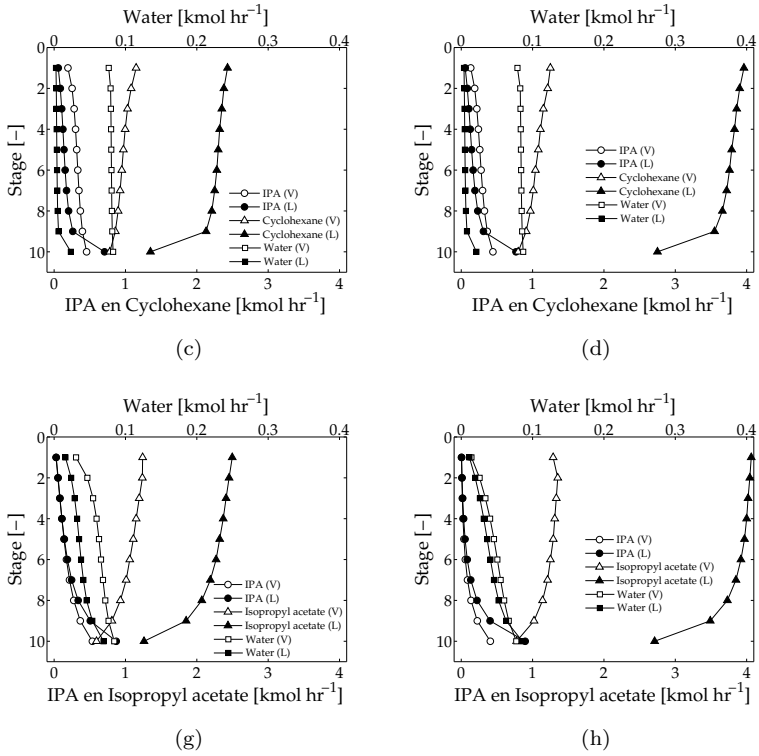


Figure 2.13: continued

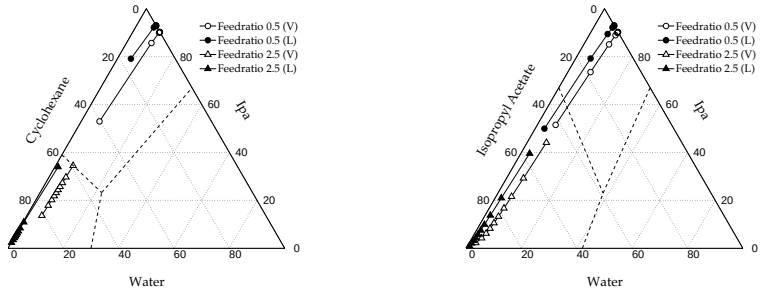


(a) (b)

Figure 2.14: Ternary vapour and liquid phase profiles of the isopropanol system in the distillation section simulation for a entrainer/feed ratio of 0.5 and 2.5 for a) cyclohexane and b) isopropyl acetate as entrainer with (--) = distillation boundaries

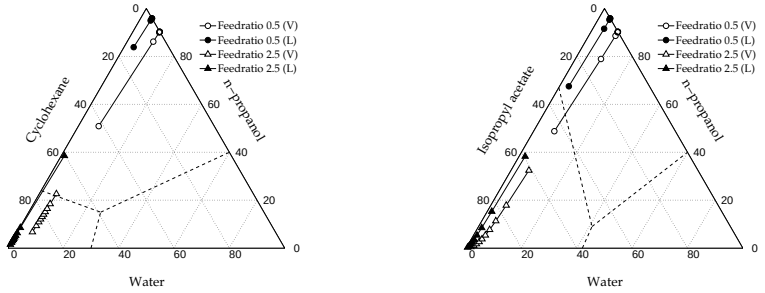


(a) (b)

Figure 2.15: Ternary vapour and liquid phase profiles of the propanol system in the distillation section simulation for a entrainer/feed ratio of 0.5 and 2.5 for a) cyclohexane and b) isopropyl acetate as entrainer with (--) = distillation boundaries

less isopropyl acetate than cyclohexane is necessary to cross the distillation border. This supports the values, mentioned before, for the entrainer ratios where the entrainer starts to have effect, and that isopropyl acetate initially pushed more isopropanol to the bottom than cyclohexane.

It can be concluded that both entrainers reduce the amount of water in the bottom stream of the distillation section. This reduction is more effective when cyclohexane is used than when isopropyl acetate is used. This is illustrated by the values of the relative volatility of water compared to isopropanol. Using cyclohexane as entrainer the relative volatility is raised from 1.4 to 9.1, while in the case of isopropyl acetate it is only raised to a value of 1.9.

### 2.4.3 Column simulations total concept

To see the combined influence of the distillation section and liquid-liquid split on the reaction, the overall concept (Entrainer-based Reactive Distillation column and decanter) for the esterification of myristic acid with isopropanol as well as with *n*-propanol, was simulated in Aspen Plus, see Figure 2.16. The Entrainer-based Reactive Distillation column is designed such that 99.0% conversion of myristic acid and a 99.0% product purity is obtained. The input parameters of the feed streams are based on a production of 1000 kg $hr^{-1}$ (3697 mol $hr^{-1}$) (iso)propyl myristate and 99% conversion of the myristic acid. The

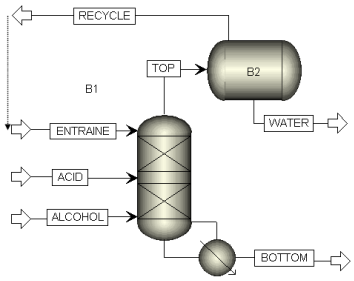


Figure 2.16: Flowsheet Entrainer-based Reactive Distillation column

ratio of myristic acid:alcohol is fixed at 1:1. The corresponding feeds are 3735 mol $hr^{-1}$ myristic acid and 3735 mol $hr^{-1}$ alcohol. The operating pressure is 1 bar and 5 bar. Cyclohexane is used as the entrainer. The temperature of the decanter is 60°C.

The kinetics of the reactions are experimentally determined, they are described in Chapter 3. The reaction rate for the esterification of myristic acid and isopropanol using *p*-toluene sulphonic acid is

$$\begin{aligned} r_E \;=\; & 3.33 \cdot 10^5 [\text{cat}] \exp\left(\frac{-58.9 \cdot 10^3}{RT}\right)[A][B] \\ & - 2.18 \cdot 10^3 [\text{cat}] \exp\left(\frac{-45.9 \cdot 10^3}{RT}\right)[E][W] \text{ mol L}^{-1}\text{s}^{-1} \end{aligned} \tag{2.1}$$

For the esterification with *n*-propanol using *p*-toluene sulphonic acid this is

$$\begin{aligned} r_E \;=\; & 6.27 \cdot 10^4 [\text{cat}] \exp\left(\frac{-47.4 \cdot 10^3}{RT}\right)[A][B] \\ & - 8.44 [\text{cat}] \exp\left(\frac{-25.4 \cdot 10^3}{RT}\right)[E][W] \text{ mol L}^{-1}\text{s}^{-1} \end{aligned} \tag{2.2}$$

$r_E$ is the reaction rate, $[E]$ the concentration ester, $[A]$ the concentration alcohol, $[B]$ the concentration acid, $[W]$ the concentration water and [cat] is the catalyst concentration. The chosen catalyst concentration is 0.15 M, which is ten times larger then found in literature [19] for Reactive Distillation for the esterification of fatty acids.

Because the reaction with isopropanol is very slow at atmospheric pressure, a large liquid hold-up is required to reach 99% conversion at 1 bar. Therefore, the column consists of a reactive section of 500 stages of 17 L per stage, at an operating pressure of 5 bar this is reduced to 32 stages of 10 L per stage. For the esterification with *n*-propanol this is 89 and 16 stages of 10 L per stage, for respectively a pressure of 1 and 5 bar. Furthermore, the column has an one stage bottom section and a distillation section on top of two stages.

The number of stages in the bottom section and the distillation section were varied: a distillation section of two stages appeared already sufficient for the desired separation to take place and adding more stages did not improve this separation further.

In the esterification with isopropanol at 1 bar, the addition of the entrainer has no positive influence on the conversion. The simulation results show that, to reach 99% conversion, the entrainer amount must be as low as possible. This effect is caused by a combined effect of thermodynamics and kinetics. One of the components with the lowest boiling point in the column is the entrainer. Therefore the amount of entrainer needed for the water removal causes a decrease of the temperature in the column. This temperature decrease has an negative influence on the conversion, probably because the high activation energy of the reaction cannot be overcome. In Figure 2.17 it can be seen that with increasing entrainer amount, the column temperature and conversion decreases.

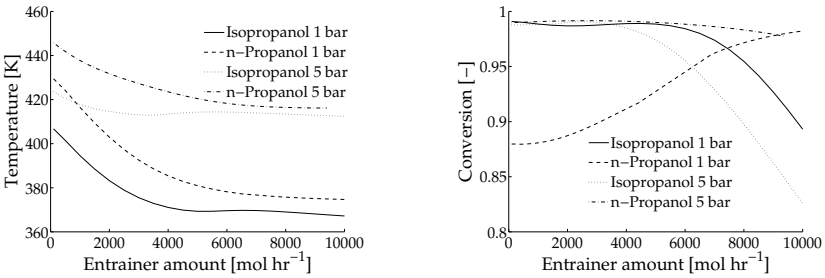


Figure 2.17: Influence of the entrainer (cyclohexane) amount on a) the column temperature and b) the conversion in the Entrainer-based Reactive Distillation for isopropanol ($-$) and *n*-propanol ($--$) for a feed of 3735 mol hr$^{-1}$ myristic acid and 3735 mol hr$^{-1}$ alcohol

However, in the esterification with *n*-propanol, the addition of the entrainer has a positive influence on the conversion. More entrainer leads to a higher con-

version. The activation energy of the esterification reaction with *n*-propanol is lower than with isopropanol. Also the *n*-propanol itself has a higher boiling point than isopropanol. Therefore the column temperature will be higher and more entrainer is needed to lower the temperature to the same level as in the case with isopropanol. Figure 2.17*a* shows that the column temperature in the case of *n*-propanol is indeed higher than in the case of isopropanol. The temperature also decreases with the amount of entrainer added, but the decrease is slower. Figure 2.17*b* shows that more entrainer leads to a higher conversion.

At an operating pressure of 5 bar the addition of the entrainer a positive influence on the conversion for both the esterification of myristic acid with *n*-propanol and isopropanol. Due to the higher pressure, the column temperature is higher and the combined effect of reaction kinetics and thermodynamics, as seen in the simulations for the esterification of myristic acid with isopropanol at 1 bar, does not take place. This can be seen in Figure 2.17. It is noticed that with increasing amount of entrainer the conversion increases till an optimum is reached at 2500 mol $hr^{-1}$ entrainer for the esterification with isopropanol and 2700 mol $hr^{-1}$ entrainer for the esterification with isopropanol at 5 bar and for the esterification with *n*-propanol at 1 and 5 bar.

In Figures 2.18 and 2.19 the vapour and liquid phase composition profiles along the stages of the Entrainer-based Reactive Distillation column are given, for the esterification of myristic acid with *n*-propanol at 1 bar for a feed of 3735 mol $hr^{-1}$ myristic acid, 3735 mol $hr^{-1}$ *n*-propanol and 14800 mol $hr^{-1}$ cyclohexane or 12800 mol $hr^{-1}$ isopropyl acetate. From the profiles can be seen that the cyclohexane does not enter the reactive section and is mainly present in the distillation section as a vapour. The isopropyl acetate does enter the reactive section slightly. The unreacted *n*-propanol leaves the column at the top. The produced water is pulled into the distillation section as a vapour, where it leaves the top in a mixture with entrainer and alcohol.

As expected, the cyclohexane is more capable of removing the water than isopropyl acetate. This is illustrated by the 'sharper' column profiles. In the case of cyclohexane the removal only takes place in the distillation section and the conversion can be achieved in a smaller column. However, more cyclo-

hexane than isopropyl acetate is needed to achieve the same conversion. This caused by the difference in size of the heterogeneous region. Since the column profile inside the top distillation section has to remain into the homogeneous region. More cyclohexane than isopropyl acetate is needed to achieve this.

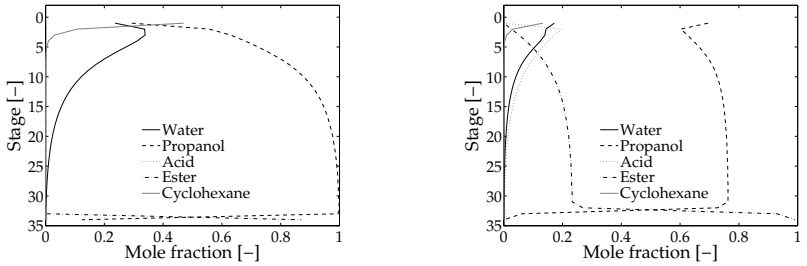


(a) (b)

Figure 2.18: (a) Vapour and (b) liquid phase profiles in the Entrainer-based Reactive Distillation column with cyclohexane

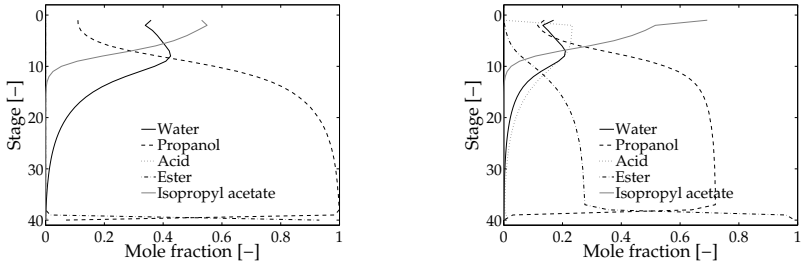


(a) (b)

Figure 2.19: (a) Vapour and (b) liquid phase profiles in the Entrainer-based Reactive Distillation column with isopropyl acetate

## 2.5 Conclusions

It was investigated whether isopropyl acetate and cyclohexane, two suitable entrainers for the azeotropic distillation of isopropanol and water, are also suitable for the Entrainer-based Reactive Distillation process.

From the residue curve maps it follows that both solvents are suitable entrainers. In the case of cyclohexane, after decantation, the entrainer phase contains almost no water but the aqueous phase contains alcohol and entrainer. In the case of isopropyl acetate the aqueous phase is almost pure water but the entrainer phase, which will be recycled back into the column, contains a significant amount of water.

The simulations of the distillation section of the column show that both entrainers reduce the amount of water in the bottom stream of the distillation section. This reduction is more effective when cyclohexane is used than when isopropyl acetate is used.

The simulations of the total Entrainer-based Reactive Distillation concept prove that both entrainers can be used as entrainer to obtain 99% conversion in one single column in the case of esterification with *n*-propanol. This is confirmed by Dimian et al. [7] in their research to Entrainer-based Reactive Distillation for the esterification of lauric acid with *n*-propanol.

As expected, because of its non-polarity, cyclohexane is a more effective entrainer than isopropyl acetate. In the esterification with isopropanol, the entrainer addition has a negative influence on the conversion, due to a combined effect of thermodynamics and kinetics.

Finally, it can be concluded that both cyclohexane and isopropyl acetate can be used as an entrainer in Entrainer-based Reactive Distillation, but cyclohexane is preferred. Apparently, for the entrainer selection in Entrainer-based Reactive Distillation the same rules can be applied as used in the entrainer selection for azeotropic distillation. However, the kinetics of the reaction can be an obstruction for the Entrainer-based Reactive Distillation concept to be feasible.

# Nomenclature

| | |
|---|---|
| $[A]$ | Fatty acid concentration [mol $L^{-1}$] |
| $[B]$ | Alcohol concentration [mol $L^{-1}$] |
| [cat] | Catalyst concentration [M] |
| $[E]$ | Ester concentration [mol $L^{-1}$] |
| $[W]$ | Water concentration [mol $L^{-1}$] |
| $R$ | Gas constant [J $mol^{-1}$ $K^{-1}$] |
| $T$ | Temperature [K] |
| $r_E$ | Reaction rate [mol $L^{-1}$ $s^{-1}$] |

# References


[1] Seader, J.; Siirola, J.; Barnicki, S. Section 13: Distillation. In *Perry's Chemical Engineers' Handbook*; Perry, R.; Green, D.; Maloney, J., Eds.; McGraw-Hill: 1999.

[2] Doherty, M. F.; Malone, M. F. *Conceptual design of distillation systems;* McGraw-Hill: Boston, 2001.

[3] Doherty, M. F.; Knapp, J. Distillation, Azeotropic, and Extractive. In *Kirk-Othmer Encyclopedia of Chemical Technology*, Vol. 8; John Wiley & Sons, Inc.: 2004.

[4] Foucher, E. R. *Ind. Eng, Chem, Res* **1991,** *30,* 760-772.

[5] Pham, H.; Doherty, M. *Chem. Eng Sc.* **1990,** *45,* 1837-1843.

[6] Pham, H.; Doherty, M. *Chem. Eng Sc.* **1990,** *45,* 1845-1854.

[7] Dimian, A. C.; Omota, F.; Bliek, A. *Chem. Eng. Process.* **2004,** *43,* 411-420.

[8] Stéger, C.; Varga, V.; Horváth, L.; Rév, E.; Fonyó, Z.; Meyer, M.; Lelkes, Z. *Chem. Eng. Process.* **2005,** *44,* 1237-1256.

[9] Seader, J.; Henley, E. *Separation Process Principles;* John Wiley & Sons, Inc.: Second Edition ed.; 2006.

[10] Robinson, C.; Gilliland, E. *Elements of Fractional Distillation;* McGraw-Hill: 4th ed. ed.; 1950.

[11] Rarey, J. *Ind. Eng. Chem.* **2005,** 7600-7608.

[12] Verhoeye, L. *J. Chem. Eng. Data* **1968,** *13,* 462-467.

[13] Verhoeye, L. *J. Chem. Eng. Data* **1971,** *15,* 222-226.

[14] Gmehling, J.; Onken, U.; Arlt, W. *Vapour-Liquid Equilibrium Data Collection 1a;* 1981.

[15] Teodorescu, M.; Aim, K.; Wichterle, I. *J. Chem. Eng. Data* **2001,** *46,* 261-266.

[16] Hong, G.; Lee, M.; Lin, H. *Fluid Phase Equilibria* **2002,** *202,* 239-252.

[17] Sørensen, J.; Arlt, W. *Liquid-Liquid Equilibrium Data Collection 2;* Dechema: 1980.

[18] Gmehling, J.; Menke, J.; Fischer, K.; Krafczyk, J. *Azeotropic Data;* VCH: Weinheim, 1994.

[19] Zhou, M. *Modelisation de reacteurs d'esterification fonctionnement semi-continu et continu,* Thesis, L'institut national polytechnique de Toulouse, 1983.

# Chapter 3

# Reaction kinetics

*In this chapter the reaction kinetics of the esterification of myristic acid with isopropanol with n-propanol are determined, using sulphated zirconia (SZ) and p-toluene sulphonic acid (pTSA) as catalysts, for a temperature range of 343-403K. SZ appeared to be an unsuitable catalyst for the esterification of myristic acid with isopropanol since it did not increase the reaction rate of the uncatalysed reaction. For the reactions with pTSA the reaction rates are determined. The reactions follow first order kinetics in all components. The kinetic model corresponds with the results for the esterification of myristic acid with isopropanol determined by Yalçinyuva et al. [1] for 333-353K and the results for the esterification of palmitic acid with isopropanol determined by Aafaqi et al. [2] for 373-443K. As expected, the reaction rate increases with increasing amount of catalyst and with increasing temperature. The reaction rate and equilibrium conversion increases with an increasing alcohol to myristic acid feed ratio. The reaction with n-propanol is considerably faster (at 373K about 3.8 times) than the reaction with isopropanol.*

## 3.1 Introduction

In the reactive section of the Entrainer-based Reactive Distillation column, the catalysed esterification reaction of a fatty acid (A) with an alcohol (B) takes place, forming a fatty acid ester (E) and water (W):

$$A + B \overset{\text{catalyst}}{\rightleftharpoons} E + W \tag{3.1}$$

Despite the low activity, harsh reaction conditions, sensitivity to poisons and diffusion problems, the important advantages of heterogenous catalysis are the easy separation from the product and the applicability in continuous processes. Furthermore, the purity of the product is higher since the side reactions can be largely eliminated and the environment is less corrosive. [1–3]

Because of these advantages, the esterification reaction is preferably catalysed by a heterogeneous catalyst, which is enclosed in a structured Reactive Distillation packing. To calculate the conversions in the reactive section, the kinetic parameters should be known. Therefore, the reaction kinetics of the esterification of isopropanol and myristic acid were investigated.

To our knowledge, one kinetic study has been reported in the literature for the esterification of myristic acid with isopropanol using $p$TSA, $H_2SO_4$, Amberlyst15 and a Degussa silica based catalyst. [1]. In this study, the kinetics were measured at 60-80°C, but for Reactive Distillation higher temperatures are needed to obtain sufficiently high conversions. Therefore, we study the reaction at a more appropriate range of 70-130°C. Also a number of studies discussed the esterification reactions of other fatty acids using homogenous and heterogeneous catalysts. [2, 4–11]. An overview is given in Table 3.1.

In other research [12, 13] , which was part of the same project, different heterogeneous catalysts, like ion exchange resins, zeolites and sulphated metal oxide (zirconia, titania an tin oxide) were compared, based on their activity and selectivity. Sulphated zirconia showed high activity and selectivity for the esterification of lauric acid with a variety of primary alcohols ranging from

| Reaction | Catalyst | Reference |
|---|---|---|
| Decanoic acid + methanol | Amberlyst 15 | Steinigeweg and Gmehling [7] |
| Lauric acid + isobutanol | $H_2SO_4$ | El-Kinawy et al. [6] |
| Myristic acid + isopropanol | *p*TSA, $H_2SO_4$, Amberlyst 15, Degussa | Yalçinyuva et al. [1] |
| Myristic acid + isobutanol | $H_2SO_4$ | El-Kinawy et al [6] |
| Palmitic acid + isopropanol | *p*TSA,zinc ethanoate | Aafaqi et al. [2] |
| Palmitic + isobutanol | $H_2SO_4$ | Goto et al. [5] |
| Stearic acid + isobutanol | $H_2SO_4$ | El-Kinawy et al [6] |
| Oleic acid + methanol | *p*TSA, $H_2SO_4$, K2411, K1481 | Unnithan and Tiwari [4], Othmer and Rao [8], Vieville et al. [9] |
| Oleic acid + 2-ethylhexanol | *p*TSA | Lacaze-Dufaure and Mouloungui [10] |
| Oleic acid + glycerol | K1481, Amberlyst 16, Amberlyst 31 | Pouilloux et al. [11] |

Table 3.1: Esterification of fatty acids with various catalysts

2-ethylhexanol to methanol. It has a high thermal stability and strong acid sites. The large pores do not limit the diffusion of the fatty acid molecules. Sulphated zirconia does not leach under the reaction conditions and does not give rise to side reactions such as etherification or dehydration. [12, 13]

*p*-Toluene sulphonic acid (*p*TSA) was used as a homogeneous catalyst, because it was reported to have a better catalytic performance compared to sulphuric acid. [1, 2, 4].

In this chapter first the heterogeneously catalysed reaction will be discussed. Because the experimental data showed that no suitable heterogeneous catalyst is available for the esterification of myristic acid, also the homogeneously catalysed reaction using *p*TSA is investigated for the esterification of myristic acid with isopropanol and with *n*-propanol. A mathematical model is used to determine the kinetic parameters from the experimental data and the influence of the reaction temperature, catalyst loading and myristic acid to alcohol feed ratio is discussed.

## 3.2 Heterogeneously catalysed reaction

### 3.2.1 Theory

Heterogeneously catalysed kinetics are quite complex, including adsorption and desorption steps to the catalyst. [14] Using reaction orders is a simplistic approach to describe the heterogeneously catalysed kinetics. In the case of homogeneously catalysed kinetics, the majority of the researchers report that an esterification reaction follows second order reversible kinetics (first order in all components). [1, 2, 4–6, 15, 16] Which is also mostly assumed to be true for simplifications of heterogeneously catalysed kinetics. [2, 7, 9, 16]

Heterogeneously catalysed kinetics can be approximated by a pseudohomogeneous model, in which the heterogeneous system is considered to be homogeneous. [7, 17] When first order kinetics in all components is assumed, the reaction rate ($r_E$) of the homogenous reaction can be described by

$$r_E[\text{cat}] = (k_1[A][B] - k_{-1}[E][W]) \tag{3.2}$$

where [cat] is the catalyst concentration, $[E]$ the ester concentration, $[A]$ the alcohol concentration, $[B]$ the acid concentration, $[W]$ the water concentration, $k_1$ the rate constant of the forward reaction and $k_{-1}$ the rate constant of the backward reaction. In this equation, the reaction rate constants $k_1$ and $k_{-1}$ are assumed to be linearly dependent on the catalyst concentration. Various studies support this assumption [3, 8, 18, 19].

During the kinetic experiments performed in this research, no water and ester will be present at the start of the reaction, only an initial concentration of alcohol $[A]_0$ and acid $[B]_0$ is present. The etherification of the alcohol is negligible. The reaction volume during the reaction is considered to be constant. Therefore, the following substitutions hold:

- $[A] = [A]_0 - [E]$: the alcohol concentration equals the initial concentration of alcohol minus the ester concentration formed.
- $[B] = [B]_0 - [E]$: the acid concentration equals the initial concentration of acid minus the ester concentration formed.
- $[W] = [E]$: the amount of water formed equals the amount of ester formed.

Implementing these substitutions in Eq. 3.2 gives

$$r_E = [\text{cat}](k_1([A]_0 - [E])([B]_0 - [E]) - k_{-1}[E]^2) \tag{3.3}$$

The temperature dependency of the rate constants can be simplified by the Arrhenius equation,

$$k = k^0 \exp\left(\frac{-E_a}{RT}\right) \tag{3.4}$$

in which $k^0$ is the pre-exponential factor, $E_a$ the activation energy, $R$ the gas constant and $T$ the temperature.

If the liquid phase non ideality is incorporated into the pseudohomogeneous model, Eq. 3.2 may be expressed in terms of activities:

$$r_E = [\text{cat}](k_1 a_A a_B - k_{-1} a_E a_W) \tag{3.5}$$

where $a_i$ are the activity coefficients of the corresponding components. Taking the liquid-phase nonideality into account is not sufficient to describe the heterogeneous kinetics. The interaction between the reactants and the solid catalyst, such as sorption effects, are neglected. To incorporate these effects, an adsorption-based model should be used. [7, 17]

Different authors reported [2, 7, 17, 20] that the esterification of acids by heterogeneous catalysts can be described by a Langmuir-Hinshelwood-Hougen-Watson (LHHW) model. The LLHW equation for a reversible esterification that is first order in all components is written as follows:

$$r_E = [\text{cat}]\left(\frac{k_1 K_A a_A K_B a_B - k_{-1} K_E a_E K_W a_W}{(1 + K_A a_A + K_B a_B + K_E a_E + K_W a_W)^2}\right) \tag{3.6}$$

in which the $K$ values are the adsorption equilibrium constants.

In the case of ion-exchange resins, water is preferably sorbed and therefore sorption effects can be summarised wit a singular sorption constant $K_{sorb}$ and the equation can be simplified to [7]:

$$r_E = [\text{cat}]\left(\frac{k_1 a_A a_B}{(K_{sorb} a_W)^2} - \frac{k_{-1} a_E}{K_{sorb} a_W}\right) \tag{3.7}$$

For other catalysts, adsorption experiments should be done to determine the adsorption of the different components.

Reactive Distillation simulation results based on the LHHW model are more accurate than those based on the pseudohomogeneous model. [7] However, the LHHW model is not easily included in AspenPlus RADFRAC. The pseudohomogeneous model on the other hand, is simple, the description of the kinetics is qualitatively good and can be easily implemented in AspenPlus RADFRAC. Therefore the use of the pseudohomogeneous model is preferred.

### 3.2.2 Experimental

#### Apparatus

The experiments are conducted in an autoclave from Büchi Glas Uster (eco-clave075) purchased at Autoclave. The autoclave has a thermostated steel vessel with a volume of 1 L. Inside the vessel, a turbine stirrer and baffle are present. The autoclave is mounted with a burette to add the alcohol. For the heterogeneous catalyst, a catalyst basket is mounted on the baffle rod. A picture of this catalyst basket can be found in Figure 3.1.

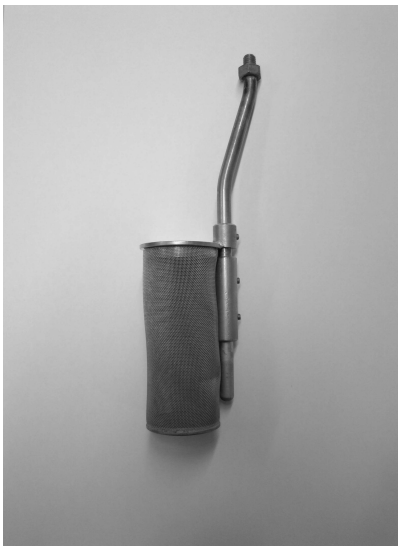

Figure 3.1: Catalyst basket

#### Materials and catalysts

Isopropanol (≥99.5%) from Acros and myristic acid (≥95%) from Sigma-Aldrich were used as the reactants. The Sulphated Zirconia (SZ) catalyst with a $SO_3$ loading of 6.5% was supplied by Norpro Saint-Gobain. Nafion

SAC13 with a capacity of 0.14 meq/g was supplied by BASF. Amberlyst 15( wet) with a capacity of 4.7 meq/g dry weight was purchased at Sigma-Aldrich. Dodecane (≥98%) and methyl ethyl ketone (≥99%), for the analysis, were obtained from Fluka.

### Analysis

All samples of the kinetic experiments were analysed by gas chromatography. The column is a Varian WCOT Fused Silica 50m x 0.32 mm column coated with CP-Sil 5CB. $H_2$ is used as carrier gas at a constant speed of 2 mL $min^{-1}$. The temperature program, 75°C for 5 min, than 40°C $min^{-1}$ to 225°C and maintain 225°C for another 11.25 min. Dodecane is used as an internal standard and methyl ethyl ketone as solvent.

### Procedure

Melted myristic acid is charged into the reactor. When the alcohol and the catalyst are added, the temperature will drop. Therefore the acid is heated above the designated temperature. The alcohol is added to the superheated acid using a burette. The temperature decreases till approximately five degrees below the desired temperature. The reaction mixture is heated, and in less than five minutes the desired temperature is reached. The reaction mixture is kept constant at the desired temperature, with a maximum deviation of 1K. Due to the applied temperature, the alcohol and water evaporate which causes the pressure to rise. There is no other gas present. In the experiments with a heterogeneous catalyst the basket in the reactor is filled with catalyst. After addition of the alcohol, the stirring is started. Because of the slow reaction, the reaction is continued for three days. The first day samples are taken every hour, the second and third day, every two hours. To determine the influence of the external mass transfer on the reaction rate, the stirrer speed was varied between 700 and 900 rpm in additional runs. No influence of the stirrer speed on the reaction rate was detected. Therefore, all further experiments were conducted at a stirrer speed of 900 rpm.

### 3.2.3 Results and Discussion

In Figure 3.2*a* the experimental results for the autocatalysis reaction and a reaction with 10 grams of Sulphated Zirconia catalyst at 130°C are shown. It can be seen that there is no significant difference between the two curves. Thus, the reaction rates for both reactions are comparable. The Sulphated Zirconia is not a successful catalyst. Also Nafion SAC13 and Amberlyst 15 were investigated. In Figure 3.2*b*, it can be seen that the activity of these catalysts was also not very high at the applied reaction conditions, the ester concentrations do not differ much from those at autocatalysis.

Yalçinyuva et al. [1] investigated the same reaction with Amberlyst 15 and a silica-based Degussa catalyst, which were reported to be successful in the esterification of carboxylic acids with short alkyl chains. [3, 18] However, in the esterification of myristic acid with isopropanol very low conversions (5-10% after 5 hours) were found. They explained this phenomenon by the diffusion problem of myristic acid into the pores of the catalyst. In Figure 3.2 it can be seen that comparable results are found in this research.

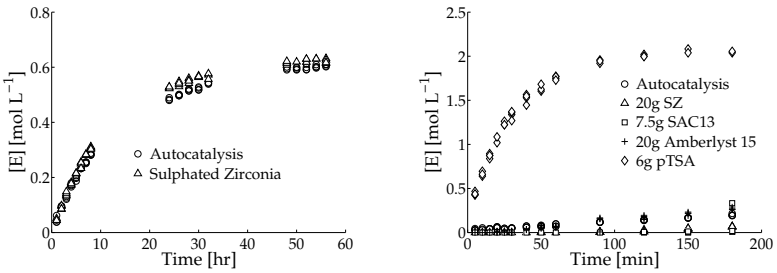


(a) (b)

Figure 3.2: Comparison of the reaction rate of the esterification of myristic acid with isopropanol for a) autocatalysis and 10 grams of Sulphated Zirconia catalyst at 130°C and a equimolar ratio of isopropanol to myristic acid and for b) autocatalysis, Sulphated Zirconia, Nafion SAC13, Amberlyst 15 and *p*TSA at 100°C and a equimolar ratio of isopropanol to myristic acid

From the above results it can be concluded that none of the investigated heterogeneous catalysts is suitable for the esterification of myristic acid and isopropanol at the desired conditions. Therefore the focus will be on a homogeneous catalyst: *p*-toluene sulphonic acid.

## 3.3 Homogeneously catalysed reaction

### 3.3.1 Theory

McCracken and Dickson [21] found that with a homogeneous catalyst the esterification of acetic acid with cyclohexanol is second order in acid and first order in alcohol. Vieville et al. [9] reported that the esterification of oleic acid with methanol is only first order in acid. However, the majority of the researchers report that an esterification reaction follows second order reversible kinetics (first order in all components). For example, Dhanuka et al. [16] showed that the esterification could be expressed by second order (first order in both reactants) reversible kinetics. The same approach was used by other researchers for fatty acid esterification reactions [1, 2, 4–6, 15].

When the most commonly reported first order kinetics in all components is assumed, the reaction rate ($r_E$)of the homogenous reaction can be described by

$$r_E = [\text{cat}](k_1[A][B] - k_{-1}[E][W]) \tag{3.8}$$

where [cat] is the catalyst concentration, $[E]$ the ester concentration, $[A]$ the alcohol concentration, $[B]$ the acid concentration, $[W]$ the water concentration, $k_1$ the rate constant of the forward reaction and $k_{-1}$ the rate constant of the backward reaction.

The reaction rate constants $k_1$ and $k_{-1}$ are assumed to be linearly dependent on the catalyst concentration. Various studies support this assumption [3, 8, 18, 19].

The liquid-phase nonideality can be taken into account by using activities instead of concentrations or mole fractions, resulting in a more consistent and

accurate description [7, 17]. However, the activity-based model is not easily included in AspenPlus RADFRAC. The concentration-based model on the other hand, is simple, the description of the kinetics is qualitatively good and can be easily implemented in AspenPlus RADFRAC. Therefore we have chosen to use the concentration-based model.

In the kinetic experiments performed in this research, no water and ester is present at the start of the reaction, only an initial concentration of alcohol $[A]_0$ and acid $[B]_0$ is present. The etherification of the alcohol is negligible. The reaction volume during the reaction is considered to be constant. Therefore, the following substitutions can be made based on the reaction stoichiometry:

- $[A] = [A]_0 - [E]$: the alcohol concentration equals the initial concentration of alcohol minus the ester concentration formed.

- $[B] = [B]_0 - [E]$: the acid concentration equals the initial concentration of acid minus the ester concentration formed.

- $[W] = [E]$: the amount of water formed equals the amount of ester formed.

Implementing these substitutions in Eq. 3.8 gives

$$\frac{d[E]}{dt} = [\text{cat}](k_1([A]_0 - [E])([B]_0 - [E]) - [\text{cat}]k_{-1}[E]^2 \tag{3.9}$$

The temperature dependency of the rate constants can be expressed by the Arrhenius equation [22]:

$$k = k^0 \exp\left(\frac{-E_a}{RT}\right) \tag{3.10}$$

in which $k^0$ is the pre-exponential factor, $E_a$ the activation energy, $R$ the gas constant and $T$ the temperature. Combining Eq. 3.9 and 3.10 gives

$$r_E = [\text{cat}]k_1^0 \exp\left(\frac{-E_{a,1}}{RT}\right)([A]_0 - [E])([B]_0 - [E]) - [\text{cat}]k_{-1}^0 \exp\left(\frac{-E_{a,-1}}{RT}\right)[E]^2 \tag{3.11}$$

This model contains four model parameters ($k_1^0$,$k_{-1}^0$,$E_{a,1}$ and $E_{a,-1}$), that can be estimated in Matlab using a nonlinear least squares algorithm, as discussed by Levenberg and Marquardt [23].

The equilibrium constant $K_{eq}$ gives information on the maximum conversion that can be reached when the reaction is performed in a closed vessel. $K_{eq}$ is given as:

$$K_{eq} = \frac{[E][W]}{[A][B]} \tag{3.12}$$

with the concentrations at equillibrium. At equillibrium the net rates are equal to zero:

$$\frac{d[E]}{dt} = k_1[A][B] - k_{-1}[E][W] = 0 \tag{3.13}$$

Combining Eq. 3.12 and 3.13 yields:

$$K_{eq} = \frac{[E][W]}{[A][B]} = \frac{k_1}{k_{-1}} \tag{3.14}$$

Yalçinyuva et al. [1] obtain the backward reaction rate constant by dividing the forward reaction rate constant by the equilibrium constant, which was determined experimentally. They reported that phase splitting occurs, resulting in inaccurate measured values of the equilibrium constant based on the overall composition, since phase splitting causes the overall composition to be different from the composition in the separate phase. Therefore, the backward reaction rate constant is obtained from the model, since this was considered to be a more reliable approach.

### 3.3.2 Experimental

#### Apparatus

The experiments are conducted in an autoclave from Büchi Glas Uster (eco-clave075) purchased at Autoclave. A picture of the set-up can be found in Figure 3.3. The autoclave has a thermostated steel vessel with a volume of 1 L. Inside the vessel, a turbine stirrer and baffle are present. The autoclave is mounted with a burette to add the alcohol.

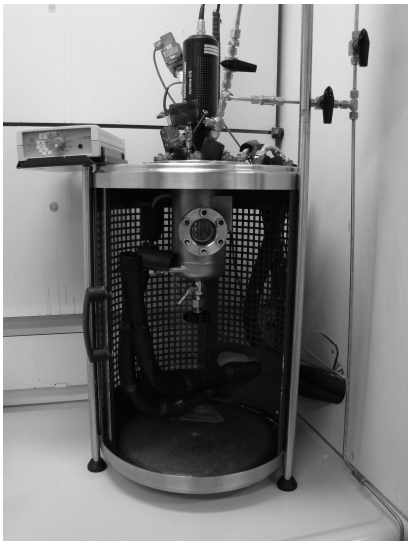

Figure 3.3: Experimental setup for measuring the reaction kinetics

#### Materials and catalysts

Isopropanol (≥99.5%) from Acros or *n*-propanol (≥99.5%) from Sigma-Aldrich and myristic acid (≥95%) from Sigma-Aldrich were used as the reactants. The *p*-toluene sulphonic acid (*p*TSA) catalyst was obtained as *p*-toluene sulphonic acid monohydrate (98.5%) from Aldrich. Dodecane (≥98%) and methyl ethyl

ketone (≥99%), for the analysis, were obtained from Fluka.

#### Analysis

All samples of the kinetic experiments were analysed by gas chromatography. The column is a Varian WCOT Fused Silica 50m x 0.32 mm column coated with CP-Sil 5CB. $H_2$ is used as carrier gas at a constant speed of 2 mL $min^{-1}$. The temperature program, 75°C for 5 min, than 40°C $min^{-1}$ to 225°C and maintain at 225°C for another 11.25 or 14.25 min for respectively the reaction with isopropanol or *n*-propanol. Dodecane is used as an internal standard and methyl ethyl ketone as solvent.

#### Procedure

Melted myristic acid is charged into the reactor. When the alcohol and the catalyst are added, the temperature will drop. Therefore the acid is heated above the designated temperature. The alcohol is added to the superheated acid using a burette. The temperature decreases till approximately five degrees below the desired temperature. The reaction mixture is heated, and in less than five minutes the desired temperature is reached, the reaction mixtures is kept constant at this temperature. Due to the applied temperature, the alcohol and water will evaporate which causes the pressure to rise. There is no other gas present. The *p*TSA is mixed with the alcohol. After addition of the alcohol, the stirring is started. Samples are taken at 5, 10, 15, 20, 25, 30, 40, 50, 60, 90, 120 and 180 minutes.

### 3.3.3 Results and discussion

#### Kinetic Model

During the experiments the temperature was varied between 75°C and 130°C, the catalyst amount used during the experiments was varied between 0.017 and 0.052 M *p*TSA and alcohol:myristic acid feed ratios were varied between 0.5 and 2. In the case of isopropanol, the concentration profiles of twelve of

these experiments were used to determine the unknown parameters from Eq. 3.11. The other three datasets were used to validate the model. In the case of *n*-propanol, the concentration profiles of all nine experiments were used to determine the unknown parameters. Table 3.2 and 3.3 contains the computed kinetic parameters.

| | | isopropanol | 95% confidence bounds |
|---|---|---|---|
| $k_1^0$ | $[\mathrm{L\,mol^{-1}s^{-1}}]$ | $3.33 \cdot 10^5$ | $2.85 \cdot 10^5$ |
| $k_{-1}$ | $[\mathrm{L\,mol^{-1}s^{-1}}]$ | $2.18 \cdot 10^3$ | $6.54 \cdot 10^3$ |
| $E_{a,1}$ | $[\mathrm{J\,mol^{-1}}]$ | $-58.9 \cdot 10^3$ | $2.64 \cdot 10^3$ |
| $E_{a,-1}$ | $[\mathrm{J\,mol^{-1}}]$ | $-45.9 \cdot 10^3$ | $9.40 \cdot 10^3$ |
| $R^2$ | | 0.9823 | |
| $R^2$ validation | | 0.9933 | |

Table 3.2: Kinetic parameters for the reaction with isopropanol

| | | *n*-propanol | 95% confidence bounds |
|---|---|---|---|
| $k_1^0$ | $[\mathrm{L\,mol^{-1}s^{-1}}]$ | $6.27 \cdot 10^4$ | $6.21 \cdot 10^4$ |
| $k_{-1}$ | $[\mathrm{L\,mol^{-1}s^{-1}}]$ | 8.44 | 17.38 |
| $E_{a,1}$ | $[\mathrm{J\,mol^{-1}}]$ | $-47.4 \cdot 10^3$ | $3.07 \cdot 10^3$ |
| $E_{a,-1}$ | $[\mathrm{J\,mol^{-1}}]$ | $-25.4 \cdot 10^3$ | $9.26 \cdot 10^3$ |
| $R^2$ | | 0.9288 | |

Table 3.3: Kinetic parameters for the reaction with *n*-propanol

The coefficient of determination ($R^2$) is the ratio of variance in the model and the variance in the data. A value close to unity means that the values predicted by the model equal the experimental values. The higher value for $R^2$ for the reaction with isopropanol means that the model for the reaction with isopropanol gives a better description of the experimental values than the model for the reaction with *n*-propanol. The actual rate constant $k$ at the corresponding reaction temperature is largely dependant of the activation energy. Therefore the values for $k^0$ cannot be compared with each other, since the activation energies for the forward and backward reaction are different.

In Figure 3.4 the ester concentrations calculated by the kinetic model and

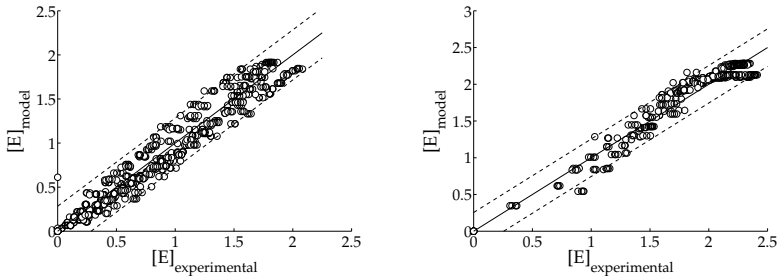


(a) (b)

Figure 3.4: Ester concentrations calculated by the kinetic model versus experimental values for a) isopropanol and b) *n*-propanol, (–) = model equal to experimental, (--)= deviation of twice the standard deviation

the experimental values are compared. The dashed lines from the error bounds are on the basis of twice the standard deviation. Statistically, in a normal distribution, 95% of the values will be in this area. As can be seen, almost all values are within these boundaries. This means, that the model is sufficiently accurate to describe the experimental reaction kinetics.

Yalçinyuva et al. [1] performed a kinetic study of the esterification of myristic acid with isopropanol using *p*-toluene sulphonic acid at a temperature range of 60-80°C. In Figure 3.5*a* the conversions calculated by the kinetic model are compared to the experimental values of Yalçinyuva et al. [1]. The dashed lines from the error bounds are on the basis of twice the standard deviation. As can be seen, all values are within these boundaries.

In Figure 3.5*b* the forward reaction rate constants ($k_1$) and the backward reaction rate constants ($k_{-1}$) for the kinetic model and the experimental data of Yalçinyuva et al. [1] are compared. For the forward reaction rate constant there is a good correspondence between the model and literature values. For the backward reaction rate constant, one point shows a strong deviation, the rest of the point are show a good correspondence between the model and literature values. Yalçinyuva et al. [1] obtain the backward reaction rate

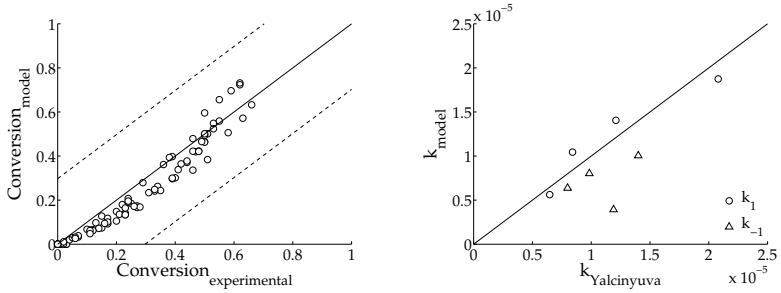


(a) (b)

Figure 3.5: a) Conversions and b) reaction rate constants calculated by the kinetic model versus experimental values of Yalçinyuva(–) = model equal to experimental, (--)= deviation of twice the standard deviation

constant by dividing the forward reaction rate constant by the equilibrium constant, which was determined experimentally. They reported that phase splitting occurs, therefore there will be a discrepancy between the experimental equilibrium constants and those calculated via the kinetic model as discussed previously.

Aafaqi et al. [2] studied the esterification of palmitic acid with isopropanol using *p*-toluene sulphonic acid as catalyst at a temperature range of 373-443K. In Figure 3.6 the calculated ester concentration profiles of the esterification of myristic acid and palmitic acid (reaction kinetics from Aafaqi et al. [2]) with isopropanol are compared for a reaction temperature of 393K and a catalyst concentration of 0.029 M. It can be seen that the difference between both curves is small. The esterification of palmitic acid is slightly faster, despite the longer carbon chain. El-Kinawy et al. [6] showed for the esterification of propionic, butyric, lauric, myristic and stearic acid with isobutanol that there is no unambiguous relationship between the esterification rate constant and the acid chain length.

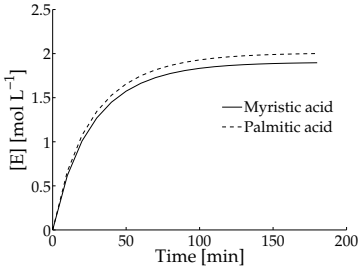


Figure 3.6: Ester concentration of the esterification reactions of myristic acid and palmitic acid with isopropanol with [cat]=0.029 M, at a temperature of 393K and an acid to alcohol feed ratio equal to unity

### Effect of reaction temperature

Figure 3.7 shows the experimental results and the model for different temperatures. It should be remarked that the model prediction shown in the figure are those for the single parameter set fitted to all experiments, in case the model

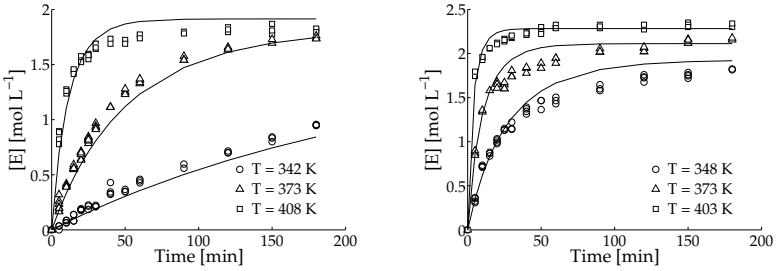


(a) (b)

Figure 3.7: Effect of reaction temperature on the esterification reaction of myristic acid with a) isopropanol ([cat]=0.036 M) and b) *n*-propanol ([cat]=0.032 M), at a myristic acid to alcohol feed ratio equal to unity

would have been fitted to only the experimental results shown in the figure, it could have matched the experiments more closely. However, the parameters obtained in this case, would have had a smaller range of conditions for which they would be valid. It can be seen that the model corresponds quite well with the experimental results, especially in the initial phase of the experiments. At longer times, the deviations become larger, the occurrence of a phase separation may be a possible explanation for these deviations [1]. The reaction rate increases with increasing temperature, also the equilibrium conversion increases with increasing reaction temperature. At a higher temperature more collisions and more successful collisions occur. These successful collisions have sufficient energy to break the bonds, form products and thus result in higher values of myristic acid conversion. [19]

### Effect of catalyst loading

The amount of catalyst influences the reaction rate, because more $H^+$-ions become available when the amount of catalyst in the mixture increases. Figure 3.8 shows a plot of the initial reaction rate ($r_{E,0}$) for both the experimental results and the model, for different catalyst concentrations. It can be seen that the model corresponds quite well with the experimental results. As expected,

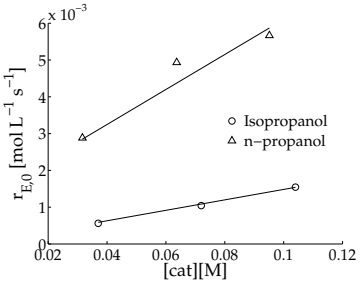


Figure 3.8: Effect of catalyst loading on the initial reaction rate for the esterification of myristic acid with isopropanol $n$-propanol, at a temperature of 373K and a myristic acid to alcohol feed ratio equal to unity

the initial reaction rate increases with increased amounts of catalyst.

### Effect of myristic acid to alcohol feed ratio

In Figure 3.9 the experimental results and the model of the esterification reactions are given for different myristic acid to alcohol feed ratios. For both reactions it can be seen that the model corresponds quite well with the experimental results.

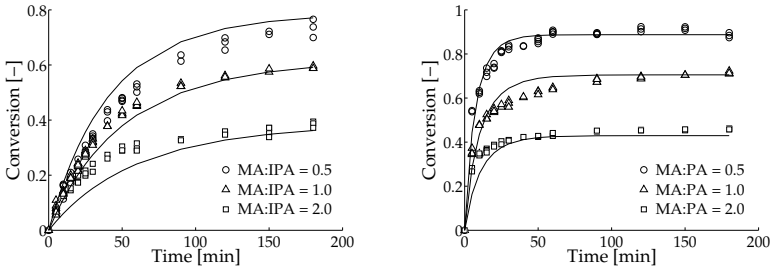


(a) (b)

Figure 3.9: Effect of myristic acid to alcohol feed ratio on the esterification reaction of myristic acid with a) isopropanol and b) $n$-propanol at a temperature of 373K

Figure 3.9 shows that the reaction rate and equilibrium conversion increases with a decreasing myristic acid to alcohol feed ratio. At a ratio of 2, the conversion is significantly lower: due to the lower alcohol concentration the reaction equilibrium is shifted towards the reactant side. At a ratio of 0.5, more myristic acid reacts because of the excess of alcohol. Yalçinyuva et al. [1] also reported a increasing conversion with a decreasing myristic acid to alcohol feed ratio.

### Isopropanol versus *n*-propanol

In Figure 3.10 the experimental results and the model are given for the esterification with isopropanol (T = 373K, [cat] = 0.070 M) and *n*-propanol (T = 373K, [cat] = 0.064 M). It can be seen that the reaction with *n*-propanol is indeed much faster than the reaction with isopropanol. The initial slope of the *n*-propanol curve is about 3.8 times steeper than of the isopropanol curve. The equilibrium concentrations are of the same order, thus the maximum conversions are approximately the same.

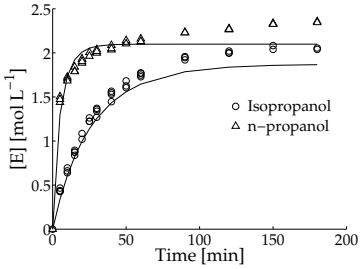


Figure 3.10: Comparison of the reaction rate between the esterification of myristic acid and isopropanol ([cat] = 0.070 M) and with *n*-propanol ([cat] = 0.064 M), at a reaction temperature of 373K and a myristic acid to alcohol feed ratio equal to unity

### Equilibrium constant

Using Eq. 3.10 and 3.14 together with the computed kinetic parameters, the equilibrium constant can be calculated. For the reaction with isopropanol this is

$$K_{eq} = \frac{k_1}{k_{-1}} = \frac{k_1^0 \exp(\frac{-E_{a,1}}{RT})}{k_{-1}^0 \exp(\frac{-E_{a-1}}{RT})} = 152.29 \exp\left(\frac{-12.93 \cdot 10^3}{RT}\right) \tag{3.15}$$

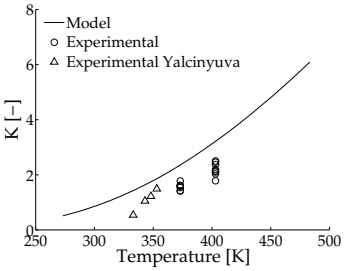


Figure 3.11: Experimentally determined and calculated equilibrium constants

Figure 3.11 shows the equilibrium constant calculated from the model as described above, experimental values and experimental values of Yalçinyuva et al. [1]. It can be seen that the experimental data are slightly below the model prediction. This is likely caused by phase splitting. At higher conversions, the water formed during the esterification reaction causes a multiphase reaction medium. A correct measurement of the sample will then be difficult. However, the experimental values and the experimental values of Yalçinyuva et al. [1] both show the same trend as the model prediction.

### 3.3.4 Phase separation

The phenomenon of phase separation reported by Yalçinyuva et al. [1] may be a possible explanation for the deviation of the model regarding to experimental data, at higher conversions. The used kinetic model describes a pseudohomogeneous reaction, therefore it applies only to a single liquid phase. When two phases are present, the model can no longer be applied.

The phase separation is caused by the immiscibility of water and myristic acid and water and isopropyl myristate. Maeda et al. [24] reported liquid-liquid immiscibility data on the ethanol-water-myristic acid system at a range of 318.2-323.2K. Using isopropanol instead of ethanol will give comparable results. Because myristic acid is more polar than isopropyl myristate, the

system with isopropyl myristic instead myristic acid will give a slightly larger immiscibility region. Assuming ethanol and isopropanol and myristic acid and isopropyl myristate give the same results regarding to immiscibility, two liquid phases are present according to the ternary diagram of Maeda et al. [24] at conversions higher than 50%, when a equimolar feedratio of isopropanol to myristic acid is used. Therefore, below 50% conversion, definitely only one liquid phase will exist and the kinetic model will be valid. After this, a transition region is reached in where phase splitting may or may not occur, depending of the reaction conditions like feed ratio and temperature. The validity of the kinetic model at these higher conversions is uncertain.

## 3.4 Conclusion

A study on the reaction kinetics of the esterification of myristic acid and isopropanol has been done, using *p*TSA and SZ as catalyst.

The reaction catalysed with the heterogeneous SZ catalyst had the same reaction rate as the uncatalysed reaction. SZ is not a suitable catalyst for the esterification of myristic acid with isopropanol.

The resulting reaction rate for the esterification of myristic acid and isopropanol using *p*TSA is

$$\begin{aligned} r_E = {} & [\text{cat}]3.33 \cdot 10^5 \exp\left(\frac{-58.9 \cdot 10^3}{RT}\right)[A][B] \\ & - [\text{cat}]2.18 \cdot 10^3 \exp\left(\frac{-45.9 \cdot 10^3}{RT}\right)[E][W] \ \text{mol}\,\text{L}^{-1}\text{s}^{-1} \end{aligned} \tag{3.16}$$

The resulting reaction rate for the esterification of myristic acid and *n*-propanol using *p*TSA is

$$r_E = [\text{cat}]6.27 \cdot 10^4 \exp\left(\frac{-47.4 \cdot 10^3}{RT}\right)[A][B] - [\text{cat}]8.44 \exp\left(\frac{-25.4 \cdot 10^3}{RT}\right)[E][W] \text{ mol L}^{-1}\text{s}^{-1} \quad (3.17)$$

The reaction rate as well as the equilibrium conversion increase with increasing reaction temperature. As expected, the initial reaction rate increases with increasing amount of catalyst, but the equilibrium conversion is not influenced by the catalyst. The reaction rate and equilibrium conversion increases with a decreasing myristic acid to alcohol feed ratio. The reaction with *n*-propanol is considerably faster than the reaction with isopropanol. This is due to less steric hindrance of a secondary alcohol compared to a tertiary alcohol.

# Nomenclature

| | |
|---|---|
| $[A]$ | Fatty acid concentration [mol $L^{-1}$] |
| $[B]$ | Alcohol concentration [mol $L^{-1}$] |
| [cat] | Catalyst concentration [M] |
| $[E]$ | Ester concentration [mol $L^{-1}$] |
| $[W]$ | Water concentration [mol $L^{-1}$] |
| $a$ | Activity [-] |
| $E_a$ | Activation energy [J $mol^{-1}$] |
| $K_{eq}$ | Equilibrium constant [-] |
| $K$ | Adsorption equilibrium constant [L $mol^{-1}$] |
| $k$ | Rate constant [L $mol^{-1}$ $s^{-1}$] |
| $R$ | Gas constant [J $mol^{-1}$ $K^{-1}$] |
| $r_{E,0}$ | Initial reaction rate [mol $L^{-1}$ $s^{-1}$] |

$r_E$ Reaction rate [mol $L^{-1}$ $s^{-1}$]
$T$ Temperature [K]

# References

[1] Yalçinyuva, T.; Deligöz, H.; Boz, I.; Gürkaynak, M. *Int. J. Chem. Kinet.* **2008,** *40,* 136-144.

[2] Aafaqi, R.; Mohamed, A.; Bhatia, S. *J. Chem. Technol. Biotechnol.* **2004,** *79,* 1127-1134.

[3] Altiokka, M.; Çitak, A. *Applied Catalysis A: General* **2003,** *239,* 141-148.

[4] Unnithan, U.; Tiwari, K. *Indian Journal of Technology* **1987,** *25,* 477-479.

[5] Goto, S.; Tagawa, T.; Yusoff, A. *Int. J. Chem. Kin.* **1991,** *23,* 17-26.

[6] El-Kinawy, O.; Megahed, O.; Zaher, F. *Modelling, Measurement and Control C* **2002,** *63,* 27-38.

[7] Steinigeweg, S.; Gmehling, J. *Ind. Eng. Chem. Res.* **2003,** *42,* 3612-3619.

[8] Othmer, D.; Rao, S. *Ind. Eng. Chem.* **1950,** *42,* 1912-1919.

[9] Vieville, C.; Mouloungui, Z.; Gaset, A. *Ind. Eng. Chem. Res.* **1993,** *32,* 2065-2068.

[10] Lacaze-Dufaure, C.; Mouloungui, Z. *Applied Catalysis A: General* **2000,** *204,* 223-227.

[11] Pouilloux, Y.; Abro, S.; Vanhove, C.; Barrault, J. *J. Mol. Catal. A: Chem.* **1999,** *149,* 243-254.

[12] Kiss, A.; Dimian, A.; Rothenberg, G. *Adv. Synth. Catal.* **2006,** *348,* 75-81.

[13] Kiss, A.; Omota, F.; Dimian, A.; Rothenberg, G. *Topics in Catalysis* **2006,** *40,* 141-150.

[14] Nijhuis, T.; Beers, A.; Kapteijn, F.; Moulijn, J. *Chem. Eng Sc.* **2002,** *57,* 1627-1632.

[15] Bart, H.; Reideschläger, J.; Schatka, K.; Lehmann, A. *Ind. Eng. Chem. Res.* **1994,** *33,* 21-25.

[16] Dhanuka, V.; Malshe, V.; Chandalia, S. *Chem. Eng Sc.* **1977,** *32,* 551-556.

[17] Pöpken, T. *Ind. Eng. Chem. Res.* **2000,** *39,* 2601-2611.

[18] Yadav, G.; Mehta, P. H. *Ind. Eng. Chem. Res.* **1994,** *33,* 2198-2208.

[19] Ali, S.; Tarakmah, A.; Merchant, S.; Al-Sahhaf, T. *Chem. Eng. Sc.* **2007,** *62,* 3197-3217.

[20] Song, W.; Venimadhavan, G.; Manning, J.; Malone, M.; Doherty, M. *Ind. Eng. Chem. Res.* **1998,** *37,* 1917-1928.

[21] McCracken, D.; Dickson, P. *Ind. Engng. Chem. Proc. Des. Develop.* **1967,** *6,* 286-293.

[22] Atkins, P. *Physical Chemistry;* Oxford University Press: Fifth ed.; 1994.

[23] Marquardt, D. *J. Soc. Indust. Appl. Math.* **1963,** *11,* 431-441.

[24] Maeda, K.; Yamada, S.; Hirota, S. *Fluid Phase Equilibria* **1997,** *130,* 281-294.

# Chapter 4

# Feasibility analysis

*In this chapter the gains that can be obtained using Entrainer-based Reactive Distillation with regard to conventional Reactive Distillation are discussed. Five process configurations for the esterification of myristic acid with isopropanol and n-propanol using a homogeneous catalyst, are compared, by simulation in Aspen Plus. In the esterification with isopropanol at 1 bar, the addition of the entrainer has no positive influence on the conversion, because the amount needed for water removal causes a temperature decrease in the column. This temperature decrease has a negative influence on the conversion, because the high activation energy of the reaction cannot be overcome. However, in the esterification with isopropanol at 5 and 10 bar and in the esterification with n-propanol (either 1, 5 or 10 bar), the addition of the entrainer has a positive influence on the conversion. More entrainer leads to a higher conversion. Surprising is the observation that the conventional Reactive Distillation configuration (RD1) reaches the desired purity and conversion. Because of its polarity, water is pressed out of the liquid phase, in which the reaction takes place, so the reaction can reach nearly complete conversion. Because the decrease of the reaction volume due to the addition of the entrainer is rather small and the energy consumption are comparable, conventional Reactive Distillation (RD1) is the preferable configuration for the esterification of myristic*

*acid with either isopropanol or n-propanol.*

## 4.1 Introduction

The conceptual feasibility of Entrainer-based Reactive Distillation for the synthesis of fatty acid esters is already shown by Dimian et al. [1] and Wang and Wong [2]. This chapter will therefore focus on the gains that can be obtained by applying Entrainer-based Reactive Distillation with regard to conventional Reactive Distillation. The objective of this feasibility analysis is to compare several possible process configurations from conventional Reactive Distillation to Entrainer-based Reactive Distillation for the synthesis of fatty acid esters:

- Conventional Reactive Distillation (one column)
- Conventional Reactive Distillation (two columns)
- Conventional plus azeotropic Reactive Distillation (two columns)
- Entrainer-based Reactive Distillation (one column)
- Entrainer-based Reactive Distillation (two columns)

In this chapter first the theory of modelling Reactive Distillation processes is discussed. After the description of the process conditions and the process configurations, which will be investigated, a comparison between the five configurations will be made.

The comparison is done on the basis of process models constructed in Aspen Plus for the esterification of myristic acid with isopropanol using *p*-toluene sulphonic acid (*p*TSA) as homogeneous catalyst, because it has a better catalytic performance than sulphuric acid. [3–5]. The models contain the required conditions (i.e. capacity, conversion and purity), derived from industrial preferences, to produce fatty acid esters. Because the reaction with isopropanol is rather slow, also the esterification with *n*-propanol and an operating pressure

of 5 and 10 bar is investigated. For both alcohols and each operating pressure, the processes are evaluated on their ability to meet the requirements by comparing column size and energy consumption.

## 4.2 Modelling Reactive Distillation

A Reactive Distillation process model consists of sub-models for mass transfer, reaction kinetics and hydrodynamics. The completion of these sub-models can vary from simple to complex. [6] The different approaches are depicted schematically in Figure 4.1. Mass transfer between the vapour and liquid phase can be described by the equilibrium stage model in which physical equilibrium between both phases is assumed, or by a rigourous rate-base approach with the Maxwell-Stefan diffusion equations. In homogeneous catalysed and autocatalysed Reactive Distillation, transport and reaction take place in a two-phase system with an interface. The reaction can take place in the bulk liquid and in the film phase. For slow reactions it is sufficient to only account for the reaction in the bulk phase. For heterogeneous systems it is necessary to also

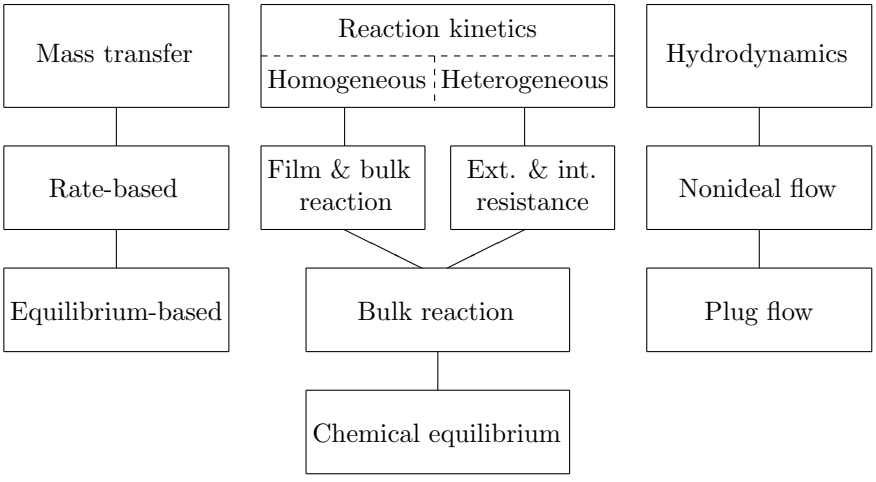


Figure 4.1: Modelling approaches for Reactive Distillation

include the phenomena insise the solid catalyst particles. However, the system can be considered as pseudo-homogeneous, when all internal and external mass transfer resistances are lumped. If the reaction is sufficiently fast, both systems can be described by the chemical equilibrium. As for the hydrodynamics, the system can be described as an ideal plug flow, or correlations concerning axial dispersion, liquid hold-up and pressure drop can be included into the model. [6]

**Phase equilibrium versus chemical equilibrium**

In the extreme, the equilibrium behaviour of a Reactive Distillation process is either controlled by chemical equilibrium or phase equilibrium. In general it will be in between those two extremes. To quantify this variation the Damköhler number can be used. [7, 8]

$$Da = \frac{H_0 k_1}{V} \tag{4.1}$$

where $H_0$ is the liquid hold-up, $k_1$ is a pseudo-first-order rate constant and $V$ is the vapour rate. The Damköhler number is the ratio of a characteristic liquid residence time to the characteristic reaction time. For low values of $Da$ ($Da < 0.5$) the reaction rate is slow compared to the residence time and the system is dominated by phase equilibrium. For large values of $Da$ ($Da > 10$) the reaction rate is fast and chemical equilibrium is approached on the reactive stages. [7] However, Bock and Wozny [9] showed that the assumption of chemical equilibrium is inappropriate for many Reactive Distillation processes. If the Damköhler number lies between these values neither phase equilibrium nor chemical equilibrium is controlling and a rate-based model must be used [7]. For the system used in this research $Da \approx 0.02$. This is much smaller than 0.5 and the system can be assumed to be dominated by phase equilibrium.

In this chapter the simplest possible model for all three parts (mass transfer, reaction kinetics and hydrodynamics) is used. For comparing the different configurations, such models are adequate. As explained above, the mass transfer can be described by physical equilibrium. Chemical equilibrium is not

reached, therefore the reaction will be described by a kinetic model of the bulk reaction. The hydrodynamics are considered to be ideal (plug flow).

### 4.2.1 Equilibrium stage model

In the equilibrium stage model the vapour and liquid streams leaving the stage are assumed to be in equilibrium with each other. The model is formed by the MESH equations. MESH is an acronym referring to the different types of equations. The M equations are the material balance equations; the total material balance (Eq. 4.2) and the component material balance (Eq. 4.3):

$$\frac{dU_j}{dt} = V_{j+1} + L_{j-1} + F_j - (1+r_j^V)V_j - (1+r_j^L)L_j + \sum_{m=1}^{r}\sum_{i=1}^{c}\nu_{i,m}R_{m,j}\epsilon_j \quad (4.2)$$

$$\begin{aligned}\frac{dU_j x_{i,j}}{dt} &= V_{j+1}y_{i,j+1} + L_{j-1}x_{i,j-1} + F_j z_{i,j} - (1+r_j^V)V_j y_{i,j} - (1+r_j^L)L_j x_{i,j} \\ &\quad + \sum_{m=1}^{r}\nu_{i,m}R_{m,j}\epsilon_j \end{aligned} \quad (4.3)$$

in which $U_j$ is de hold-up at stage j. Generally $U_j$ is considered to be the hold-up of only the liquid phase. $r_j$ are the ratios of side stream flows to interstage flows. $\nu_{i,m}$ represents the stoichiometric coefficient of component $i$ in reaction $m$ and $\epsilon_j$ represents the reaction volume.

$$r_j^V = S_j^V/V_j; \qquad r_j^L = S_j^L/L_j; \quad (4.4)$$

The E equations are the phase equilibrium relations

$$y_{i,j} = K_{i,j}x_{i,j} \quad (4.5)$$

The S equations are the summation equations:

$$\sum_{i=1}^{c} x_{i,j} = 1; \qquad \sum_{i=1}^{c} y_{i,j} = 1; \tag{4.6}$$

The H equations are the heat balance equations

$$\begin{aligned} \frac{dU_j H_j}{dt} &= V_{j+1}H_{j+1}^V + L_{j-1}H_{j-1}^L + F_j H_j^F - (1 + r_j^V)V_j H_j^V \\ &\quad -(1 + r_j^L)L_j H_j^L - Q_j \end{aligned} \tag{4.7}$$

where the superscripted $H$'s are the enthalpies of the appropriate phase. Because the enthalpies are referred to their elemental states. the heat of reaction is accounted for automatically. Under steady-state conditions, all the time derivatives in the above equations are equal to zero. [8, 10]

The equilibrium stage model can be modelled in Aspen Plus using a inside-out algorithm known as RADFRAC. Inside-out methods involve the introduction of new parameters, e.g. physical parameters, into the model equations (Eq. 4.2 - 4.7) to be used as primary interaction variables. The complex physical properties are approximated by simple models at the outer loop, while the inner loop solves the model equations simultaneously by Newton's method using analytical derivatives. [8, 11]

## 4.3 Modelling

### 4.3.1 Process conditions and requirements

In the reactive section of the Entrainer-based Reactive Distillation column, the esterification reaction of myristic acid (A) with an alcohol (B), isopropanol or *n*-propanol, takes place, forming a fatty acid ester (E) and water (W):

$$\mathrm{A} + \mathrm{B} \overset{\text{catalyst}}{\rightleftharpoons} \mathrm{E} + \mathrm{W} \tag{4.8}$$

All the configurations are designed, in Aspen Plus using RADFRAC, such that a 99.0% conversion of myristic acid and a 99.9% product purity, requirements which makes the process attractive for the industry, is obtained. The input parameters of the feed streams are based on a production of 1000 kg/hr (3697 mol/hr) ester, which is representative for an industrial process [12] and 99% conversion of the myristic acid. The ratio of myristic acid:alcohol is fixed at 1:1 because it is an equimolar reaction. The operating pressure is 1 bar, which was also used by Dimian et al. [1] and Wang and Wong [2]. To investigated the effect of pressure, which causes higher temperatures in the column, the conventional Reactive Distillation (RD1) and the Entrainer-based Reactive Distillation (ERD1) configuration are also evaluated at 5 and 10 bar. Cyclohexane and isopropyl acetate are used as entrainer, these follow from the entrainer selection in Chapter 2.

The kinetics of the reactions are experimentally determined and are described in Chapter 3. The reaction rate for the esterification of myristic acid and isopropanol using $p$TSA is

$$\begin{aligned} r_E \;=\; & 3.33 \cdot 10^5 [\text{cat}] \exp\left(\frac{-58.9 \cdot 10^3}{RT}\right)[A][B] \\ & - 2.18 \cdot 10^3 [\text{cat}] \exp\left(\frac{-45.9 \cdot 10^3}{RT}\right)[E][W] \ \text{mol}\,\text{L}^{-1}\text{s}^{-1} \end{aligned} \tag{4.9}$$

For the esterification with $n$-propanol using $p$TSA this is

$$\begin{aligned} r_E \;=\; & 6.27 \cdot 10^4 [\text{cat}] \exp\left(\frac{-47.40 \cdot 10^3}{RT}\right)[A][B] \\ & - 8.44 [\text{cat}] \exp\left(\frac{-25.38 \cdot 10^3}{RT}\right)[E][W] \ \text{mol}\,\text{L}^{-1}\text{s}^{-1} \end{aligned} \tag{4.10}$$

$r_E$ is the reaction rate, $[E]$ the concentration ester, $[A]$ the concentration alcohol, $[B]$ the concentration acid, $[W]$ the concentration water and [cat] is

the catalyst concentration. In order to establish significant conversions, the chosen catalyst concentration is 0.15 M, which is ten times larger then found in literature [12] for Reactive Distillation for the esterification of fatty acids.

Typical liquid hold-up values derived from Reactive Distillation structured packing, like Katapak-S are 0.06-0.18 $m^3m^{-3}$ [13]. For non-reactive structured packing like Sulzer BX this is 0.02-0.12 $m^3m^{-3}$ [14]. For random packing this is 0.05-0.2 $m^3m^{-3}$ [15]. For tray columns, the liquid hold-up can be calculated from equations determined by Zuiderweg [16]. In Chapter 6 the hold-up calculations will be discussed more in detail. The liquid hold-up strongly depends on the densities and therefore on the operating pressure. Using standard tray geometry parameters given by Sinnott [17] liquid loads of 0.05-0.40 $m^3m^{-3}$ are obtained for pressures of 5-15 bar. Every internal has his own HETP (Height Equivalent to the Theoretical Plate). In Table 4.1 this internal specific HETP [17–19]and the corresponding liquid hold-up volumes for a columndiameter of 0.5m, which is a common diameter for the capacity used in this chapter, are given for the different internals.

| Internals | HETP [m] | Hold-up [L] |
|---|---|---|
| Reactive structured packing | ∼0.5 | 6-18 |
| Non-reactive structured packing | ∼0.2 | 0.8-5 |
| Random packing | 0.4-1 | 4-39 |
| Trays | 0.5 | 5-39 |

Table 4.1: Typical liquid hold-ups for a columndiameter of 0.5 m and different internals

For the simulations in this chapter a liquid hold-up of 10 L per stage is used, this is an average value resulting from Table 4.1.

Because the reaction with isopropanol is very slow at atmospheric pressure, a large hold-up is required to obtain 99% conversion. For comparison the number of stages is set to 500 and the hold-up per stage is varied to obtain the required conversions and purity. In this case the liquid hold-up of 10 L per stage will be exceeded.

### 4.3.2 Thermodynamics

For the simulations in Aspen Plus a property model has to be selected. Parameters based on vapour-liquid equilibrium data do not provide good predictions for the liquid-liquid equilibria and vice versa. [20] Therefore a combination is used: NRTL parameters based on vapour-liquid equilibrium data are used for the interaction between isopropanol and water and isopropanol and cyclohexane, and NRTL parameters based on liquid-liquid equilibrium data will be used for the interaction between water and cyclohexane. In Chapter 2 vapour-liquid equilibrium data and liquid-liquid equilibrium data from literature for water-isopropanol-cyclohexane [21] and water-isopropanol-isopropyl acetate [22, 23] are compared to different property models in Aspen Plus. In the case of *n*-propanol, only liquid-liquid equilibrium data is available for the water-propanol-cyclohexane system [24].

The set of NRTL parameters developed by Aspen Tech based on data from the Dortmund Data Bank, was found to correspond the best with the experimental vapour-liquid equilibria literature data, which is described in Chapter 2 , and is therefore used further. The binary coefficients used in the simulations can be found in Table 4.2.

The liquid-liquid equilibrium data do not correspond well. The decanter should be simulated with a separate set of NRTL parameters obtained from liquid-liquid equilibrium data. Because insufficient experimental data is available, it is decided to use the current NRTL parameters. As result, the amount of entrainer predicted by simulation is somewhat overestimated.

For the reactive section, the same property model is used. The unknown interaction parameters are estimated using UNIFAC, these are all parameters concerning the myristic acid or the ester. UNIFAC predicts an azeotrope between myristic acid and isopropyl myristate. It is unlikely that this will occur, because the components have similar polarities. Therefore it was decided to set the interaction between those components to zero, to approximate reality.

Propyl myristate is not present in the Aspen Plus database and because it is not a commercial product no data is available. Its boiling point was estimated

| Component i | Water | Water | Isopropanol | Water |
|---|---|---|---|---|
| Component j | Isopropanol | Cyclohexane | Cyclohexane | Isopropyl acetate |
| Source | VLE-IG | LLE-ASPEN | VLE-IG | LLE-ASPEN |
| aij | 6.8284 | 13.1428 | 0 | 26.9 |
| aji | -1.3115 | -10.4585 | 0 | -1.4234 |
| bij | -1483.46 | -1066.98 | 105.7733 | -6530.3008 |
| bji | 426.3978 | 4954.897 | 689.9346 | 618.5185 |
| cij | 0.3 | 0.2 | 0.3 | 0.2 |
| | | | | |
| Component i | Isopropanol | Water | Cyclohexane | *n*-propanol |
| Component j | Isopropyl acetate | *n*-propanol | *n*-propanol | Isopropyl acetate |
| Source | VLE-IG | VLE-IG | VLE-IG | R-PCES |
| aij | 0 | 5.4486 | 6.8277 | 0 |
| aji | 0 | -1.7411 | -4.1888 | 0 |
| bij | 110.5442 | -861.179 | -1548.27 | 191.351326 |
| bji | 100.1164 | 576.4458 | 1490.146 | 157.849157 |
| cij | 0.3 | 0.3 | 0.3 | 0.3 |

Table 4.2: The binary coefficients of the NRTL model used in the simulations

by estimating the difference in boiling point between isopropyl myristate and myristate using the Joback method [25]. Because the difference in boiling point is negligible (0.44K), isopropyl myristate is used in the simulations to represent being propyl myristate

### 4.3.3 Process descriptions

Five possible process configurations based on Reactive Distillation for the synthesis of fatty acid esters are compared to evaluate what can be gained using the Entrainer-based Reactive Distillation process:

- the conventional Reactive Distillation configuration (RD1) is the most basic Reactive Distillation concept.
- the conventional Reactive Distillation with water/alcohol separation configuration (RD2) is a process already discussed by Bock et al. [26].
- the conventional Reactive Distillation combined with azeotropic Reactive Distillation (RD3) is a logic step between RD1 and ERD1
- the Entrainer-based Reactive Distillation configuration (ERD1) is the process of interest in this research.
- the Entrainer-based Reactive Distillation with distillative entrainer/alcohol separation(ERD2), that enables alcohol recycling to the optimal position along the ERD column, is a variant on the ERD1.

#### Conventional Reactive Distillation (RD1)

In conventional Reactive Distillation only one column is present in which the reaction takes place. The myristic acid is fed at the top of the column and the alcohol at the bottom. Between those feed points the reaction takes place. The (iso)propyl myristate is collected at the bottom and the unreacted myristic acid and alcohol will come out at the top together with the formed water. The reflux has a high water content because no water removal takes place. Therefore it is expected that a conversion of 99% cannot be obtained.

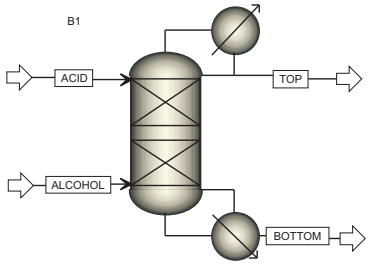


Figure 4.2: Process scheme for conventional Reactive Distillation

### Conventional Reactive Distillation with water/alcohol separation (RD2)

In this configuration the conventional Reactive Distillation column is taken but the top vapour is condensed and fed into a second column. In this column pure water is drawn off and an azeotropic mixture of water and alcohol is recycled back to the Reactive Distillation column.

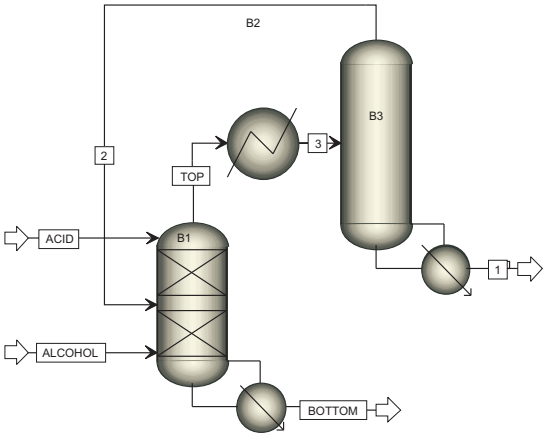


Figure 4.3: Process scheme for conventional Reactive Distillation with water/alcohol separation

### Conventional Reactive Distillation combined with Azeotropic Distillation (RD3)

In this configuration the conventional Reactive Distillation is combined with azeotropic distillation in the second column. An entrainer is fed to obtain pure alcohol at the bottom and a water/entrainer mixture at the top. The entrainer is chosen such that it forms an immiscibility region with water and the mixture can be separated by decantation. The entrainer phase can be recycled back into the column and the alcohol stream is recycled back to the Reactive Distillation column.

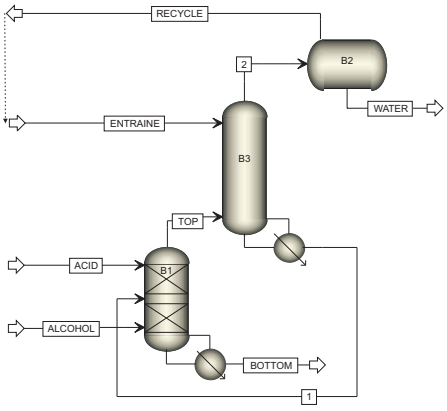


Figure 4.4: Process scheme for conventional Reactive Distillation combined with azeotropic distillation

### Entrainer-based Reactive Distillation (ERD1)

The Entrainer-based Reactive Distillation column consists of a reactive section with a distillation section placed on top, in which the entrainer is responsible for removing the water from the reactive section. The top vapour, which consists of entrainer, water and alcohol, is condensed and two phases are obtained through decantation: an aqueous phase and an entrainer rich phase which is refluxed back to the column.

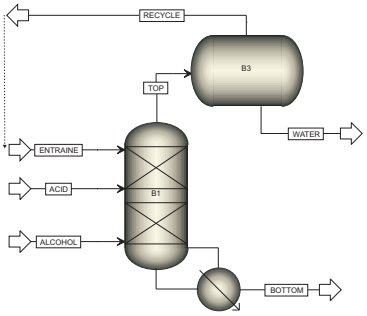


Figure 4.5: Process scheme for Entrainer-based Reactive Distillation

### Entrainer-based Reactive Distillation with entrainer/alcohol separation (ERD2)

In this configuration the Entrainer-based Reactive Distillation configuration is taken and the entrainer rich stream is separated in an additional column into a pure entrainer stream and an alcohol stream, which both are recycled back to the Entrainer-based Reactive Distillation column.

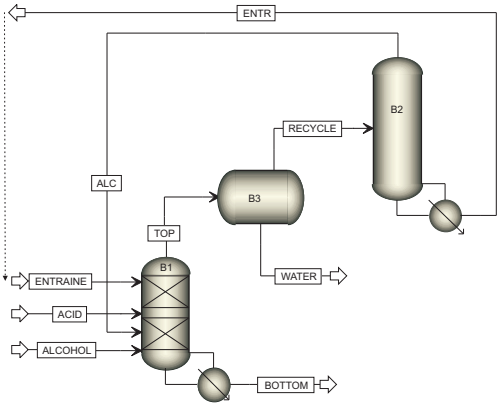


Figure 4.6: Process scheme for Entrainer-based Reactive Distillation with entrainer/alcohol separation

## 4.4 Results and discussion

### 4.4.1 Esterification with isopropanol at 1 bar

In Table 4.3 and 4.4 the obtained conversion, product purity and the required design and operating parameters for all five configurations are summarised for the esterification of myristic acid with isopropanol. Table 4.3 gives the results for the configuration without entrainer (RD1 and RD2), and the results for cyclohexane as entrainer in the configurations with entrainer (RD3, ERD1 and ERD2). Table 4.4 gives the results for isopropyl acetate as entrainer in the

| | RD1 | RD2 | RD3 | ERD1 | ERD2 |
|---|---|---|---|---|---|
| Conversion [%] | 99.0 | 99.2 | 99.0 | 99.1 | 99.1 |
| Product purity [%] | 99.0 | 99.2 | 99.0 | 99.1 | 99.1 |
| *Reactive column* | | | | | |
| Number of reactive stages | 499 | 499 | 499 | 499 | 499 |
| Hold-up reactive stages [l] | 18 | 17 | 18 | 17 | 17 |
| Feed stage recycle | - | 84 | 2 | - | 32 |
| Purification stages bottom | 1 | 0 | 0 | 0 | 0 |
| Distillation stages top | 1 | 1 | 1 | 1 | 1 |
| Condensor/decanter duty [kW] | 48 | 49 | 47 | 47 | 46 |
| Reboiler duty [kW] | 145 | 141 | 144 | 141 | 141 |
| Boilup ratio [-] | 1 | 1 | 1 | 1 | 1 |
| Reflux ratio [-] | 0.1 | - | - | - | - |
| *Distillation column* | | | | | |
| Stages distillation column | - | 2 | 2 | - | 3 |
| Reboiler duty [kW] | - | 5 | 4 | - | 0.1 |
| Boilup ratio [-] | - | 0.1 | 12 | - | 0.1 |
| | | | | | |
| Entrainer amount [mol/hr] | - | - | 100 | 100 | 100 |
| Total energy [kW] | 193 | 195 | 195 | 188 | 187 |
| Water purity [%] | 99.0 | 99.1 | 99.0 | 99.1 | 99.1 |

Table 4.3: Results for the feasibility analysis of different configurations for the esterification with isopropanol and cyclohexane as entrainer

| | RD3 | ERD1 | ERD2 |
|---|---|---|---|
| Conversion [%] | 99.0 | 99.1 | 99.1 |
| Product purity [%] | 99.0 | 99.1 | 99.1 |
| *Reactive column* | | | |
| Number of reactive stages | 499 | 499 | 499 |
| Hold-up reactive stages [l] | 18 | 17 | 17 |
| Feed stage recycle | 1 | - | 46 |
| Purification stages bottom | 0 | 0 | 0 |
| Distillation stages top | 1 | 1 | 1 |
| Condensor/decanter duty [kW] | 47 | 47 | 47 |
| Reboiler duty [kW] | 145 | 141 | 141 |
| Boilup ratio [-] | 1 | 1 | 1 |
| *Distillation column* | | | |
| Stages distillation column | 2 | - | 2 |
| Reboiler duty [kW] | 4 | - | 0.2 |
| Boilup ratio [-] | 10 | - | 0.2 |
| | | | |
| Entrainer amount [mol/hr] | 100 | 100 | 100 |
| Total energy [kW] | 196 | 188 | 187 |
| Water purity [%] | 99.0 | 98.8 | 99.0 |

Table 4.4: Results for the feasibility analysis of different configurations for the esterification with isopropanol and isopropyl acetate as entrainer

configurations with entrainer (RD3, ERD1 and ERD2). The concentration profiles can be found in Appendix 4.A.1.

Surprisingly, the conventional Reactive Distillation configuration (RD1) reaches the desired purity and conversion. It was expected that equilibrium would occur, because no water is removed, thus the backward reaction takes place as well. However, the formed water is only present in very small quantities in the liquid phase at the bottom stages, where most of the reaction takes place. The largest amount of water is present in the upper stages of the column (see Figure 4.7). Water is the most polar component in the col-

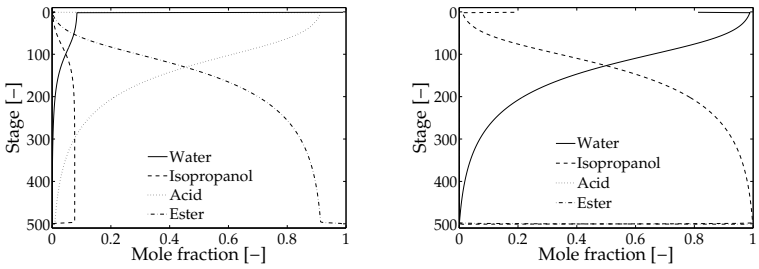


Figure 4.7: Concentration profiles of (a) liquid phase and (b) vapour phase, for the RD1 configuration for the esterification with isopropanol at 1 bar

umn; which means that the other components dissolve better in each other compared to water. The water is therefore pushed out of the liquid phase, in which the reaction takes place and the reaction can reach nearly complete conversion. Apparently, a form of reactive stripping takes place in which the water is stripped from the liquid phase by the alcohol vapour stream, due to the relatively high activity of water in the fatty acid-fatty acid ester mixture. This is supported by the activity coefficient of water, which is increased to a value of approximately five, while the activity coefficient of isopropanol is approximately two and those of the acid and the ester are around one.

When conventional Reactive Distillation is combined with a water/alcohol

separation (RD2) the excess of water above the azeotropic composition of the binary alcohol-water azeotrope is drawn off in the second column. The azeotrope is recycled back to the reactive column. In Table 4.3 it can be seen that the reaction volume and energy consumption, needed to achieve the desired conversion, are comparable to those in the conventional Reactive Distillation (RD1). However, an additional column to perform the separation is required.

The three configurations in which an entrainer is added (RD3, ERD1 and ERD2) all yield similar results. Compared with the configurations without entrainer (RD1 and RD2) the energy consumption is somewhat lower (see Table 4.3 and 4.4). However, addition of the entrainer has no positive influence on the conversion. To reach a 99% conversion, the entrainer amount should be as low as possible. This effect is caused by a combined effect of temperature on thermodynamics and kinetics.

The temperature in a distillation column is determined by the boiling points of the components, their azeotropes and their concentrations, which are determined by the reaction kinetics. One of the components with the lowest boiling point in the column is the entrainer. Therefore the amount of entrainer needed for water removal causes a decrease of the temperature in the column. This temperature decrease has a negative influence on the conversion because the high activation energy of the reaction cannot be overcome. In Figure 4.8 it can be seen that with increasing entrainer amount, the column temperature and conversion decreases.

As expected, in all configurations the required column size to obtain the desired conversion is not realistic. With the number of theoretical stages per metre (NTSM) of two and 500 stages, the columns are 250 metre high. Furthermore, also the common value of common liquid hold-up is exceeded. Therefore it is concluded that, under the used operating conditions neither of these configurations is preferable. But with application of higher pressure, the column size can be reduced. This will be investigated in Section 4.4.3.

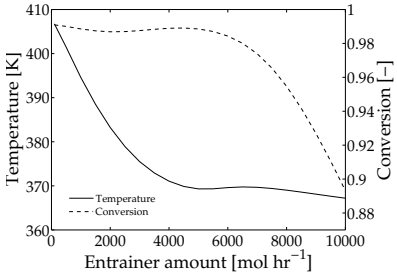


Figure 4.8: Influence of the entrainer amount on the column temperature and the conversion in the Entrainer-based Reactive Distillation for isopropanol at 1 bar

### 4.4.2 Esterification with *n*-propanol at 1 bar

Because the slow reaction with isopropanol requires very large Reactive Distillation columns to obtain the required conversion, also the esterification of myristic acid with *n*-propanol is investigated. Since the reaction is much faster, the size of the reactive section is expected to be significantly smaller than for isopropanol.

In Table 4.5 and 4.6 the obtained conversion, product purity and the required design and operating parameters for all five configurations are summarised for the esterification of myristic acid with *n*-propanol. Table 4.5 gives the results for the configuration without entrainer (RD1 and RD2), and the results for cyclohexane as entrainer in the configurations with entrainer (RD3, ERD1 and ERD2). Table 4.6 gives the results for isopropyl acetate as entrainer in the configurations with entrainer (RD3, ERD1 and ERD2). The concentration profiles can be found in Appendix 4.A.2.

From the number of reactive stages in Table 4.5 and 4.6, it can be immediately seen that they are, for all five configurations, significantly lower than in the esterification with isopropanol, where 499 reactive stages were needed. Also the liquid hold-up of 10 litre per stage can be maintained.

| | RD1 | RD2 | RD3 | ERD1 | ERD2 |
|---|---|---|---|---|---|
| Conversion [%] | 99.0 | 99.0 | 99.0 | 99.0 | 99.0 |
| Product purity [%] | 99.0 | 99.1 | 99.0 | 99.0 | 99.0 |
| *Reactive column* | | | | | |
| Number of reactive stages | 60 | 77 | 52 | 32 | 32 |
| Hold-up reactive stages [l] | 10 | 10 | 10 | 10 | 10 |
| Feed stage recycle | - | 10 | 2 | - | 1 |
| Purification stages bottom | 0 | 0 | 0 | 1 | 2 |
| Distillation stages top | 0 | 1 | 1 | 1 | 1 |
| Condensor/decanter duty [kW] | 111 | 91 | 180 | 196 | 198 |
| Reboiler duty [kW] | 190 | 126 | 207 | 269 | 266 |
| Boilup ratio [-] | 1 | 1 | 1 | 1 | 1 |
| Reflux ratio [-] | 1.6 | - | - | - | - |
| *Distillation column* | | | | | |
| Stages distillation column | - | 2 | 3 | - | 2 |
| Reboiler duty [kW] | - | 44 | 48 | - | 15 |
| Boilup ratio [-] | - | 1 | 0.6 | - | 0.1 |
| | | | | | |
| Entrainer amount [mol/hr] | - | - | 14500 | 14800 | 14600 |
| Total energy [kW] | 301 | 261 | 444 | 465 | 479 |
| Water purity [%] | 99.0 | 98.9 | 95.3 | 93.3 | 92.8 |

Table 4.5: Results for the feasibility analysis for different configurations for the esterification with *n*-propanol and cyclohexane as entrainer

| | RD3 | ERD1 | ERD2 |
|---|---|---|---|
| Conversion [%] | 99.0 | 99.0 | 99.0 |
| Product purity [%] | 99.0 | 99.0 | 99.0 |
| | | | |
| *Reactive column* | | | |
| Number of reactive stages | 46 | 38 | 37 |
| Hold-up reactive stages [l] | 10 | 10 | 10 |
| Feed stage recycle | 2 | - | 2 |
| Purification stages bottom | 2 | 0 | 0 |
| Distillation stages top | 1 | 1 | 1 |
| Condensor/decanter duty [kW] | 243 | 180 | 725 |
| Reboiler duty [kW] | 231 | 254 | 251 |
| Boilup ratio [-] | 1 | 1 | 1 |
| *Distillation column* | | | |
| Stages distillation column | 3 | - | 6 |
| Reboiler duty [kW] | 87 | - | 568 |
| Boilup ratio [-] | 0.1 | - | 5 |
| | | | |
| Entrainer amount [mol/hr] | 18900 | 12800 | 12200 |
| Total energy [kW] | 571 | 434 | 1544 |
| Water purity [%] | 98.8 | 98.2 | 97.9 |

Table 4.6: Results for the feasibility analysis of different configurations for the esterification with *n*-propanol and isopropyl acetate as entrainer

As shown in the results of the esterification with isopropanol, in the esterification with *n*-propanol the desired purity and conversion can also be reached in conventional Reactive Distillation (RD1).

When the conventional Reactive Distillation is combined with a water/alcohol separation (RD2), the excess of water above the azeotropic composition of the binary alcohol-water azeotrope is drawn off in the second column. The azeotrope is recycled back into the reactive column.

Reviewing the concentration profiles of the liquid and vapour phase, which can be found in Figure 4.9 it can be seen that the alcohol and the water are mainly present in the vapour phase. This is due to the relatively high

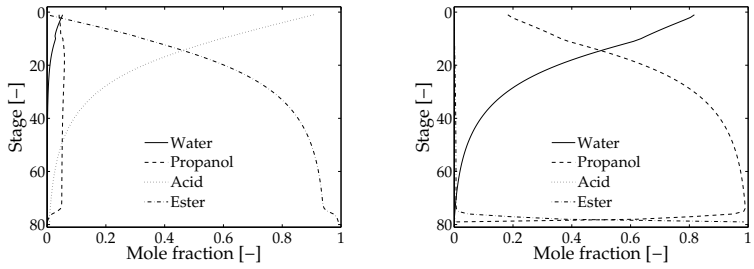


Figure 4.9: Concentration profiles of (a) liquid phase and (b) vapour phase, for the RD2 configuration for the esterification with *n*-propanol at 1 bar

temperature in the column and explains why more stages are required then in conventional Reactive Distillation (RD1). However, the additional alcohol water separation unit does not lead to any improvement of the reactive column, but it does lead to a significant decrease of the energy consumption.

In all configurations where an entrainer is added (RD3, ERD1 and ERD2) the entrainer has a positive effect on the conversion, in contrast with what was found for the esterification with isopropanol. In Figure 4.10 the influence of the entrainer amount on the temperature and conversion is shown for the Entrainer-based Reaction Distillation configuration (ERD1). More entrainer leads to a higher conversion, which results in a smaller reactive section. Comparing Table 4.5 and 4.6 with Table 4.3 and 4.4 it can be seen that in the esterification with *n*-propanol the energy consumption is much higher than in the esterification with isopropanol. This is caused by the higher entrainer amounts.

When the conventional Reactive Distillation was combined with azeotropic distillation (RD3) it appeared from the simulations that a pure alcohol recycle could only be obtained if the top stream of the reactive column has a low water content which means a low conversion. The azeotropic distillation imposes a constraint on the conversion in the reactive column. However, a conversion of

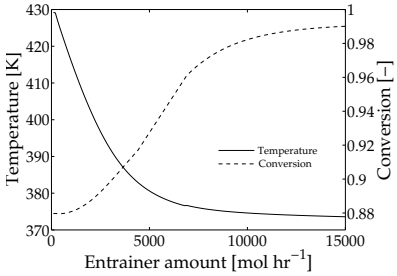


Figure 4.10: Influence of the entrainer amount on the column temperature and the conversion in the Entrainer-based Reactive Distillation for *n*-propanol at 1 bar

99.0% is possible in this configuration. The entrainer ends up in the bottom stream of the second column and enters therefore the reactive column. Strictly speaking this is no longer azeotropic distillation but also a form of Entrainer-based Reactive Distillation.

The Entrainer-based Reactive Distillation with entrainer/alcohol separation (ERD2) shows no additional advantages over Entrainer-based Reactive Distillation (ERD1). The number of stages is more or less the same, and the energy consumption is higher. Also, the number of equipment units increased, and the water purity decreased. The results show a large difference in the energy consumption between the two entrainer. In the case of isopropyl acetate the energy consumption increases due to the separation of the alcohol and entrainer in the second column. In the case of cyclohexane, the separation in the second column hardly takes place. Because of the cyclohexane-*n*-propanol azeotrope more pure cyclohexane cannot be obtained in this column.

In the case of cyclohexane, the required entrainer amount is for all three configurations more or less the same. In the case of isopropyl acetate it seems that the conventional Reactive Distillation combined with azeotropic distillation (RD3) configuration needs significant more entrainer than the other two configurations. However, the amount of pure entrainer entering the reactive

column from the recycle of the separation column is comparable to the required entrainer amount for the other two configurations.

As expected, the cyclohexane is more effective in removing the water than isopropyl acetate. This is illustrated by the 'sharper' column profiles, as shown in Figure 4.11. However, in the Entrainer based Reactive Distillation configurations (ERD1 and ERD2), slightly more cyclohexane than isopropyl acetate is needed to achieve the same conversion. his caused by the size of the hetero-

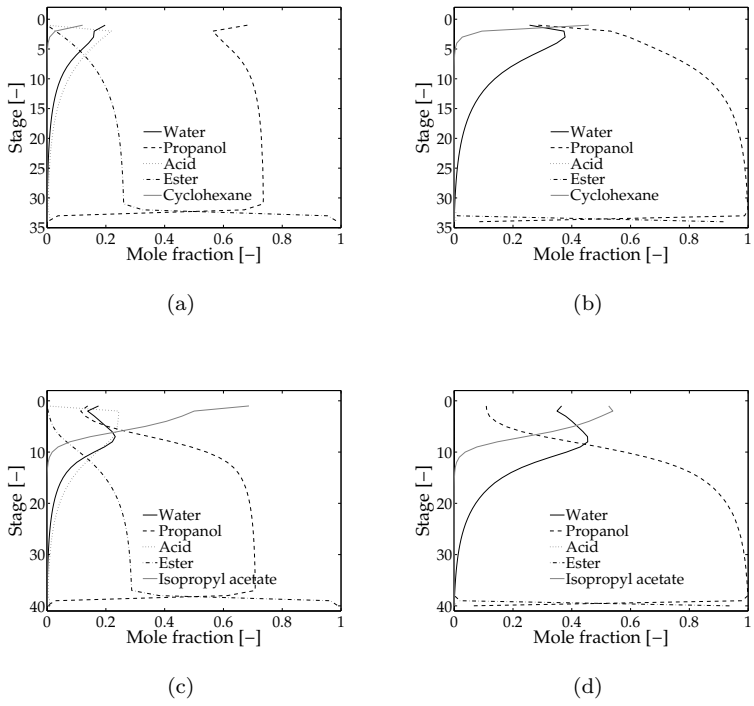


Figure 4.11: Concentration profiles of (a) liquid phase and (b) vapour phase with cyclohexane as entrainer and (c) liquid phase and (d) vapour phase with isopropyl acetate as entrainer, for the ERD1 configuration for the esterification with *n*-propanol at 1 bar

geneous region. The column profile inside the top distillation section has to remain into the homogeneous region. More cyclohexane than isopropyl acetate is needed to achieve this.

Due to the higher boiling temperature of isopropyl acetate, more energy is required to fully separate the entrainer from the other components (water and alcohol). Therefore the energy consumption is higher for isopropyl acetate than for cyclohexane.

Reviewing the results of the configurations and the different entrainers, the concepts are technically feasible. Looking at equipment requirements only, like column size and number of column, the most appropriate option should result in an Entrainer-based Reactive Distillation (ERD1) configuration using cyclohexane as entrainer. This configuration has the smallest required number of reactive stages. However, the energy requirements are higher than the configurations without entrainer. An economic evalution should point out which configuration is the optimal one. The results show that conventional Reactive Distillation (RD1) can also be used to achieve the desired conversion and purity.

### 4.4.3 Esterification with isopropanol and with *n*-propanol at 5 and 10 bar

At an operating pressure of 1 bar, the required column size for a conversion of 99% is too large to realise for the esterification of myristic acid with isopropanol. Besides, the amount of entrainer needed for the water removal causes a decrease of the temperature in the column, which has in the esterification of myristic acid with isopropanol an negative influence on the conversion. By increasing the pressure also temperatures will increase. Therefore, the conventional Reactive Distillation (RD1) and the Entrainer-based Reactive Distillation (ERD1) configuration are also investigated at 5 and 10 bar with cyclohexane as entrainer. In Table 4.7 and 4.8 the obtained conversion, product purity, the required design and operating parameters are summarised for both esterifications at a pressure of respectively 5 and 10 bar. The concentra-

tion profiles can be found in Appendix 4.A.3and 4.A.4.

| | isopropanol | | *n*-propanol | |
|---|---|---|---|---|
| | RD1 | ERD1 | RD1 | ERD1 |
| Conversion [%] | 99.0 | 99.0 | 99.1 | 99.0 |
| Product purity [%] | 99.1 | 98.3 | 99.1 | 99.0 |
| *Reactive column* | | | | |
| Number of reactive stages | 94 | 94 | 16 | 16 |
| Hold-up reactive stages [l] | 10 | 10 | 10 | 10 |
| Purification stages bottom | 1 | 1 | 1 | 1 |
| Distillation stages top | 1 | 1 | 1 | 1 |
| Condensor/decanter duty [kW] | 45 | 46 | 45 | 78 |
| Reboiler duty [kW] | 223 | 225 | 191 | 241 |
| Boilup ratio [-] | 1 | 1 | 1 | 1 |
| Reflux ratio [-] | 0.1 | - | 0.1 | - |
| | | | | |
| Entrainer amount [mol/hr] | - | 800 | - | 4800 |
| Total energy [kW] | 268 | 271 | 196 | 319 |
| Water purity [%] | 99.0 | 99.0 | 99.0 | 99.4 |

Table 4.7: Results for the feasibility analysis for different configurations for the esterification with isopropanol and with *n*-propanol and cyclohexane as entrainer at 5 bar

As shown in the results of the esterifications at 1 bar, the desired purity and conversion also can be reached in conventional Reactive Distillation (RD1). The required column size for the esterification with isopropanol now also becomes realistic. Due to the higher pressure, the column temperature is higher and the reaction rate faster.

In the esterification with isopropanol, the addition of the entrainer has now, in contrast with the simulation at one bar, a positive influence on the conversion: fewer reactive stages are needed compared to conventional Reactive Distillation (RD1) at 10 bar. At 5 bar, the the effect is too small to result in a decrease of the reaction volume. Due to the higher pressure, the column temperature is higher and the combined effect of reaction kinetics and thermodynamics, as seen in the simulations at one bar, does not take place. This can

| | isopropanol | | *n*-propanol | |
|---|---|---|---|---|
| | RD1 | ERD1 | RD1 | ERD1 |
| Conversion [%] | 99.1 | 99.0 | 99.1 | 99.1 |
| Product purity [%] | 99.1 | 98.0 | 99.1 | 99.1 |
| *Reactive column* | | | | |
| Number of reactive stages | 36 | 32 | 10 | 10 |
| Hold-up reactive stages [l] | 10 | 10 | 10 | 10 |
| Purification stages bottom | 1 | 1 | 1 | 1 |
| Distillation stages top | 1 | 1 | 1 | 1 |
| Condensor/decanter duty [kW] | 43 | 62 | 43 | 50 |
| Reboiler duty [kW] | 241 | 260 | 216 | 213 |
| Boilup ratio [-] | 1 | 1 | 1 | 1 |
| Reflux ratio [-] | 0.1 | - | 0.1 | - |
| | | | | |
| Entrainer amount [mol/hr] | - | 3100 | - | 100 |
| Total energy [kW] | 284 | 322 | 259 | 263 |
| Water purity [%] | 99.0 | 99.4 | 99.0 | 99.2 |

Table 4.8: Results for the feasibility analysis for different configurations for the esterification with isopropanol and with *n*-propanol and cyclohexane as entrainer at 10 bar

be seen in Figure 4.12. It is noticed that with increasing amount of entrainer the conversion increases till a maximum is reached at 1600 mol $hr^{-1}$ entrainer at 5 bar. In the esterification with *n*-propanol, the required entrainer amount is much lower compared to the required amount at 1 bar, which results in a much lower energy consumption.

Looking at equipment requirements alone, the most appropriate option should result in an Entrainer-based Reactive Distillation (ERD1) configuration. However, the results show that conventional Reactive Distillation (RD1) can also be used to achieve the desired conversion and purity. Because the decrease of the reaction volume due to the addition of the entrainer is rather small and the energy consumption increases when using an entrainer, conventional Reactive Distillation (RD1) remains a interesting alternative, especially because the risk of contamination of the product by adding an extra compo-

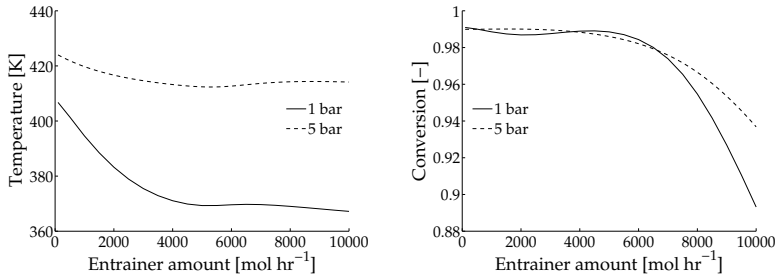


(a) (b)

Figure 4.12: Influence of the entrainer amount on a) the column temperature and b) the conversion in the Entrainer-based Reactive Distillation for the esterification with isopropanol at 5 bar

nent is eliminated.

To research the influence of the required conversion on the decrease of reaction volume by Entrainer-based Reactive Distillation, the conventional Reactive Distillation (RD1) and the Entrainer-based Reactive Distillation (ERD1) configuration are also investigated at 5 bar with for a required conversion of 90% and 99.9%. In Table 4.9 the corresponding decrease in reaction volume is given.

| | Decrease in reaction volume | |
|---|---|---|
| Conversion | Isopropanol | *n*-propanol |
| 90.0% | 0% [1] | 0%[1] |
| 99.0% | 0% | 0% |
| 99.9% | 1.9% | 14.3% |

Table 4.9: Influence of the required conversion on the decrease in reaction volume in the Entrainer-based Reactive Distillation compared to conventional Reactive Distillation for the esterification with isopropanol and *n*-propanol at 5 bar

[1]Entrainer does not have a positive influence on the conversion

For a conversion of 90.0% the entrainer does not have a positive influence on the conversion. At a conversion of 99%, which was already mentioned previously, the entrainer does have a positive influence on the conversion. However this effect is too small to result in a decrease of the reaction volume. At a conversion of 99.9% it results in a limited decrease of the reaction volume. At lower conversions less water will be produced and the amount of unreacted isopropanol is larger. Thus, the ratio of water to isopropanol becomes smaller which makes it more difficult to remove the water.

## 4.5 Conclusions

Five process configurations from conventional Reactive Distillation to Entrainer-based Reactive Distillation for the synthesis of fatty acid esters were compared by simulations with process models made in Aspen Plus for the esterification of myristic acid.

In the esterification with isopropanol at 1 bar, the addition of the entrainer has, against expectations, no positive influence on the conversion. To reach 99% conversion, the entrainer amount must be as low as possible. This effect is caused by a combined effect of thermodynamics and kinetics. The amount of entrainer needed for water removal causes a decrease of the temperature in the column. This temperature decrease has a negative influence on the conversion, because the high activation energy of the reaction cannot be overcome. However, in the esterification with isopropanol at 5 and 10 bar and in the esterification with *n*-propanol (either 1, 5 or 10 bar), the addition of the entrainer has a positive influence on the conversion. More entrainer leads to a higher conversion.

Conventional Reactive Distillation configuration (RD1) also reaches the desired purity and conversion. Because of its polarity, water is pressed out of the liquid phase, wherein the reaction takes place, so the reaction can reach nearly complete conversion.

Looking at equipment requirements alone, the most appropriate option should result in an Entrainer-based Reactive Distillation (ERD1) configura-

tion, on the condition that suitable operating conditions are applied. However, the decrease of the reaction volume due to the addition of the entrainer is rather small and the energy requirements are comparable. Therefore, conventional Reactive Distillation (RD1) remains an interesting alternative, especially because the risk of contamination of the product by adding an extra component is eliminated.

# Nomenclature

| | |
|---|---|
| $[A]$ | Fatty acid concentration [mol $L^{-1}$] |
| $[B]$ | Alcohol concentration [mol $L^{-1}$] |
| [cat] | Catalyst concentration [M] |
| $[E]$ | Ester concentration [mol $L^{-1}$] |
| $[W]$ | Water concentration [mol $L^{-1}$] |
| $Da$ | Damköhler number [-] |
| $\epsilon$ | Reaction volume [$m^3$] |
| $F$ | Feed stream [mol $s^{-1}$] |
| $H_0$ | Liquid hold-up [mol] |
| $H$ | Molar enthalpy [J $mol^{-1}$] |
| $K$ | Vapour-liquid equilibrium constant [-] |
| $k_1$ | Pseudo-first-order rate constant [$s^{-1}$] |
| $L$ | Liquid flowrate [mol $s^{-1}$] |
| $\nu$ | Stoichiometric coefficient [-] |
| $Q$ | Heat duty [J $s^{-1}$] |
| $R$ | Gas constant [J $mol^{-1}$ $K^{-1}$] |
| $R_{m,j}$ | Reaction rate [$mol^{-3}s^{-1}$] |
| $r_E$ | Reaction rate [mol $L^{-1}$ $s^{-1}$] |
| $r_j$ | Ratio of side stream flow to interstage flow on stage $j$ [-] |
| $S$ | Side draw-off [mol $s^{-1}$] |

$T$ Temperature [K]
$t$ Time [s]
$U$ Molar hold-up [mol]
$V$ Vapour rate [mol $s^{-1}$]
$x$ Mole fraction in the liquid phase [-]
$y$ Mole fraction in the vapour phase [-]
$z$ Mole fraction in either vapour or liquid phase [-]

### Subscripts

$i$ Component index
$j$ Stage index
$m$ Reaction index

### Superscripts

$F$ Referring to feed stream
$L$ Referring to liquid phase
$V$ Referring to vapour phase

## References

[1] Dimian, A. C.; Omota, F.; Bliek, A. *Chem. Eng. Process.* **2004,** *43,* 411-420.

[2] Wang, S.; Wong, D. *Ind. Eng. Chem. Res.* **2006,** *45,* 9042-9049.

[3] Aafaqi, R.; Mohamed, A.; Bhatia, S. *J. Chem. Technol. Biotechnol.* **2004,** *79,* 1127-1134.

[4] Yalçinyuva, T.; Deligöz, H.; Boz, I.; Gürkaynak, M. *Int. J. Chem. Kinet.* **2008,** *40,* 136-144.

[5] Unnithan, U.; Tiwari, K. *Indian Journal of Technology* **1987,** *25,* 477-479.

[6] Noeres, C.; Kenig, E.; Górak, A. *Chem. Eng. Process.* **2003,** *42,* 157-178.

[7] Towler, G. P.; Frey, S. J. Reactive distillation. In *Reactive Separation Process*; Kulprathipanja, S., Ed.; Taylor & Francis: 2002.

[8] Taylor, R.; Krishna, R. *Chem. Eng. Sc.* **2000,** *55,* 5183-5229.

[9] Bock, H.; Jimoh, M.; Wozny, G. *Chem. Eng. Technol.* **1997,** *20,* 182-191.

[10] Taylor, R.; Kooijman, H.; Klamt, A.; Eckert, F. Distillation simulation with cosmo-rs. In *Proceedings of the Distillation and Absorption Conference*; Baden-Baden, 2002.

[11] Venkataraman, S.; Chan, W.; Boston, J. *Chem. Eng. Prog.* **1990,** 45-54.

[12] Zhou, M. *Modelisation de reacteurs d'esterification fonctionnement semi-continu et continu,* Thesis, L'institut national polytechnique de Toulouse, 1983.

[13] Moritz, P. *Scale-up der Reaktivdestillation mit Sulzer Katapak-S,* Thesis, Universität Stuttgart, 2002.

[14] Brunazzi, E.; Paglianti, A. *AIChE Journal* **1997,** *43,* 317-327.

[15] Stichlmair, J. G.; Fair, J. R. *Distillation principles and practice;* Wiley-VCH: New York, 1998.

[16] Zuiderweg, F. *Chem. Eng Sc.* **1982,** *37,* 1441-1464.

[17] Sinnott, R. *Chemical Engineering Design;* volume 6 of *Coulson & Richardson's Chemical Engineering* Butterworth Heinemann: Oxford, Third ed.; 1999.

[18] Götze, L.; Bailer, O.; Moritz, P.; Scala, C. v. *Catalysis Today* **2001,** *69,* 201-208.

[19] Sulzer Chemtech, *Structured Packings, for Distillation, Absorption and Reactive Distillation 22.13.06.20-I.05-30* .

[20] Rarey, J. *Ind. Eng. Chem.* **2005,** 7600-7608.

[21] Verhoeye, L. *J. Chem. Eng. Data* **1968,** *13,* 462-467.

[22] Teodorescu, M.; Aim, K.; Wichterle, I. *J. Chem. Eng. Data* **2001,** *46,* 261-266.

[23] Hong, G.; Lee, M.; Lin, H. *Fluid Phase Equilibria* **2002,** *202,* 239-252.

[24] Sørensen, J.; Arlt, W. *Liquid-Liquid Equilibrium Data Collection 2;* Dechema: 1980.

[25] Poling, B.; Prausnitz, J.; O'Conell, J. *The Properties of Gases and Liquids;* McGraw Hill: Fifth ed.; 2007.

[26] Bock, H.; Wozny, G.; Gutsche, B. *Chem. Eng. Process.* **1997,** *36,* 101-109.

# Appendix 4.A Concentration profiles

## 4.A.1 Esterification with isopropanol at 1 bar

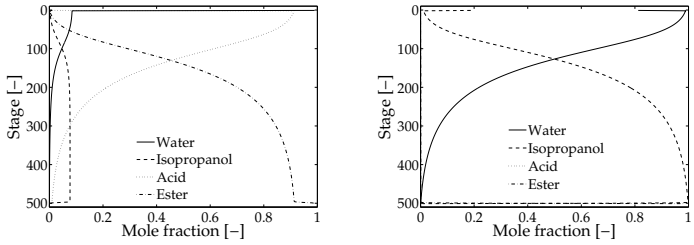


(a) (b)

Figure 4.13: Concentration profiles of (a) liquid phase and (b) vapour phase, for the RD1 configuration

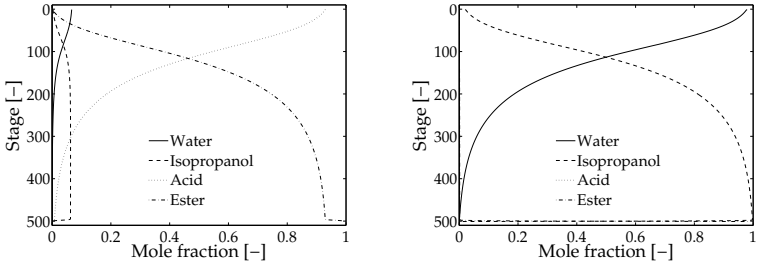


(a) (b)

Figure 4.14: Concentration profiles of (a) liquid phase and (b) vapour phase, for the RD2 configuration

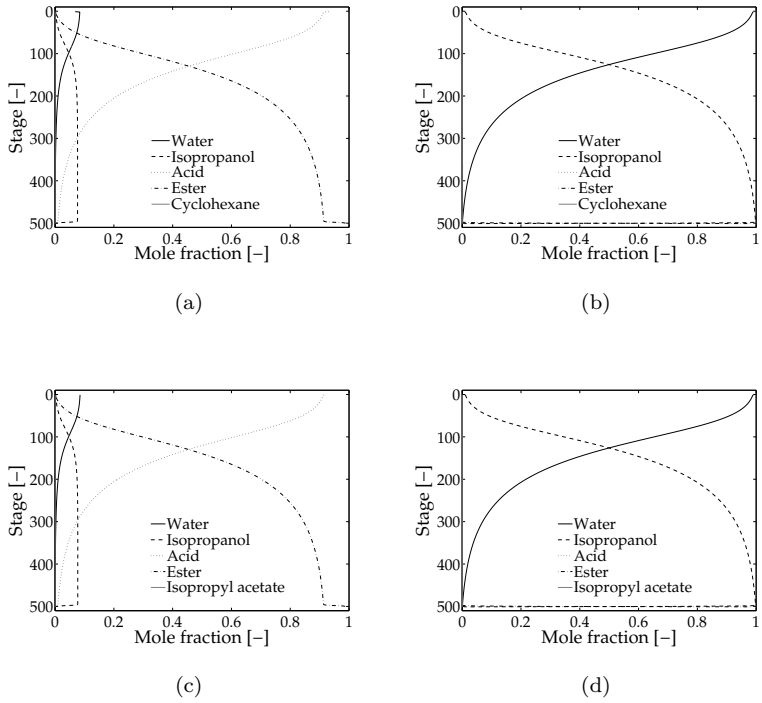


Figure 4.15: Concentration profiles of (a) liquid phase and (b) vapour phase with cyclohexane as entrainer and (c) liquid phase and (d) vapour phase with isopropyl acetate as entrainer, for the RD3 configuration

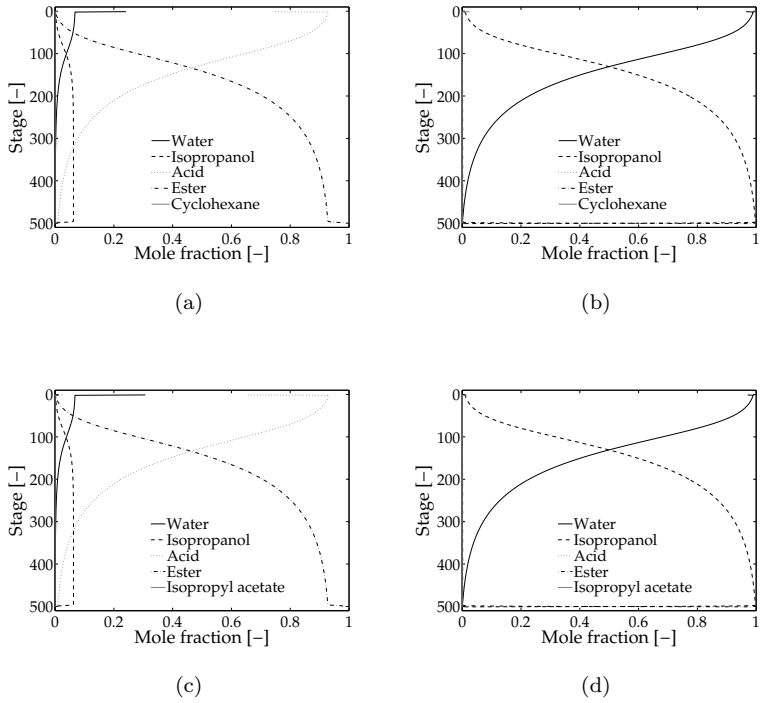


Figure 4.16: Concentration profiles of (a) liquid phase and (b) vapour phase with cyclohexane as entrainer and (c) liquid phase and (d) vapour phase with isopropyl acetate as entrainer, for the ERD1 configuration

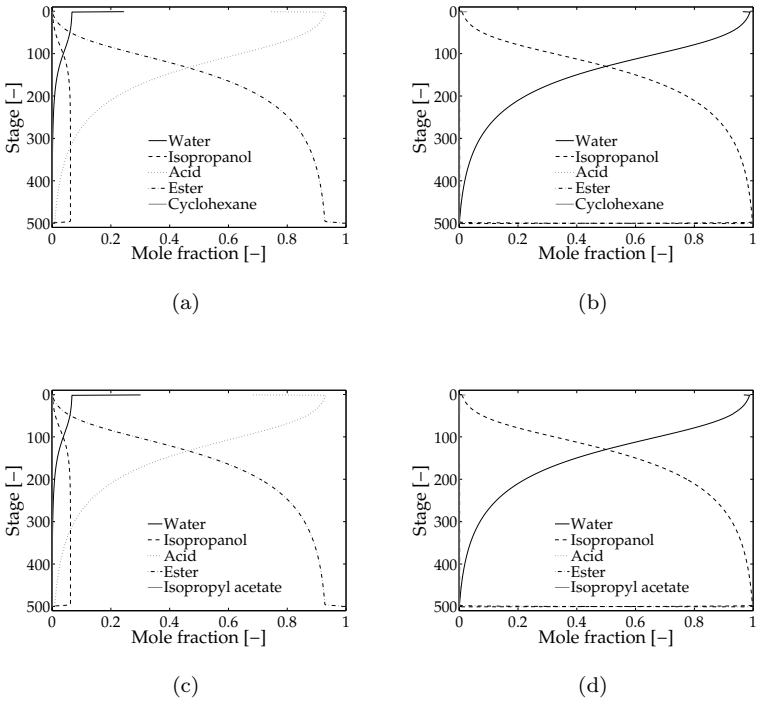


Figure 4.17: Concentration profiles of (a) liquid phase and (b) vapour phase with cyclohexane as entrainer and (c) liquid phase and (d) vapour phase with isopropyl acetate as entrainer, for the ERD2 configuration

### 4.A.2 Esterification with *n*-propanol at 1 bar

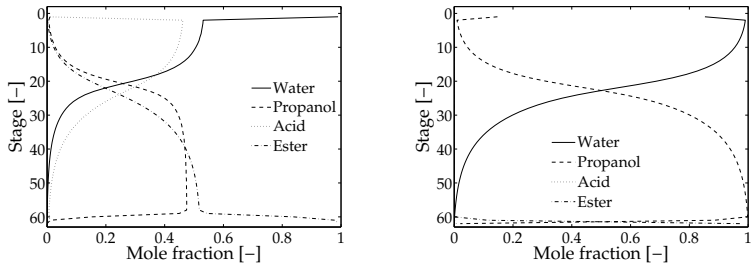


Figure 4.18: Concentration profiles of (a) liquid phase and (b) vapour phase, for the RD1 configuration

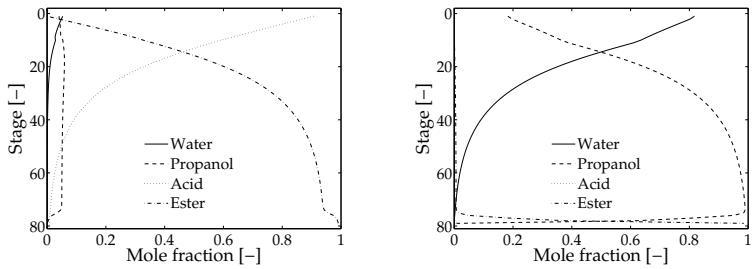


Figure 4.19: Concentration profiles of (a) liquid phase and (b) vapour phase, for the RD2 configuration

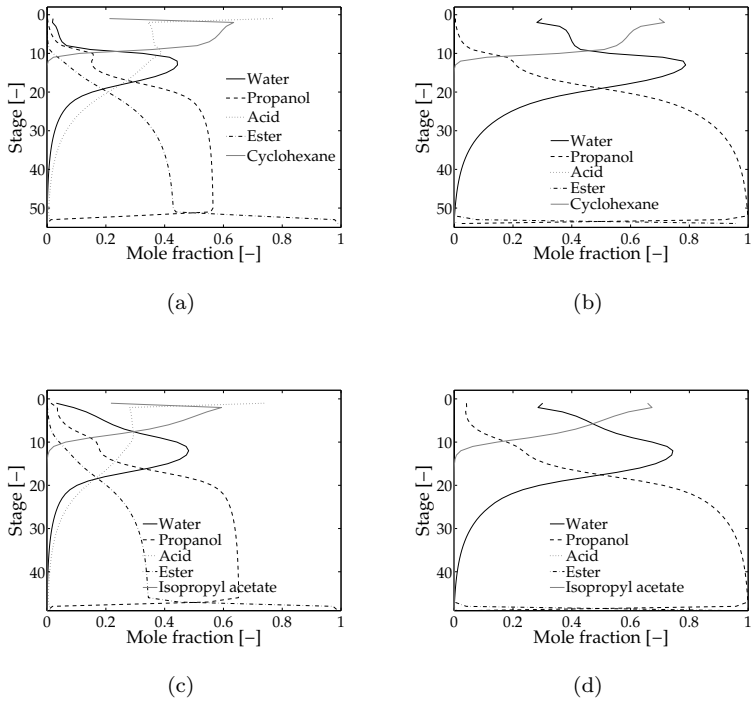


Figure 4.20: Concentration profiles of (a) liquid phase and (b) vapour phase with cyclohexane as entrainer and (c) liquid phase and (d) vapour phase with isopropyl acetate as entrainer, for the RD3 configuration

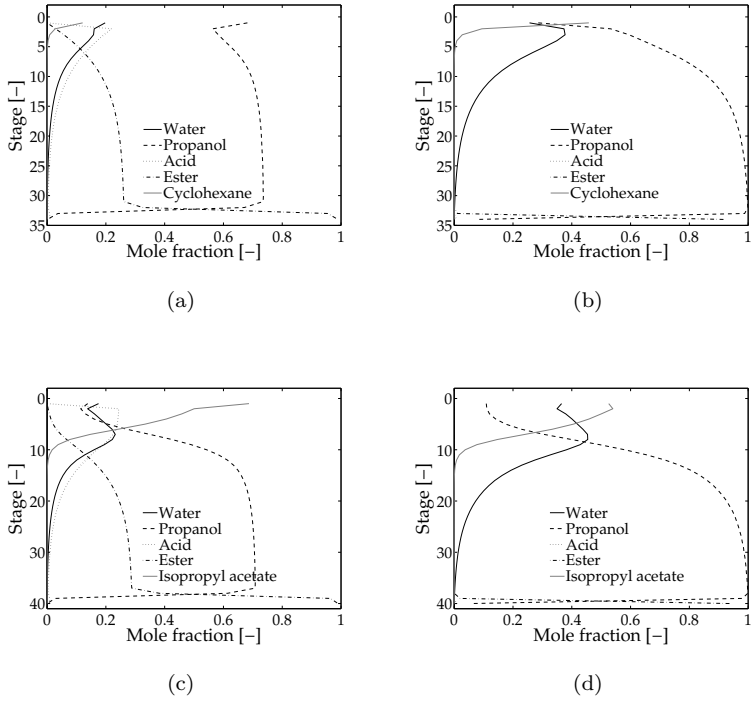


Figure 4.21: Concentration profiles of (a) liquid phase and (b) vapour phase with cyclohexane as entrainer and (c) liquid phase and (d) vapour phase with isopropyl acetate as entrainer, for the ERD1 configuration

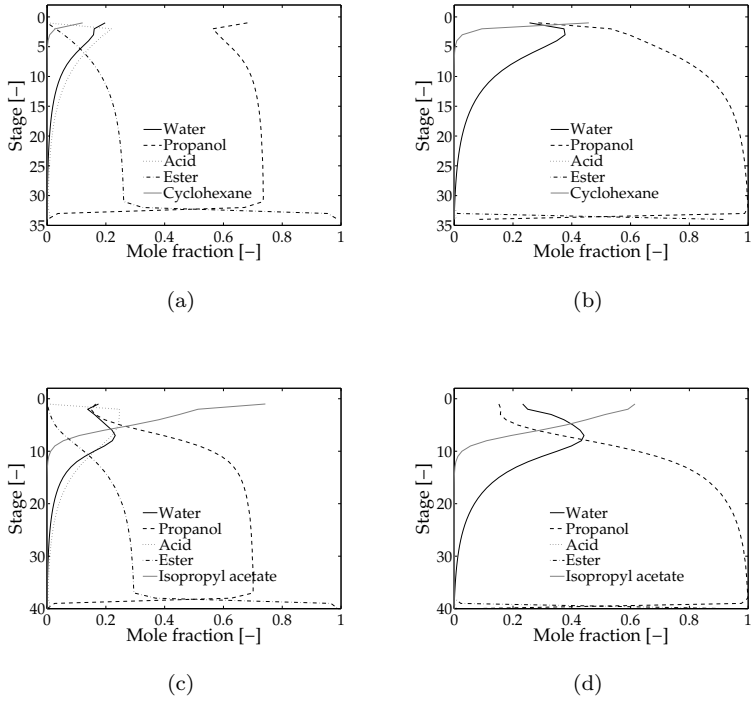


Figure 4.22: Concentration profiles of (a) liquid phase and (b) vapour phase with cyclohexane as entrainer and (c) liquid phase and (d) vapour phase with isopropyl acetate as entrainer, for the ERD2 configuration

### 4.A.3 Esterification with isopropanol and with *n*-propanol at 5 bar

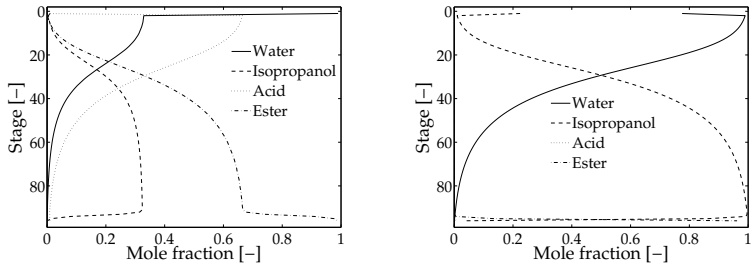


Figure 4.23: Concentration profiles of (a) liquid phase and (b) vapour phase, for the RD1 configuration

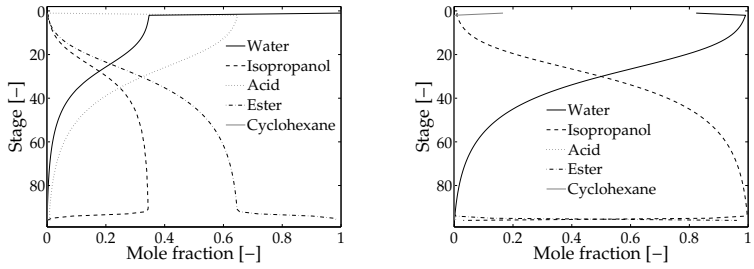


Figure 4.24: Concentration profiles of (a) liquid phase and (b) vapour phase with cyclohexane as entrainer for the ERD1 configuration

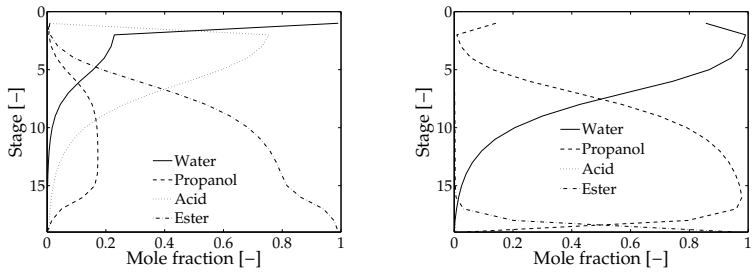


Figure 4.25: Concentration profiles of (a) liquid phase and (b) vapour phase, for the RD1 configuration

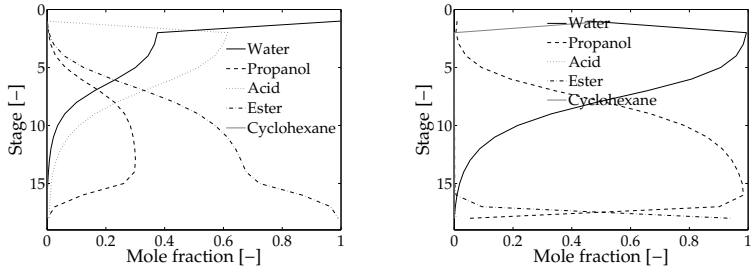


Figure 4.26: Concentration profiles of (a) liquid phase and (b) vapour phase with cyclohexane as entrainer for the ERD1 configuration

### 4.A.4 Esterification with isopropanol and with *n*-propanol at 10 bar

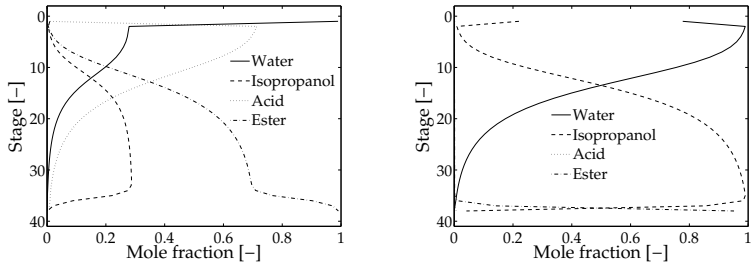


Figure 4.27: Concentration profiles of (a) liquid phase and (b) vapour phase, for the RD1 configuration

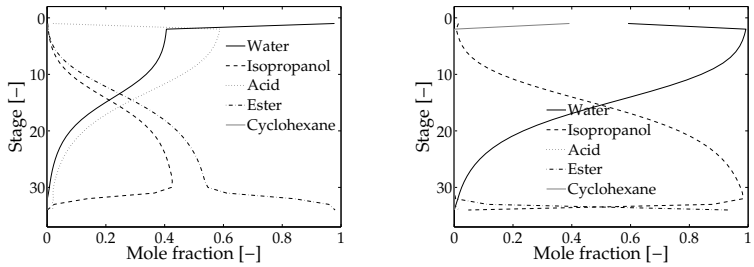


Figure 4.28: Concentration profiles of (a) liquid phase and (b) vapour phase with cyclohexane as entrainer for the ERD1 configuration

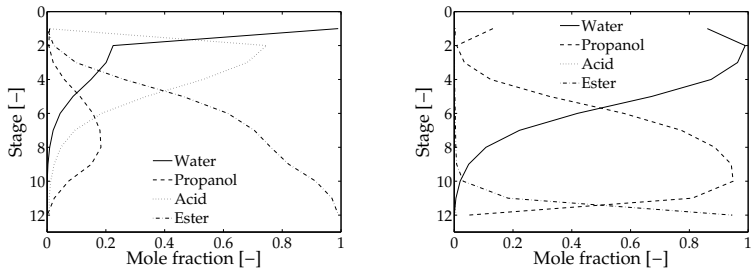


(a) (b)

Figure 4.29: Concentration profiles of (a) liquid phase and (b) vapour phase, for the RD1 configuration

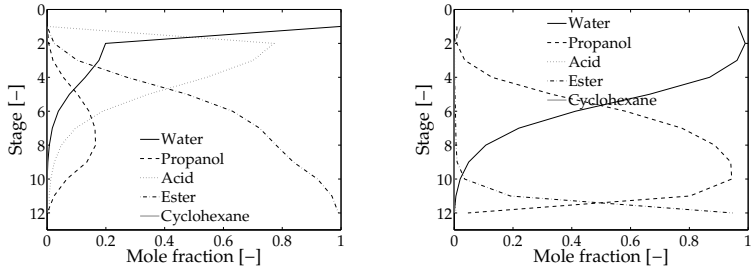


(a) (b)

Figure 4.30: Concentration profiles of (a) liquid phase and (b) vapour phase with cyclohexane as entrainer for the ERD1 configuration

# Chapter 5

# Pilot column

*In this chapter the Aspen Plus process for the Reactive Distillation was validated through pilot plant experiments. A detailed model of the pilot plant is created for different operating conditions. Experiments with a pilot column are performed to verify the model. The conducted experiments correspond well with the predicted values, therefore the model describes the column well and can be used to construct a conceptual design. However, not all the intended validation experiments could be performed, because of the practical difficulties that arise when negligible liquid level in the column has to be ensured. Also break down of the pumps due to clogging is a limiting factor in the experiments.*

## 5.1 Introduction

In the previous chapter an Aspen Plus model for the Reactive Distillation of myristic acid with isopropanol was proposed. In order to expand this model to a conceptual design, experimental validation is required. However, experimental data on the esterification of fatty acids by Reactive Distillation at pilot plant scale is scarce. A few processes with various fatty esters and alcohols are described.

Jeromin et al. [1] describe the esterification of different fatty acids with

methanol in a tray column. Zhou [2] report the experimental validation of a model for the esterification of oleic acid with methanol. Zaidan et al. [3] investigated the Reactive Distillation with a pre-reactor for the esterification of oleic acid with methanol, ethanol, *n*-propanol and isopropanol. Steinigeweg and Gmehling [4] investigated the esterification of decanoic acid with methanol using a heterogenous catalyst in a packed column. Bhatia et al. [5] report the experimental validation of a rate-based model for the production of isopropyl palmitate in a packed Reactive Distillation column using a heterogeneous catalyst. Schleper et al. [6] mention the esterification of an unknown fatty acid with isopropanol in a tray column. Some of these studies involve the esterification with isopropanol but none of them in the combination with myristic acid.

Investigations about the esterification of myristic acid with isopropanol with a homogeneous catalyst in a tray column have been performed by Bock et al. [7]. A process including a recovery column for isopropanol was presented. However, the reported experimental data is limited. The results of only one experiment are reported without including the operating conditions.

No information on the used system, a packed Reactive Distillation column for the esterification of myristic acid with isopropanol is available. Little information on the Reactive Distillation for the esterification of myristic acid with isopropanol in a tray column is available. However, this is not enough to validate the model used in the present work. Therefore, this chapter contains a pilot plant study on the esterification of myristic acid with isopropanol in a packed column, in order to validate the proposed Aspen Plus model.

In Chapter 4 the hydrodynamics were described as an ideal plug flow, while in this chapter the liquid hold-up and pressure drop correlations are included for a more accurate model. Therefore first the theory about modelling the hydrodynamics of a packed Reactive Distillation column are discussed. Based on the model from Chapter 4 and the hydrodynamics relations a model for the pilot plant is formulated. In order to validate this model experiments are performed. Finally the experimental results are compared with the simulation results obtained by the model.

## 5.2 Modelling Reactive Distillation

A Reactive Distillation process model consists of sub-models for mass transfer, reaction kinetics and hydrodynamics. The completion of these sub-models can vary from simple to complex, as described in Chapter 4. [8]

It was described that the Damköhler number can be used to see if a Reactive Distillation process is controlled by chemical equilibrium, phase equilibrium or something in between those two extremes.

For the system used in this research $Da \approx 0.02 - 0.18$. This is much smaller than 0.5, which means that the system can be assumed to be dominated by phase equilibrium, just like in the feasibility analysis in Chapter 4.

In this chapter the simplest possible model for all three parts (mass transfer, reaction kinetics and hydrodynamics) is used. As explained above, the mass transfer can be described by physical equilibrium. This equilibrium stage model is described in Chapter 4, section 4.2.1. Chemical equilibrium is not reached, therefore the reaction will be described by a kinetic model of the bulk reaction. The hydrodynamics are described by liquid hold-up and pressure drop correlations, while in Chapter 4 the system was described as an ideal plug flow.

### 5.2.1 Hydrodynamics

The pressure drop of a gas flowing upwards through a packing countercurrent to a liquid flow is shown in Figure 5.1. At low liquid rates, the effective cross section of the packing is similar to that of the dry packing. The pressure drop is due to flow through a series of openings in the bed. The pressure drop is proportional approximately to the square of the gas velocity, as indicated in region AB. At higher liquid rates liquid is present in and de the effective open cross section is smaller. The energy of the upflowing gas stream is partially used to support an increasing quantity of liquid in the column (region A'B'). When the pressure drop is proportional to a gas-flow-rate power distinctly higher then two, the loading zone is reached, as indicated in Figure 5.1. There are two possibilities when the liquid holdup increases: 1) The effective orifice

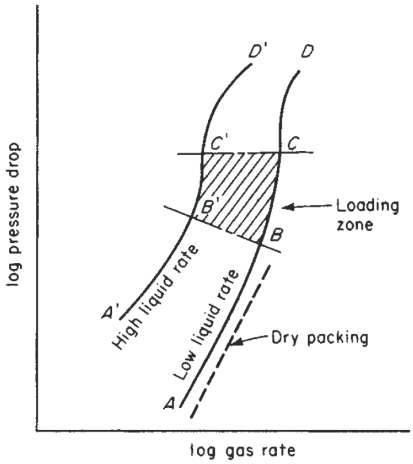


Figure 5.1: Pressure-drop characteristics of packed columns [9]

diameter becomes so small that the liquid surface becomes continuous across the cross section of the column. A slight change in gas rate results in a large change in pressure drop, and flooding occurs. 2) Phase inversion occurs, and gas starts bubbling through the liquid. The increase in the pressure drop will also be significant analogous to the first case. However stable operation is still possible. [9]

### Pressure drop

In the RADFRAC model in Aspen Plus, the pressure drop is accounted for by the model of Bravo et. al. [9–12]. This is a widely applied model for structured packings and can be used for both sheet metal and gauze packing. The correlation is as follows:

$$\Delta P = \left[0.171 + \left(\frac{92.7}{Re_g}\right)\right]\left[\frac{\rho_g u_{ge}^2}{d_{eq} g_c}\right]\left[\frac{1}{(1 - C_0 Fr^{0.5})}\right]^5 \tag{5.1}$$

with $u_{ge}$ is the effective gas velocity inside the flow channel, $C_0$ a packing specific constant (Sulzer Bx: 3.38), $d_{eq}$ the packing equivalent diameter and $\rho_g$ the gas density. The gas Reynolds number $Re_g$ is defined as:

$$Re_g = \frac{d_{eq} u_{ge} \rho_g}{\mu_g} \tag{5.2}$$

in where $\mu_g$ is viscosity of the gas. The effective gas velocity inside the flow channel $u_{ge}$ is defined as:

$$u_{ge} = \frac{u_g}{\varepsilon \sin \theta} \tag{5.3}$$

with $u_g$ being the superficial gas velocity and $\varepsilon$ the void fraction of packing. The Froude number $Fr$ is defined as:

$$Fr = \frac{u_l^2}{d_{eq} g} \tag{5.4}$$

in where $u_l$ is the superficial liquid velocity, $\theta$ the angle of inclination with flow and $g$ the gravitational constant.

This model is valid in the region below the loading point, and it cannot predict the flood point because it does not include the effects of gas velocity on liquid hold-up. [9, 12]

### Operating region

In packed columns the vapour load can be reduced to extremely low values, but the liquid load must be within a certain range. Below a certain liquid load the surface of the packed column is no longer completely wetted and gas and liquid are no longer in intimate contact. This results in a serious drop of separation efficiency. The minimum liquid flow is considered as the wetting border of the feasible operating region of a packed column. In practice, minimum liquid loads for a random packing are in the order of 10 $\mathrm{m^3 m^{-2} hr^{-1}}$. For structured

packing this number can be as low as 0.05 $m^3m^{-2}hr^{-1}$. [13, 14]

The flooding point represents the column load at which liquid can no longer flow countercurrent to the rising vapour. Liquid flow is obstructed by the high vapour load to such an extent that it accumulates in the bed. As already stated, the flooding point is characterised by a steep increase in the pressure drop. In general the operating region of a packed column is therefore enclosed between a wetting and a flooding border. This is depicted in Figure 5.2.

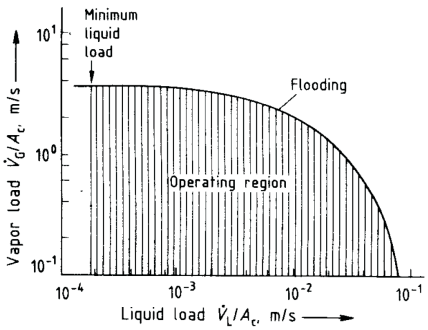


Figure 5.2: Operating region of a packed column [13, 14]

### Liquid hold-up

For the liquid hold-up of a packing two scenarios can be distinguished. Below the load point, the liquid hold-up is solely dependant on the liquid rate. Above the load point it is also a function of vapour rate. The liquid in the packing is held back by friction forces imposed on it by the gas as well as the static pressure gradient produced by the pressure drop. The influence of the gas rate on hold-up in the loading region is complex. However the following relation can be derived between the pressure drop and the hold-up [15]:

$$h = h_0 \left[ 1 + 20 \left( \frac{\Delta P}{Z \rho_g g} \right)^2 \right] \tag{5.5}$$

where $Z$ is the total height of packing. The variable $h_0$ is the liquid hold-up below the loading point:

$$h_0 = 0.555 Fr_L^{1/3} \tag{5.6}$$

with the Froude number, $Fr$, defined as:

$$Fr = \frac{u_L^2 a}{g\varepsilon^{4.65}} \tag{5.7}$$

where $a$ is the specific surface of the packing.

The pressure drop in this equation is accounted for by the Stichlmair model [15], because it takes hold-up into account:

$$\frac{\Delta P}{\Delta P_{dry}} = \left[\frac{1-\varepsilon(1-\frac{h}{\varepsilon})}{1-\varepsilon}\right]^{(2+c)/3} \left(1-\frac{h}{\varepsilon}\right)^{-4.65} \tag{5.8}$$

with $\Delta P_{dry}$ being the dry pressure drop:

$$\frac{\Delta P_{dry}}{Z} = 0.75 f_0 \left(\frac{1-\varepsilon}{\varepsilon^{4.65}}\right)\left(\frac{\rho_g u_g^2}{d_p}\right) \tag{5.9}$$

where the friction factor for flow past a single particle, $f_0$ is defined as:

$$f_0 = \frac{C_1}{Re_g} + \frac{C_2}{Re_g^{0.5}} + C_3 \tag{5.10}$$

and the exponent $c$ in Eq. 5.8 as:

$$c = \frac{\frac{-C_1}{R_g} - \frac{C_2}{2Re_g^{0.5}}}{f_0} \tag{5.11}$$

with $C_1$, $C_2$ and $C_3$ constants, specific for the packing. For the Sulzer BX packing these constants are respectively, 15, 2 and 0.35.

In here the gas Reynolds number $Re_g$ is not defined as in Eq. 5.2 but as:

$$Re_g = \frac{d_p u_g \rho_g}{\mu_g} \tag{5.12}$$

The particle diameter $d_p$ in Eq. 5.9 is defined as:

$$d_p \equiv \frac{6(1-\varepsilon)}{a} \tag{5.13}$$

with a void fraction ($\varepsilon$) of 0.86 and a specific surface area ($a$) of 450 for the Sulzer BX packing.

## 5.3 Modelling

Simulations of the pilot column are conducted using the commercial software package Aspen plus. First the column capacity has to be determined to determine the boundaries of the operating window. Subsequently, a base case is simulated as a reference for further simulations. Based on this case, the operating conditions of the experiments are chosen and a simulation for each experiment is made.

### 5.3.1 Column specifications

The column specifications are listed in Table 5.1. The packing used in the column is the Sulzer BX packing, see Figure 5.3. This is the most suitable packing from Sulzer which is available in sizes suitable for lab scale experiments. It has a high surface area and it can be used with a homogeneous catalyst, for a heterogenous catalyst Sulzer Katapak packing should be used. The data

| | |
|---|---|
| Diameter | 0.05 m |
| Packing height | 1.19 m |
| Number of stages | 7 |
| Condensor | - |
| Reboiler | - |

Table 5.1: Specifications pilot column

for this packing is already included in the software. The number of stages is estimated from HETP data used by others for Sulzer BX in literature. [16, 17] A HETP value of $\sim$ 0.15-0.2 $m^{-1}$ is reported; this indicates approximately 6-8 stages. In this research the average of 7 stages is used.

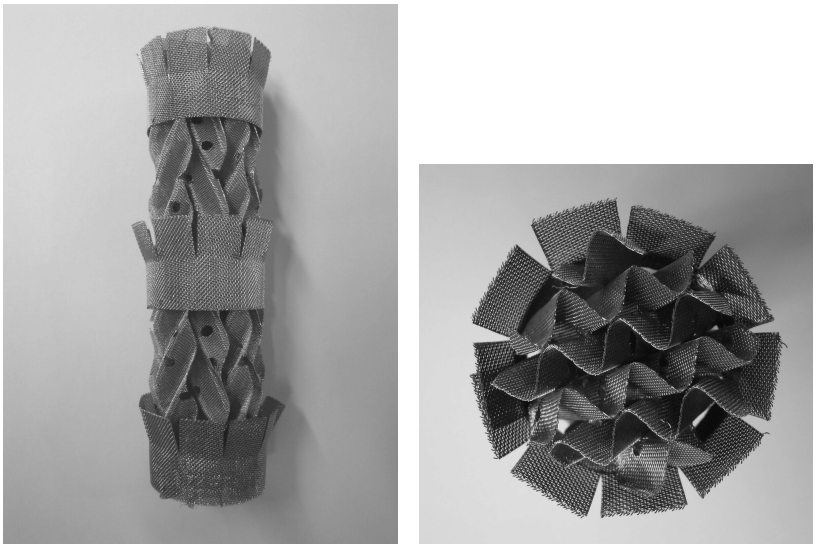

(a) (b)

Figure 5.3: Sulzer BX packing a) frontal view b) view from above

### 5.3.2 Column capacity

For the pilot plant experiments and simulations it is important to determine the operating region of the pilot column. As discussed before, the operation of a packed column is limited by a minimum liquid flow because the column is not sufficiently wetted otherwise. Also at a certain vapour load flooding of the column will occur. Stable operation is only possible between these boundaries. In order to determine the operating region of the column both the minimum liquid load and the maximum vapour load have to be determined.

### Minimum liquid load

According to Sulzer [17], the minimum liquid load for the Sulzer BX packing is approximately 0.05 $m^3$ $m^2hr^{-1}$. From this, the minimum liquid flow can be determined using the formula below:

$$F_{l,min} = \frac{u_{l,min} A \rho_l}{M_l} = 0.34 \,\mathrm{mol\,hr^{-1}} \tag{5.14}$$

where $F_{l,min}$ is the minimum liquid flow rate, $u_{l,min}$ the minimum liquid load, $\rho_l$ the liquid density, $M_l$ the liquid molar mass and $A$ the column cross sectional area.

The minimum liquid load is determined to be 0.34 mol $hr^{-1}$ of myristic acid, corresponding to 0.08 kg $hr^{-1}$. Packed columns can be operated at very low vapour flows. Because of the equimolar reaction stoichiometry, the minimum vapour flow should contain at least the same amount of moles as the liquid flow. Therefore the minimum vapour flow can be determined to be about 0.02 kg $hr^{-1}$.

### Maximum column load

The maximum column load of the pilot plant column has been estimated using the commercial program SULPAK 3.1 from Sulzer Chemtech. The column is simulated using RADFRAC model to generate estimates for the vapour and liquid densities, which serve as input parameters for SULPAK. By fixing the liquid feed and varying the vapour load, the maximum vapour flow for a given liquid feed can be determined. In Figure 5.4 a capacity plot generated with Sulpak is shown. The black line indicates the point at which flooding occurs for a given flow parameter, the grey line is at 80% from this point.

The flow parameter is determined with the following equation. Flows are defined on mass basis in this case:

$$F_{LG} = \frac{L}{G}\sqrt{\frac{\rho_g}{\rho_l}} \tag{5.15}$$

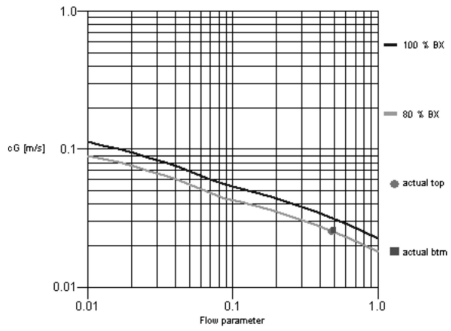


Figure 5.4: Capacity plot of Sulzer BX packing. The myristic acid flowrate is 50 kg $hr^{-1}$, while the isopropanol flowrate is chosen to get 80% capacity

The capacity factor is defined as:

$$c_G = u_g \Big( \frac{\rho_g}{\rho_l - \rho_g} \Big)^{1/2} \tag{5.16}$$

By fixing the liquid flow and varying the vapour flow in Aspen for several vapour flows the operating region of the column can be determined. In Figure 5.5 the results from these simulations are shown. The acquired curve agrees with the literature. In addition, the curve for equimolar vapour and liquid feed flow is plotted. Operation below the dashed line will result in a low conversion, because the amount of isopropanol in the system is too low for full conversion. The dotted line marks the point at which the liquid flow is minimal.

The operating region for the pilot plant is defined by a triangle between the flooding line, the minimum liquid load and the ratio of the feed flow. The feed of myristic acid should be between 0.08 kg $hr^{-1}$ and 55 kg $hr^{-1}$ (0.05 $m^3$ $m^{-2}hr^{-1}$ - 32.5 $m^3$ $m^{-2}$ $hr^{-1}$). The corresponding maximum isopropanol feed flows are 46 and 15 kg $hr^{-1}$. Although the flows through the column can be quite large, it is important to keep the final conversion in mind. During the determination of the operating window it was observed that conversion is higher at lower flow rates. This is probably due to a higher residence time

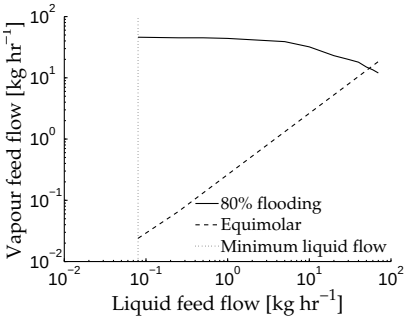


Figure 5.5: Plot of the liquid feed flow versus the vapour feed flow. The solid line shows the vapour flow at 80% from the flooding point. The dashed line is when the vapour and liquid flow are the same amount of moles, the dotted line indicates the minimum liquid flow

despite the fact the liquid holdup is lower. Therefore relatively low flow rates are chosen for the simulation base case.

### 5.3.3 Process conditions and requirements

The kinetics of the reactions are experimentally determined and are described in Chapter 3. The reaction rate for the esterification of myristic acid and isopropanol using $p$TSA is

$$\begin{aligned} r_E \;=\; & 3.33 \cdot 10^5 [\text{cat}] \exp\left(\frac{-58.9 \cdot 10^3}{RT}\right)[A][B] \\ & - 2.18 \cdot 10^3 [\text{cat}] \exp\left(\frac{-45.9 \cdot 10^3}{RT}\right)[E][W] \;\text{mol}\,\text{L}^{-1}\text{s}^{-1} \end{aligned} \tag{5.17}$$

$r_E$ is the reaction rate, $[E]$ the concentration ester, $[A]$ the concentration alcohol, $[B]$ the concentration acid, $[W]$ the concentration water and [cat] is the catalyst concentration.

In order to establish significant conversions, the chosen catalyst concentration of the base case is 0.05 M. The operating pressure is 3 bar and the column temperature is 180°C. A feed of 1.01 kg $hr^{-1}$ myristic acid and 1.32 kg $^{-1}$ isopropanol is used, corresponding to a feed ratio of 1:5 mole myristic acid over isopropanol. This large excess of isopropanol is needed to maintain the pressure in the column. In further simulations one parameter from the base case will be varied to study the influence of that parameter. The other conditions will be kept at a constant value.

In Table 5.2 the physical properties of the vapour and liquid stream in the pilot column can be found.

| | Vapour stream | Liquid stream |
|---|---|---|
| Density [kg $m^{-3}$] | 4.8 | 760 |
| Surface tension [N $m^{-1}$] | - | $1.7 \cdot 10^{-2}$ |
| Viscosity [Pa.s] | $1.2 \cdot 10^{-5}$ | $5.7 \cdot 10^{-4}$ |

Table 5.2: Physical properties of the vapour and liquid streams in the pilot column

### 5.3.4 Thermodynamics

For the simulations in Aspen Plus a property model has to be selected. In Chapter 2 vapour-liquid equilibrium data from literature for different water-isopropanol systems [18–20] are compared to different NRTL property models in Aspen Plus.

The set of NRTL parameters developed by Aspen Tech based on data from the Dortmund Data Bank, was found to correspond the best with the experimental literature data and is therefore used further.

The unknown interaction parameters are estimated using UNIFAC, these are all parameters concerning the myristic acid or the ester. UNIFAC predicts an azeotrope between myristic acid and isopropyl myristate. It is unlikely that this will occur, because the components have similar polarities. Therefore it is better to set the interaction between those components to zero, to approximate

reality.

## 5.4 Experimental

### 5.4.1 Apparatus

In Figure 5.6 the pilot plant set-up is drawn schematically. In Figure 5.7 pictures of the column and storage vessels can be seen. The pilot plant set-up consists of a thermostated steel column of 1.7 metres. The column is filled with Sulzer BX packing, the total packing height is 1.19 metres. Pumps (Bronkhorst

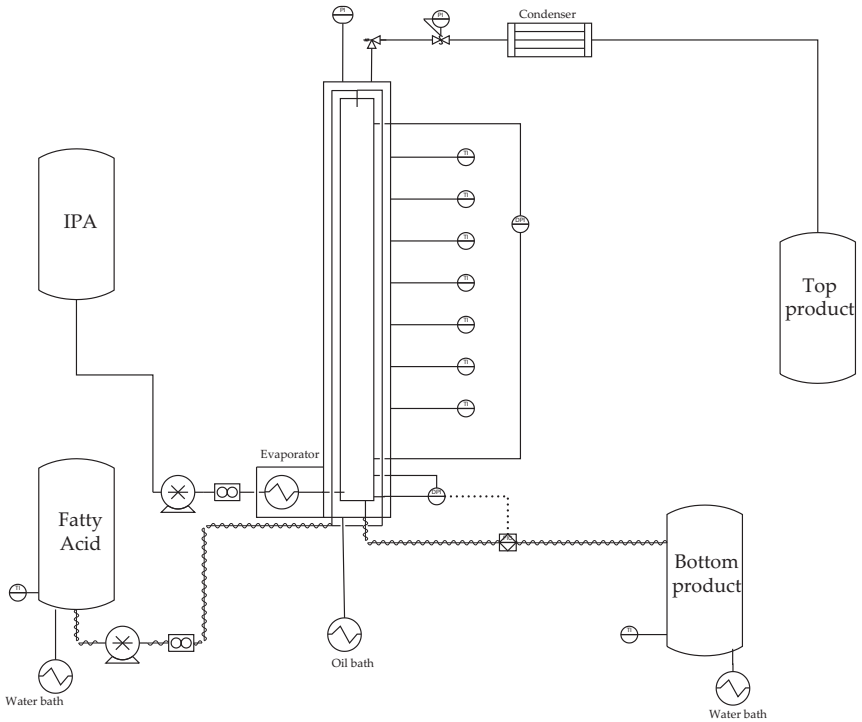


Figure 5.6: Schematic presentation of the pilot plant set-up

MZR-7255)are used to transport the reactants tot the column. Coriolis mass flow controllers (Bronkhorst M53-RAD-22-0-B) are use to measure and control the flow.The myristic acid is fed, together with the catalyst, at the top of the column after being heated inside the wall. The isopropanol is evaporated by an evaporator (A-steam) and fed at the bottom of the column. The bottom product (myristic acid and isopropyl myristic) goes via a mass flow controller, which is connected to a differential pressure transmitter(GE Sensing LX8381, span: 10 mbar differential pressure), to its storage vessel. The top vapour (isopropanol and water) flows via a mass flow controller, which is controlled by a pressure measurement, through a condenser to its storage vessel. The maximum operating pressure is 5 bar. Along the column the temperature is measured at 7 points and samples can be taken at the bottom of the column. The process is monitored and controlled by the custom made graphical user interface in LabVIEW.

(a) (b)

Figure 5.7: Pilot plant set-up a) column and b) storage vessels

### 5.4.2 Materials and catalysts

Isopropanol (≥99.5%) from Merck and myristic acid (≥95%) from Sigma-Aldrich were used as the reactants. The *p*-toluene sulphonic acid (*p*TSA) catalyst was obtained as *p*-toluene sulphonic acid monohydrate (98.5%) from Aldrich. Dodecane (≥98%) and methyl ethyl ketone (≥99%), for the analysis, were obtained from Fluka.

### 5.4.3 Analysis

All samples of the kinetic experiments were analysed by gas chromatography. The column is a Varian WCOT Fused Silica 50m x 0.32 mm column coated with CP-Sil 5CB. $H_2$ is used as carrier gas at a constant speed of 2 mL $min^{-1}$. The temperature program, 75°C for 5 min, than 40°C $min^{-1}$ to 225°C and maintain at 225°C for another 11.25. Dodecane is used as an internal standard and methyl ethyl ketone as solvent.

### 5.4.4 Procedure

The storage vessel containing the myristic acid and the vessel for the bottom product are heated to 100°C to melt the myristic acid and to ensure that the content of the vessels remain liquid. This high temperature is needed because the catalyst increases the melting point of the myristic acid. The piping from these vessels to the column and vice versa are traced at 130°C to prevent solidification. The column wall is also heated. Because the catalyst and myristic acid react to an unidentified black insoluble substance, the catalyst is added as a liquid to the myristic acid vessel just before the start of the experiment. First the isopropanol is introduced into the column. The set-up has to be operated for 15-30 minutes to make sure all the isopropanol passing through the evaporator will we evaporated. At high flowrates the flow should be increased stepwise to prevent an unstable regulation of the evaporator. Secondly, the operating pressure has to be set. When the top vapour flow has become stable, the myristic acid flow can be set. Every half an hour, samples will be taken

at the bottom the column.

## 5.5 Results and discussion

In Table 5.3 the operating parameters of the performed experiments and the conversion predicted by the model are shown. Experiment 1 is used as the reference case. In experiment 2 both the feed flows are increased. This results in a shorter residence time and therefore in a lower conversion. From experiments 3 and 4, it can be seen that an increase in temperature or pressure give higher conversions. The influence of the pressure is larger than that of temperature. The smaller increase as a result of temperature is also confirmed by comparing experiments 4 and 5. As seen in experiment 6, doubling the catalyst concentration will double the conversion.

| Exp. [-] | [cat] [$M$] | MA:IPA [-] | IPA flow [kg/hr] | MA flow [kg/hr] | P [bar] | T [C] | Conversion [%] |
|---|---|---|---|---|---|---|---|
| 1 | 0.05 | 1:5 | 1.32 | 1.012 | 3 | 180 | 7 |
| 2 | 0.05 | 1:5 | 3.00 | 2.288 | 3 | 180 | 5 |
| 3 | 0.05 | 1:5 | 1.32 | 1.012 | 3 | 220 | 9 |
| 4 | 0.05 | 1:5 | 1.32 | 1.012 | 5 | 180 | 11 |
| 5 | 0.05 | 1:5 | 1.32 | 1.012 | 5 | 220 | 14 |
| 6 | 0.10 | 1:5 | 1.32 | 1.012 | 5 | 180 | 22 |

Table 5.3: Operating parameters and model prediction for the conversion of the pilot column experiments

In order to validate the model, the absence of a liquid level in the bottom of the column has to be ensured. If there is a liquid level present, the column contains extra reaction volume which is not accounted for in the model. Besides that, evaporation takes place which, influences the vapour-liquid equilibrium and concentrations. The liquid level of the column is indicated by the pressure difference over the bottom section of the column, measured via a differential pressure transmitter. This pressure difference is automatically regulated in the LabVIEW software by opening a valve to reach a certain set-point. Due

to a bug in the control mechanism the actual pressure difference has a variable deviation from the set-point, dependant of the moment the set-point is given. Therefore the actual point with a pressure difference of zere has to be found during the experiment. This can be done by, choosing a set-point of the pressure difference at which a liquid level is present and then lowering this set-point stepwise. If the set-point is very low, the valve is opened completed although there is not enough liquid in the column to flow out. This causes a pressure loss. For the experiment at 3 bar and 180°C the results for this method can be found in Figure 5.8.

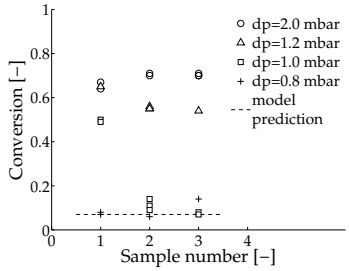


Figure 5.8: Influence of the pressure difference set-point on the conversion in the pilot column experiments at 3 bar and 180°C

In this figure it can be seen that with decreasing value of the set-point the conversion decreases as well; the final values correspond well with the value predicted by the model. Samples number three show the same conversions as samples number two, this means that steady state was reached already at samples number two (one hour).

With a liquid level present, in the column the conversions are unexpectedly high compared to the predicted model values. Such conversions cannot be reached with the available reaction volume. To obtain these high conversions an extra 2.5 L reaction volume should have been available on top of the liquid volume of approximately 0.02 L in the column. The total column volume is

2.3 L, so the higher conversion cannot be caused by a difference in predicted and actual liquid hold-up. The most likely explanation is the presence of dead volume in the bottom section of the column. Due to the geometry of this section there are areas in which the liquid does not flow but stand still, and the arising very high residence times result in a higher conversion. Due to time restrictions, it was not possible to modify the set-up to overcome this problem.

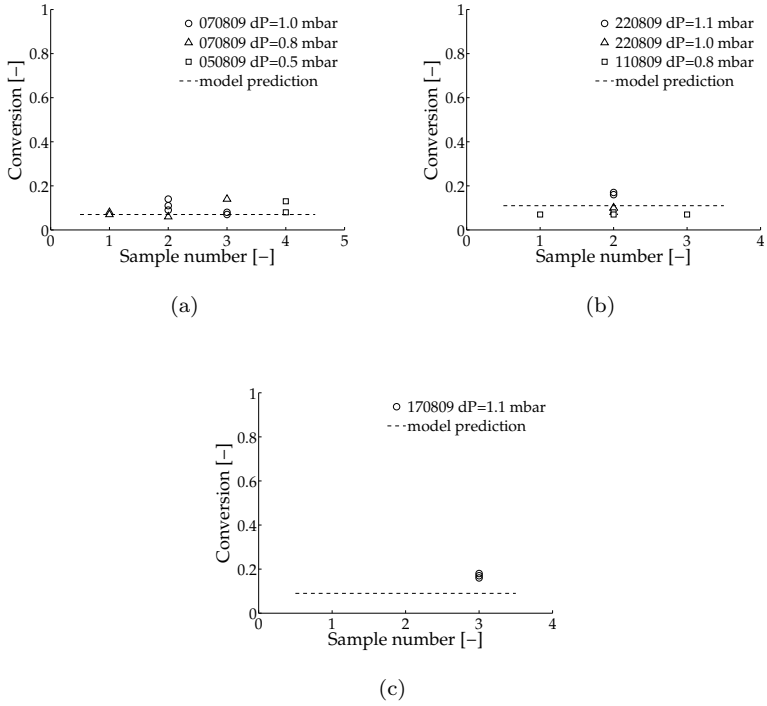


Figure 5.9: Pilot column experiments at a) 3 bar and 180°C, b) 5 bar and 180°C and c) 3 bar and 220°C

In Figure 5.9 the results of the conducted experiments are given together with the model prediction. In Figure 5.9*a* the experiments at 3 bar and 180°C are shown (Experiment 1 from Table 5.3). Figure 5.9*b* contains the results of

the experiment at 5 bar and 180°C (Experiment 4 from Table 5.3). Figure 5.9*c* shows the results of the experiment at 3 bar and 220°C (Experiment 3 from Table 5.3). The experimental values correspond well with the predicted values. Although the number of experiments which can be compared is limited, it can be concluded that the model describes the column adequately and can therefore be used to construct a conceptual design.

Due to the practical difficulties to ensure negligible liquid level in the column and have no pressure loss and because the pumps broke down by clogging with the insoluble black substance, not all the experiments could be performed. In hind side it would have probably been better to operate the column with a liquid level in the bottom and add a bottom section in the simulation model. Experiments 2, 5 and 6 from Table 5.3 were not performed, this are the experiments with higher feed flow, 5 bar and 220°C and the higher catalyst concentration. The performed experiments are the reference case (3 bar and 180°C), the experiment at 3 bar and 220°C and the one at 5 bar and 180°C (experiments 1, 3 and 4).

In hind side it would have probably been better to operate the column with a liquid level in the bottom and add a bottom section in the simulation model.

## 5.6 Conclusion

In this chapter the process model used in Aspen Plus was validated through pilot plant experiments. A detailed model of the pilot plant was created for different operating conditions. Experiments with a pilot column were performed to verify the model. The conducted experiments correspond well with the predicted values, therefore the model describes the column adequately to be used for the constructing of a conceptual design.

# Nomenclature

| | |
|---|---|
| $[A]$ | Fatty acid concentration [mol $L^{-1}$] |
| $[B]$ | Alcohol concentration [mol $L^{-1}$] |
| $[E]$ | Ester concentration [mol $L^{-1}$] |
| $[W]$ | Water concentration [mol $L^{-1}$] |
| [cat] | Catalyst concentration [M] |
| $A$ | Column cross sectional area [$m^2$] |
| $a$ | Specific surface area of packing [$m^2$ $m^{-3}$] |
| $C_0$ | Packing specific constant [-] |
| $C_1$ | Packing specific constant [-] |
| $C_2$ | Packing specific constant [-] |
| $C_3$ | Packing specific constant [-] |
| $c_G$ | Capacity factor [m $s^{-1}$] |
| $c$ | Exponent [-] |
| $\Delta P_{dry}$ | Pressure drop through an unirrigated bed [N $m^{-2}$] |
| $\Delta P$ | Pressure drop per unit height of packing [Pa $m^{-1}$] |
| $d_{eq}$ | Packing equivalent diameter [m] |
| $d_p$ | Particle diameter [m] |
| $\varepsilon$ | Void fraction [-] |
| $F_{LG}$ | Flow parameter [-] |
| $f_0$ | Friction factor for flow past a single particle [-] |
| $F_{l,min}$ | Minimum liquid flow rate [mol $hr^{-1}$] |
| $Fr$ | Froude number [-] |
| $G$ | Gas flow [kg $s^{-1}$] |
| $g_c$ | Gravity conversion factor (unity in SI system) [-] |
| $g$ | Gravitational constant [m $s^{-2}$] |
| $h_0$ | Liquid hold-up below the loading point(unity in SI system) [$m^3$ $m^{-3}$] |

| | |
|---|---|
| $h$ | Liquid hold-up in a packed bed [$m^3$ $m^{-3}$] |
| $L$ | Liquid flow [kg $s^{-1}$] |
| $M_l$ | Liquid molar mass [-] |
| $\mu_g$ | Gas viscosity [kg $m^{-1}$ $s^{-1}$] |
| $R$ | Gas constant [J $mol^{-1}$ $K^{-1}$] |
| $Re_g$ | Gas Reynolds number [-] |
| $r_E$ | Reaction rate [mol $L^{-1}$ $s^{-1}$] |
| $\rho_g$ | Gas density [kg $m^{-3}$] |
| $\rho_l$ | Liquid density [kg $m^{-3}$] |
| $T$ | Temperature [K] |
| $\theta$ | Angle of flow channel based on horizontal [deg] |
| $u_{ge}$ | Effective gas velocity inside the flow channel [m $s^{-1}$] |
| $u_g$ | Superficial gas velocity [m $s^{-1}$] |
| $u_l$ | Superficial liquid velocity [m $s^{-1}$] |
| $Z$ | Total height of packing [m] |

# References

[1] Jeromin, L. M.; Bremus, N.; Peukert, E. *Fette, Seifen, Anstrichmittel* **1981,** *83,* 493-504.

[2] Zhou, M. *Modelisation de reacteurs d'esterification fonctionnement semi-continu et continu,* Thesis, L'institut national polytechnique de Toulouse, 1983.

[3] Zaidan, M.; Domenech, S.; Gilot, B. *Entropie* **1986,** *129,* 62-68.

[4] Steinigeweg, S.; Gmehling, J. *Ind. Eng. Chem. Res.* **2003,** *42,* 3612-3619.

[5] Bhatia, S.; Ahmad, A.; Mohamed, A.; Chin, S. *Chem. Eng Sc.* **2006,** *61,* 7436-7447.

[6] Schleper, B.; Gutsche, B.; Wnuck, J.; Jeromin, L. *Chem. Ing. Tech.* **1990,** *62,* 226-227.

[7] Bock, H.; Wozny, G.; Gutsche, B. *Chem. Eng. Process.* **1997,** *36,* 101-109.

[8] Noeres, C.; Kenig, E.; Górak, A. *Chem. Eng. Process.* **2003,** *42,* 157-178.

[9] Fair, J.; Steinmeyer, D.; Penney, W.; Crocker, B. Section 14: Gas absorption and gas-liquid system design. In *Perry's Chemical Engineers' Handbook*; Perry, R.; Green, D.; Maloney, J., Eds.; McGraw-Hill: 1999.

[10] Spiegel, L.; Meier, W. *I. Chem. E. Symposium Series 104(Distill. Absorpt. 1987, Vol. 1* **1988,** *104 (Distill. Absorpt. 1987, Vol. 1),* A203-A215.

[11] Bravo, J.; Rocha, J.; Fair, J. *Hydrocarbon proc.* **1986,** *65,* 45-49.

[12] Fair, J.; Bravo, J. *Chem. Eng. Prog.* **1990,** *86,* 19-29.

[13] Stichlmair, J. Distillation and Rectification. In *Ullmann's Encyclopedia of Industrial Chemistry*; John Wiley & Sons, Inc.: 2002.

[14] de Haan, A.; Bosch, H. *Fundamentals of Industrial Separations;* 2006.

[15] Stichlmair, J.; Bravo, J.; Fair, J. *Gas Separation & Purification* **1989,** *3,* 19-28.

[16] Bhatia, S.; Mohamed, A.; Ahmad, A.; Chin, S. *Comp. Chem. Eng.* **2007,** *31,* 1187-1198.

[17] Sulzer Chemtech, *Structured Packings, for Distillation, Absorption and Reactive Distillation 22.13.06.20-I.05-30* .

[18] Verhoeye, L. *J. Chem. Eng. Data* **1968,** *13,* 462-467.

[19] Teodorescu, M.; Aim, K.; Wichterle, I. *J. Chem. Eng. Data* **2001,** *46,* 261-266.

[20] Hong, G.; Lee, M.; Lin, H. *Fluid Phase Equilibria* **2002,** *202,* 239-252.

# Chapter 6

# Continuous processes versus Batch Process

*In this chapter the process model from Chapter 5 is used to construct a conceptual design for the esterification of myristic acid with isopropanol through Reactive Distillation (packed and tray column). A parameter optimisation study is performed to investigate the influence of the different process parameters. Finally all results are integrated in conceptual designs for the industrial scale Reactive Distillation process, which are evaluated against the batch process based on required reaction volumes. Also a Bubble Column is investigated, since a much larger liquid hold-up can be obtained. The required reactor volume can be decreased with 27 or 79%, allowing a maximum temperature of respectively 170 and 220°C, using a packed Reactive Distillation column. Using a tray Reactive Distillation column and a maximum temperature of 220°C, the required reactor volume can be decreased with 93%. Due to the less favourable mass transfer characteristics of the Bubble Column, in here the required reactor volume can only be decreased with 78%. When a temperature of 220°C is allowed in the column, the tray Reactive Distillation is the preferable process for the esterification of myristic acid isopropanol, based on the required reaction vol-*

*umes. The influence of the maximum column temperature and the influence of a larger liquid hold-up per stage as a result of a different column configuration are of equal importance for the required reaction volume.*

## 6.1 Introduction

In this chapter the developed process model, which was proposed and validated in Chapter 5 is used to construct a conceptual design for the esterification of myristic acid with isopropanol through Reactive Distillation. Because packed columns have a small liquid hold-up also a Reactive Distillation tray column and a packed reactive Bubble Column (Bubble Column containing structured packing) are investigated. Those could be even more interesting alternatives. The tray Reactive Distillation column and the Bubble Column are introduced in this chapter for the first time in this thesis. Therefore first the theory of modelling those two processes, focussing on the differences compared to the packed Reactive Distillation column, are discussed.

For the packed Reactive Distillation column a full parameter optimisation is performed to investigate the influence of the different process parameters. For the tray Reactive Distillation column and the Bubble Column a simplified parameter optimisation is performed. All results are integrated in conceptual designs for the industrial scale Reactive Distillation processes (packed and tray) and the Bubble Column process, which are evaluated against the batch process. Because insufficient information on the batch process is available to make a detailed simulation model, this evaluation was done based on required reaction volumes.

The processes are designed for are a production capacity of 1000 kg/hr (3697 mol/hr) ester, which is representative for an industrial process [1] and 99% conversion of the myristic acid. The process is attractive for the industry when a 99.0% conversion of myristic acid and a 99.0% product purity is obtained.

To prevent ester colouration due to degradation and undesired side product formation, the temperature in the batch process is restricted to 170°C. [2, 3]

In a Reactive Distillation process the residence times are expected to be much lower. Therefore, it is expected that the temperature restriction is not that tight in Reactive Distillation. Therefore both a restriction of 170°C and 220°C are investigated.

## 6.2 Theory

### 6.2.1 Modelling Reactive Distillation

A Reactive Distillation process model consists of sub-models for mass transfer, reaction kinetics and hydrodynamics. The completion of these sub-models can vary from simple to complex, as described in Chapter 4. [4]

It was described that the Damköhler number can be used to see if a Reactive Distillation process is controlled by chemical equilibrium, phase equilibrium or something in between those two extremes.

For the system used in this research $Da \approx 0.05$ for the packed column and $Da \approx 0.12$ for the tray column. This is in both cases much smaller than 0.5, which means that the system can be assumed to be dominated by phase equilibrium, just like in the feasibility analysis in Chapter 4.

In this chapter the simplest possible model for all three parts (mass transfer, reaction kinetics and hydrodynamics) is used. As explained above, the mass transfer can be described by physical equilibrium. This equilibrium stage model is described in Chapter 4, section 4.2.1. Chemical equilibrium is not reached, therefore the reaction will be described by a kinetic model of the bulk reaction. The hydrodynamics for the packed column are described by liquid hold-up and pressure drop correlations, which can be found in Chapter 5. For the tray column, the hydrodynamics are considered to be ideal (plug flow).

#### Mass transfer packed column

Because the equilibrium model is used for modelling the Reactive Distillation column, mass transfer correlation are not included. However, they can be used to calculate the the height equivalent to a theoretical plate (HETP). Rocha et

al. [5] developed a model for describing mass transfer in distillation columns containing structured packings. The gas side mass transfer coefficient is based on the wetted-wall relationship. Dimensionless Sherwood ($Sh$), Reynolds($Re$) and Schmidt($Sc$) numbers are combined as follows:

$$Sh = 0.054 Re^{0.8} Sc^{0.33} \tag{6.1}$$

$$\frac{k_g S}{D_g} = 0.054 \left( \frac{(u_{ge} + u_{Le}) \rho_g S}{\mu_g} \right)^{0.8} \left( \frac{\mu_g}{D_g \rho_g} \right)^{0.33} \tag{6.2}$$

where the characteristic length S is the side dimension of a corrugation cross section (8.9 mm for Sulzer BX), for the diffusion constant $D_g$ a typical value of $1{\cdot}10^{-5}$ [6] is used and the effective velocities ($u_g e$ and $u_{Le}$)are defined as:

$$u_{ge} = \frac{u_{gs}}{\varepsilon (1 - h_l) \sin \theta} \tag{6.3}$$

$$u_{Le} = \frac{u_{Ls}}{\varepsilon h_l \sin \theta} \tag{6.4}$$

with $\theta$ is the inclination angle of the flow channel (60° for Sulzer BX) and $u_{gs}$ and $u_{Ls}$ the superficial velocities.

For the prediction of the liquid phase mass transfer coefficient a simple penetration model is used, with exposure time based on liquid flow across one corrugation face of the packing. For those parts of packed bed that do not encourage rapid surface renewal a correction factor $C_E \sim 0.9$ is introduced.

The liquid phase mass transfer coefficient can be calculated by

$$k_L = 2 \left( \frac{D_L C_E u_{Le}}{\pi S} \right)^{0.5} \tag{6.5}$$

For the diffusion constant $D_L$ a typical value of $1{\cdot}10^{-8}$ [6] is used.

The heights of the transfer units are then determined by the conventional relationships for distillation:

$$H_{OG} = H_G + \lambda H_L \tag{6.6}$$
$$= \frac{u_{gs}}{k_g a_e} + \lambda \frac{u_{Ls}}{k_L a_e} \tag{6.7}$$

$H_G$ is the height of a gas phase transfer unit, $H_L$ is the height of a liquid phase transfer unit and $H_{OG}$ is the height of an overall transfer unit. $k_g$and $k_L$ are obtained from Eq. 6.1 and 6.5. While the wetting of the packing surface is incomplete $a_e$ is the effective interfacial area, which is correlated to the total surface area of the packing $a$ as follows:

$$\beta = \frac{a_e}{a} = 1 - 1.203\left(\frac{uLs^2}{Sg}\right)^{0.111} \tag{6.8}$$

$\lambda$ is the stripping factor $(mV/L)$, with $m$ is the slope of the equilibrium curve $(= dy^*/dx)$. Subsequently, the value of the height equivalent to a theoretical plate (HETP) can be calculated:

$$HETP = H_{OG}\frac{\ln \lambda}{\lambda - 1} \tag{6.9}$$

In Table 6.1 the values for the mass transfer coefficients and the heights of the transfer units are given. The HETP for the isopropanol-myristic acid system varies between 0.11 and 0.30, with an average value of 0.21, dependant of the position on the equilibrium line. This average value is in the same order of magnitude as the value of 0.20 reported in literature [2]. It should be noted that the calculation is based on the equilibrium of a binary system and typical values for the diffusion coefficients were taken, which can explain the small deviation.

| | |
|---|---|
| $k_L$ [m $s^{-1}$] | $3.2 \cdot 10^{-4}$ |
| $k_g$ [m $s^{-1}$] | $1.6 \cdot 10^{-2}$ |
| $H_G[m]$ | 0.04 |
| $H_L$ [m] | 0.25 |
| $H_{OG}$ [m] | 0.04-2.50 |
| HETP [m] | 0.11-0.30 |

Table 6.1: Mass transfer coefficients and heights of the transfer units for the packed Reactive Distillation

### Hydrodynamics tray column

The liquid hold-up in a sieve tray column consists of the hold-up below the weir ($h_{l,bw}$) and the hold-up over the weir ($h_{l,ow}$) [7]:

$$h_l = h_{l,ow} + h_{l,bw} \tag{6.10}$$

The liquid hold-up over the weir is dependant of the flow regime. In the spray regime the liquid is dispersed almost completely into small droplets due to the force of the vapour jets. The transport of liquid over the weir occurs like spraying. In the emulsion regime the vapour jets are bent over and dispersed into bubbles. The transport over the weir is now mainly continuous liquid flow containing emulsified vapour. The transition from spray flow to emulsion flow is determined by the ratio of the horizontal liquid momentum flow and the vertical vapour momentum flow [7]:

$$\frac{u_l}{u_g}\left(\frac{\rho_l}{\rho_g}\right)^{0.5} = \frac{FP}{bh_l} > 3.0 \tag{6.11}$$

where $b$ is the weir length per unit bubbling area and $FP$ a flow parameter.

In the emulsion regime ($(FP/bh_l) > 3-4$) the liquid-up above the weir is calculated with the Francis equation:

$$h_{l,ow} = 1.04 g^{-0.33}\left(\frac{u_l}{b}\right)^{0.67} \tag{6.12}$$

For the spray and mixed regime ($(FP/bh_l) < 3-4$) Zuiderweg [7] deter-

mined the following:

$$h_{l,ow} = 2.4g^{-0.33}\left(\frac{u_l}{b}\right)^{0.67}\left(\frac{FP}{bh_l}\right)^{-0.33} \tag{6.13}$$

Zuiderweg [7] also determined the hold-up below the weir:

$$h_{l,bw} = 0.5H_w^{0.5}p^{0.25}\left(\frac{FP}{b}\right)^{0.25} \tag{6.14}$$

where $H_w$ is the weir height and $p$ the pitch of holes in sieve plate.

### 6.2.2 Modelling a Bubble Column

A Bubble Column can be compared to a Reactive Distillation column: both are gas-liquid contactors. Only in a Bubble Column the liquid is an continuous phase where the gas is bubbling through while in a distillation column both phases are disperse. In a Bubble Column mass transfer plays an important role. While for the modelling of the Reactive Distillation the mass transfer was considered equilibrium-based, for the Bubble Column a rate-based model should be used. This is done with the non-equilibrium stage model. The non-equilibrium stage model can be modelled in Aspen Plus using the RATEFRAC model. By changing the relation for the mass transfer coefficient using a FORTRAN user subroutine, the model can be used to simulated a Bubble Column.

#### Non-equilibrium stage model

At first the non-equilibrium stage model for a non-reactive system will be described. The component molar balances for the vapour and liquid-phases are

$$V_j y_{i,j} - V_{j+1} y_{i,j+1} - f_{i,j}^V + \mathbb{N}_{i,j}^V = 0 \tag{6.15}$$

$$L_j x_{i,j} - L_{j-1} x_{i,j-1} - f_{i,j}^L + \mathbb{N}_{i,j}^L = 0 \tag{6.16}$$

in where $\mathbb{N}_{i,j}$ is the interfacial mass transfer rate and is the product of the molar flux and the net interfacial area. The overall molar balances are obtained by summing Eq. 6.15 and 6.16 over the total number of components in the mixture. The $\mathbb{N}_{i,j}$ are obtained from a modified Maxwell-Stefan equation

$$\frac{x_{i,j}}{RT_j}\frac{\partial \mu^L_{i,j}}{\partial \eta} = \sum_{k=1}^{c} \frac{x_{i,j}\mathbb{N}^L_{k,j} - x_{k,j}\mathbb{N}^L_{i,j}}{c^L_{t,j}(\kappa^L_{i,k}a)_j} \tag{6.17}$$

The relation for the vapour phase is similar to the one for the liquid phase. The $\kappa^L_{i,k}$ represents the mass transfer coefficient of the $i-k$ pair in the liquid phase and $a$ is the interfacial area.
The enthalpy balances are

$$V_j H^V_j - V_{j+1}H^V_{j+1} - F^V_j H^{VF}_j + \mathbb{E}^V_j + Q^V_j = 0 \tag{6.18}$$

$$L_j H^L_j - L_{j-1}H^L_{j-1} - F^L_j H^{LF}_j + \mathbb{E}^L_j + Q^L_j = 0 \tag{6.19}$$

The interphase energy transfer for the liquid phase is

$$\mathbb{E}^L_j = -h^L_j a\frac{\partial T^L}{\partial \eta} + \sum_{i=1}^{c} \mathbb{N}^L_{i,j}H^L_{i,j} \tag{6.20}$$

In where $h^L_j$ is the heat transfer coefficient in the liquid phase. The relation for the vapour phase is similar to that of the liquid phase. At the vapour-liquid interface phase equilibrium is assumed

$$y_{i,j|I} = K_{i,j}x_{i,j|I} \tag{6.21}$$

The subscript $I$ denotes the equilibrium compositions and $K_{i,j}$ is the vapour-liquid equilibrium ratio for component $i$ on stage $j$.
Besides the equation mentioned above the summation equations for the mole fractions in both phases and equations expressing the continuity of fluxes of mass and energy across the the interface are needed. Furthermore the pressure drop across a stage is taken into account

$$p_j - p_{j-1} - (\Delta p_{j-1}) = 0 \tag{6.22}$$

in where $p_j$ and $p_{j-1}$ are the stage pressure and $\Delta p_{j-1}$ is the pressure drop per tray for stage $(j-1)$ to stage $j$. [8]

Extending the non-equilibrium stage model for a reactive system is not as it is for the equilibrium stage model in which we add a term to account for reaction to the liquid phase material balances. [8]

In case of a homogeneous reaction the liquid phase component molar balance becomes

$$L_j x_{i,j} - L_{j-1} x_{i,j-1} - f^L_{i,j} - N^L_{i,j} - \sum_{m=1}^{r} \nu_{i,m} R_{m,j} \varepsilon_j = 0 \tag{6.23}$$

where $R_{m,j}$ is the rate of reaction $m$ on stage $j$, $\nu_{i,m}$ represents the stoichiometric coefficient of component $i$ in reaction $m$ and $\varepsilon_j$ represents the reaction volume on stage $j$. For homogeneous reaction this equals the total liquid hold-up on stage $j$. [8]

### Mass transfer

The mass transfer between the gas and the liquid phase in a Bubble Column, accompanied with a slow reaction [9], can be described by the volumetric mass-transfer coefficient $k_L a$, which is the liquid phase mass transfer coefficient $k_L$ multiplied by the specific interfacial area $(a)$. The gas phase resistance can usually be neglected. $k_L$ depends on the gas flow rate, type of sparger and gas-liquid system. The mass transfer coefficient and the gas rate are proportional to one another. [10]

Little information can be found on quantitative relations for the mass transfer coefficients in a packed Bubble Column using structured packings. Sawant et al. [11] investigated the mass transfer in a packed Bubble Column using a wire gauze packing for the absorption of carbon dioxide diluted with air in sodium carbonate-sodium bicarbonate buffers. Because Sulzer BX packing is a wire gauze packing this relation will be used in this work:

$$k_L a = 0.008 u_G^{0.4} \tag{6.24}$$

and

$$a = 160 u_G^{0.4} \tag{6.25}$$

In Table 6.2 the physical properties of the system used by Sawant et al. [11] and the system of the present work are compared. Because no concentrations of the sodium carbonate-sodium bicarbonate buffers are known, it is assumed that the properties are close to that of water. The operating temperature used by Sawant et al. [11] is assumed to be 273K. The physical properties of isopropanol and myristic acid were taken from the Aspen Plus simulations.

| | Temperature [K] | Density [kg $m^{-3}$] | Surface Tension [N $m^{-1}$] | Viscosity [Pa.s] |
|---|---|---|---|---|
| Carbon dioxide [12] | 273 | 1.82 | - | $1.5{\cdot}10^{-5}$ |
| Water [12] | 273 | 998.2 | $7.4{\cdot}10^{-2}$ | $1.0{\cdot}10^{-3}$ |
| Isopropanol | 443 | 10.3 | - | $1.5{\cdot}10^{-4}$ |
| Myristic acid | 443 | 780.7 | $1.9{\cdot}10^{-2}$ | $8.4{\cdot}10^{-4}$ |

Table 6.2: Physical properties of the vapour and liquid streams in the pilot column

It should be noted that in the present work a different gas-liquid system is used of which the physical properties are not comparable: the actual mass transfer coefficient may be different from the used correlation.

In order to check if the assumption of neglecting in the gas phase resistance is correct, it will be estimated assuming the same relation as for the packed distillation column can be used. Because in a Bubble Column there is no liquid film, the bubble diameter should be used instead of the side dimension of a corrugation cross section, The bubble diameter ($d_b$) can be calculated from the interfacial surface area and the gas fraction [11]:

$$a = \frac{6\varepsilon_G}{d_b} \tag{6.26}$$

The gas side resistance can be neglected when

$$\frac{1}{k_g} \ll \frac{1}{mk_L} \tag{6.27}$$

with $m$ being the the distribution coefficient, which represents the ratio of the concentration in the liquid phase and the concentration in the vapour phase:

$$m = \frac{c_{iL}}{c_{iV}} = \left(\frac{c_L}{c_V}\right)_{equilibrium} \tag{6.28}$$

In Table 6.3 the values for the mass transfer coefficients can be found.

| | |
|---|---|
| $k_L$ [m $s^{-1}$] | $5.0 \cdot 10^{-5}$ |
| $k_g$ [m $s^{-1}$] | $2.5 \cdot 10^{-2}$ |

Table 6.3: Mass transfer coefficients in the Bubble Column

With a distribution coefficient along the column between 0.14 and 0.68, Eq. 6.27 holds, thus the gas side resistance can be neglected.

The heights of the transfer units are then determined following the relations used for the distillation. For the effective surface area the interfacial area is used.

| | |
|---|---|
| $H_G$ [m] | 0.01 |
| $H_L$ [m] | 0.14 |
| $H_{OG}$ [m] | 0.01-4.50 |
| HETP [m] | 0.04-0.50 |

Table 6.4: Heights of the transfer units of the Bubble Column

In Table 6.4 the values for the mass transfer coefficients and the heights of the transfer units are given. The HETP for the isopropanol-myristic acid system varies between 0.04 and 0.05, with an average value of 0.08, dependant of the position on the equilibrium line. This average value is in the same order of magnitude as the value of 0.20 reported in literature [2]. It should be noted

that the calculation is based on the equilibrium of a binary system and typical values for the diffusion coefficients were taken, which can explain the small deviation.

### Hydrodynamics

The gas hold-up is one of the most important operating parameters because it represents the total volume of bubbles throughout the column. Therefore the interfacial area and the mass transfer between the gas and liquid phase are proportional to the gas hold-up. The gas hold-up depends mainly on gas flow rate, but also on the physical properties of the gas-liquid system involved. [9, 10]. Unlike normal Bubble Columns, the effect of the column diameter on gas hold-up seems negligible in packed Bubble Columns using wire gauze packing. [11]

The gas hold-up is defined as the volume of the gas phase divided by the total volume of the dispersion [10]:

$$\varepsilon_G = \frac{V_G}{V_G + V_L} \tag{6.29}$$

Many authors studied the influence of the superficial gas velocity on the gas hold-up. [11, 13–17] However, little information can be found on quantitative relations for the mass transfer coefficients in packed Bubble Column using structured packings. Sawant et al. [11] investigated the gas hold-up in a packed Bubble Column using a wire gauze packing for the absorption of carbon dioxide diluted with air in sodium carbonate-sodium bicarbonate buffers. Because Sulzer BX packing is a wire gauze packing this relation is used in this work:

$$\varepsilon_G = \frac{0.017}{\varepsilon} u_G^{0.5} \tag{6.30}$$

It should be noted that in the present work a different gas-liquid system is used, the actual gas hold-up may be different from the used correlation. The value calculated for the gas hold-up is used to calculate the stage liquid hold-up which is given by:

$$h_l = (1 - \varepsilon_G)\left(\frac{\varepsilon_\kappa V_c}{n}\right) \tag{6.31}$$

where $\varepsilon_\kappa$ is the void fraction of the packing.

### Operating region

While operating a Bubble Column, three flow regimes can be distinguished [10]:

***Homogeneous flow regime*** Bubbles have a narrow bubble size distribution and are distributed relatively uniformly over the cross section of the apparatus.

***Heterogeneous flow regime*** Larger bubbles are formed, mainly in the axis of the column, which travel faster. Due to this, smaller bubbles are transported downwards, near the column wall.

***Slug flow regime*** Large bubbles are stabilised by the column wall and take on the characteristic slug shape.

In Figure 6.1 the different regimes are given for normal Bubble Columns. Lakota et al. [9] and Spicka et al. [18] reported that in the presence of internals

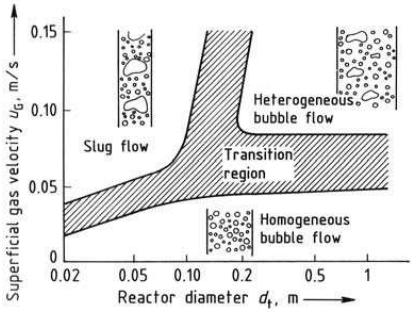


Figure 6.1: Flow regimes in Bubble Columns [10]

the homogeneous regime is extended, even up to a superficial gas velocity of 9 cm $s^{-1}$.

In the case of a slow chemical reaction small bubbles are preferred to ensure the required interfacial area [19]. This can be reached in the homogenous flow regime.

## 6.3 Modelling

To establish a feasible conceptual design for Reactive Distillation (packed and tray column) and a Bubble Column process, simulations are performed using the commercial software package Aspen Plus. First the column diameters are determined based on the vapour and liquid capacities and the desired production capacity. Subsequently, a parameter optimisation for the packed Reactive Distillation column, in which the myristic acid to isopropanol feed ratio, pressure, catalyst concentration, boil-up ratio and reflux ratio are varied, is done to obtain the optimal process configuration. Finally, based on these optimal values a conceptual design is made which is extended to the tray Reactive Distillation column and the Bubble Column.

### 6.3.1 Column sizing

The packing used in the packed Reactive Distillation column is the Sulzer BX packing. The data for this packing is already included in the software. The number of stages is estimated from HETP data used by others for Sulzer BX in literature. [2] Typical HETP values of $\sim 0.2$ $m^{-1}$ are reported in the literature.

The column diameter has been estimated using the commercial program SULPAK 3.1 from Sulzer Chemtech. The column is simulated using the RADFRAC model to generate estimates for the vapour and liquid densities, which serve as input parameters for SULPAK. The column diameter is varied till the point of 80% capacity in proportion to flooding is reached. This results in a diameter of 0.25 metres, based on a production capacity of 1000 kg $hr^{-1}$

isopropyl myristate. When the conceptual design is made it should be checked if this diameter is still valid.

For the tray column, the same diameter is used. In Aspen Plus in the tray sizing section it was checked if this was within the operating region. The minimum required diameter is 0.22 metres thus 0.25 metres is a good choice.

For the Bubble Column, the column diameter is calculated based on the different flow regimes. The Bubble Column is preferable operated in the homogeneous flow regime to ensure a large interfacial area which is beneficial for the mass transfer and subsequently the reaction rate. Lakota et al. [9] and Spicka et al. [18] reported that in the presence of internals (acrylic discs and Sulzer SMZ static mixers) the homogeneous regime is present up to a superficial gas velocity of 0.09 m $s^{-1}$. With this velocity and the production capacity of 1000 kg $hr^{-1}$ isopropyl myristate, the column diameter is calculated. Because the volume flow rate of the isopropanol depends strongly on the operating pressure, every pressure corresponds with a different diameter: an overview is given in Table 6.3.1.

| Pressure [bar] | Diameter [m] |
|---|---|
| 5 | 0.4 |
| 11 | 0.3 |
| 12 | 0.3 |
| 13 | 0.25 |

Table 6.5: Bubble Column diameters for corresponding operating pressures

### 6.3.2 Kinetics

The kinetics of the reactions are experimentally determined and are described in Chapter 3. The reaction rate for the esterification of myristic acid and isopropanol using *p*TSA is

$$r_E = 3.33 \cdot 10^5 [\text{cat}] \exp\left(\frac{-58.9 \cdot 10^3}{RT}\right)[A][B] - 2.18 \cdot 10^3 [\text{cat}] \exp\left(\frac{-45.9 \cdot 10^3}{RT}\right)[E][W] \text{ mol L}^{-1}\text{s}^{-1} \quad (6.32)$$

$r_E$ is the reaction rate, $[E]$ the concentration ester, $[A]$ the concentration alcohol, $[B]$ the concentration acid, $[W]$ the concentration water and [cat] is the catalyst concentration.

### 6.3.3 Hydrodynamics

The liquid hold-up for the packed Reactive Distillation column is calculated in Aspen Plus using the relations of Stichlmair [20] as described in Chapter 5. These values have to be specified in the model. Manual iterations have to be done till the calculated and specified values are comparable. The stage liquid-hold-up is different for every stage. To avoid complexity an average value for the stage liquid value is used.

For the tray Reactive Distillation column the liquid hold-up is calculated from Eq. 6.10 to 6.14. These equations require the input of some geometrical parameters of the tray.

The weir height will normally be between 40 to 90 mm, in the current design a value of 50 mm will be used. A good value for the weir length is 0.77 of the column diameter. The hole pitch is normally 2.5 to 4.0 times the hole diameter. In this design a pitch of 2.5 diameter is used. The preferred hole size is 5 mm. A standard tray spacing is 500 mm. [21]

For the Bubble Column the liquid hold-up is calculated from the gas hold-up, according to Eq. 6.30 and 6.31.

### 6.3.4 Thermodynamics

For the simulations in Aspen Plus a property model has to be selected. In Chapter 2 vapour-liquid equilibrium data from literature for different water-isopropanol systems [22–24] are compared to different NRTL property models in Aspen Plus.

The set of NRTL parameters developed by Aspen Tech based on data from the Dortmund Data Bank, was found to correspond the best with the experimental literature data and is therefore used further.

The unknown interaction parameters are estimated using UNIFAC, these are all parameters concerning the myristic acid or the ester. UNIFAC predicts an azeotrope between myristic acid and isopropyl myristate. It is unlikely that this will occur, because the components have similar polarities. Therefore it is better to set the interaction between those components to zero, to approximate reality.

## 6.4 Results & Discussion

### 6.4.1 Optimisation & design of the packed Reactive Distillation column

The base case used for the parameter optimisation is the RD simulation from the feasibility analysis. The pressure is 5 bar, the hold-up follows from the packing characteristics, the catalyst concentration is 0.15 M, the boil-up ratio is 1, reflux ratio is 1 and the isopropanol to myristic acid feed ratio is 1:1. In this simulation the influence of the following parameters is studied: Myristic acid to isopropanol feed ratio, pressure, catalyst concentration, boil-up ratio and reflux ratio. Three different number of stages are evaluated: 150, 200 and 300. In Figure 6.2 the influences are shown. First the parameters which cannot be optimised to obtain complete conversion are varied at constant stage liquid hold-up: Myristic acid to isopropanol feed ratio, boil-up ratio and reflux ratio. The results are verified by several simulations in which the average stage hold-

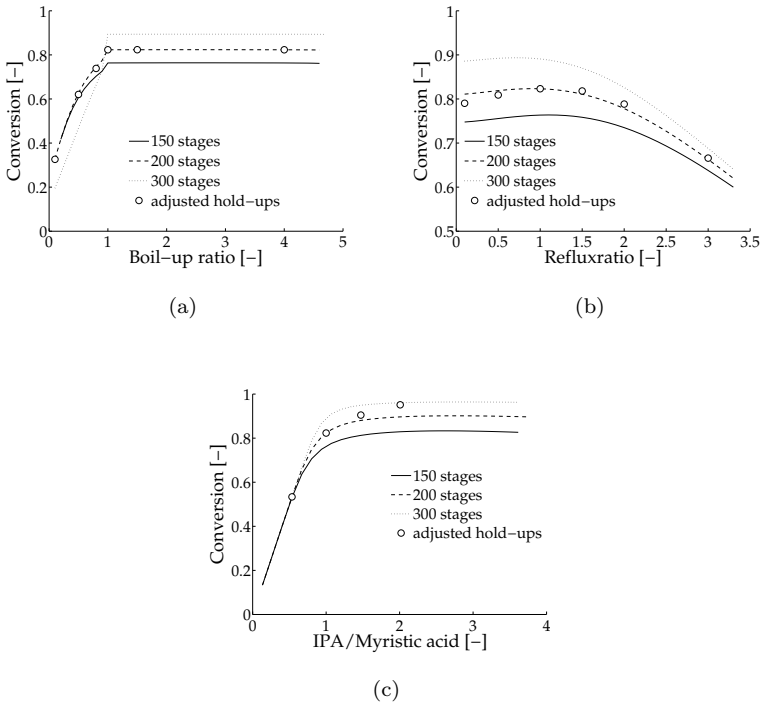


Figure 6.2: The influence of a) the boil-up ratio, b) reflux ratio and c) IPA/Myristic acid feed ratio on the conversion

up is adjusted to the operating conditions (e.g. feed flows, pressure). For all parameters, except the reflux ratio, holds that an increase in the values of the parameter results in an increase of the conversion, until a maximum value is reached. For the reflux ratio this is a rather flat optimum laying around unity, depending of the number of stages.

From these results suitable values can be selected for these parameters:

- The optimal reflux ratio is one.
- The optimal boil-up ratio is one; higher boil-up ratios do not result in a

significant higher conversion. While increasing the boil-up ratio further, a maximum increase in conversion of 0.06% can be obtained, only more energy is required.

- The optimal ipa/myristic acid feed ratio is 1.5: higher ratios can result in a increase in conversion of approximately 2% but then more isopropanol is required which also results in a higher energy consumption.

The remaining parameters (number of stages, pressure and catalyst concentration) should be used to optimise the process further. These parameters are varied while the reflux ratio is 1, the boil-up ratio is 1 and the ipa/ma feed ratio is 1.5. In Figure 6.3 the influence of the catalyst concentration is shown. Higher catalyst concentrations result in higher conversion. However, the catalyst concentration cannot be increased endlessly. The catalyst amount should be negligible compared to the myristic acid amount. In the preceding simulations a catalyst concentration of 0.15 M was used. This corresponds with 3.5 weight percent of the myristic acid amount, which is considered too much because of economical reasons. The catalyst is washed out of the product stream and will not be recycled. To keep the costs of the catalyst as low as possible a low catalyst concentration is preferred. Therefore, for the following simulations, a catalyst concentration of 0.1 M is chosen; this corresponds with 2.2 weight percent of the myristic acid amount, which is assumed to be

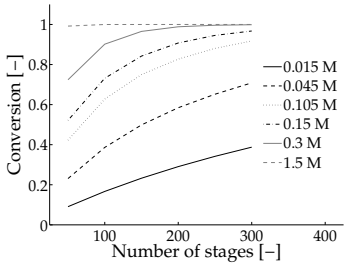


Figure 6.3: The influence of the catalyst concentration on the conversion

applicable.

With this catalyst concentration, a good combination of the pressure and number of stages needs to be found. In Figure 6.4 the conversion versus number of stages is given for different pressures. The reboiler temperature is set to 170°C or 220°C by changing the boilup-ratio. At low pressures the amount of stages has to be high, and with a small number of stages the pressure has to be high. An optimal combination can be found in the circled area. In this area 99% conversion can be obtained with the lowest possible number of stages and pressure. An operating pressure of 7 and 15 bar, respectively for the temperature restriction of 170°C and 220°C is chosen. Higher pressures hardly influence the number of stages to reach the same conversion of 99%.

For the temperature restriction of 170°C a pressure of 8 bar can increase the conversion with 3.6% with a small number of stages. With more stages this difference becomes smaller. At 300 stages and more the pressure increase results in a decrease in conversion of about 1%. This is probably caused by the fact that at 8 bar the temperature of 170°C is slightly below the water boiling point (170.5°C at 8 bar), which makes it difficult to evaporate the water. At higher pressures it is even not possible to reach such high conversions, the water cannot be evaporated anymore, which results in a decrease in conversion.

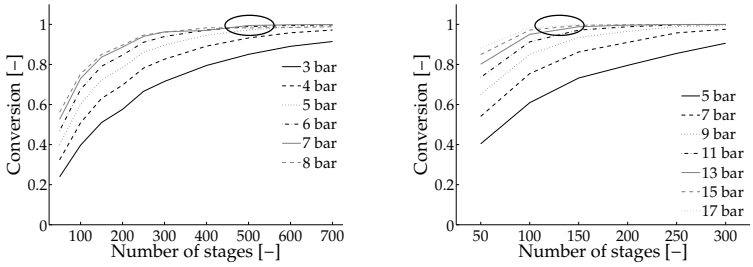


(a) (b)

Figure 6.4: The influence of the pressure on the conversion while the temperature is restricted to a maximum of a) 170°C and b) 220°C

For the temperature restriction of 220°C at a pressure of 16 bar the average increase in conversion is 0.5%, depending of the number of stages. At higher pressures this increase becomes smaller and at a pressure of 20 bar the conversion decreases, just as seen at 9 bar with a temperature restriction of 181°C, although the boiling temperature of water is not exceeded yet, this occurs at a pressure of 24 bar. Apparently, the thermodynamics hinders the evaporation of water before the boiling point is exceeded. This is supported by the activity coefficient of water which decreases with increasing pressure. At 5 bar the activity coefficient varies between 2.8 and 3.4, along the column. When increasing the pressure the whole activity coefficient profile lowers till the lowest point of the profile has reached a value of 2.0. From this point, which occurs at 20 bar when the conversion starts to decrease, the rest of the profile decreases to a value of 2.0. At 24 bar when, the maximum temperature in the column exceeds the boiling temperature of water, the activity coefficient along a major part of the column is 2.0.

At the chosen pressure the exact number of stages to obtain 99% is determined. For the temperature restriction of 170°C this results in in 419 reactive stages with an average liquid hold-up per stage of 1.16 L and a pressure of 7 bar. For the temperature restriction of 220°C this results in 121 reactive stages with an average liquid hold-up per stage of 1.26 L and a pressure of 15 bar. Because a higher temperature is allowed, a higher pressure can be applied. The liquid hold-up is correlated to the pressure drop and pressure and therefore they are different in both situations.

Because in the conceptual design the vapour flow has increased compared to the starting point in the parameter optimisation, the chosen diameter of 0.25 metres is not applicable anymore. To stay within the operating region this should be changed to 0.30 metres. A change of diameter does not effect the required liquid volume, although the number of equilibrium stages has decreased. This means that the vapour-liquid equilibrium does not play a role: the system is governed by the reaction kinetics.

A larger diameter results, at equal flows, in lower velocities. Because the liquid hold-up is dependent on those velocities a change in diameter effects

liquid hold-up per stage and therefore the required reactor volume.

For the temperature restriction of 170°C the larger diameter results in in 379 reactive stages with an average liquid hold-up per stage of 1.28 L. For the temperature restriction of 220°C this results in 108 reactive stages with an average liquid hold-up per stage of 1.42 L.

| | 170°C | 220°C |
|---|---|---|
| Pressure [bar] | 7 | 15 |
| Reactive stages [-] | 379 | 108 |
| Column height [m] | 76 | 22 |
| Liquid hold-up per stage [L] | 1.28 | 1.42 |
| Total liquid hold-up [$m^3$] | 0.49 | 0.15 |
| Total volume [$m^3$] | 5.36 | 1.53 |

Table 6.6: Results conceptual design for Reactive Distillation in a packed column

In Table 6.6 an overview is given of the resulting dimensions of the conceptual design of a packed Reactive Distillation column with two possible temperature restrictions, namely 170°C and 220°C. When the temperature restriction is 170°C the height of the reactive section of the column is 76 metres, which is not desired in this applications. With a temperature restriction of 220°C the height of the reactive section becomes 22 metres, which is more realistic. However, first it should be investigated if higher temperatures are allowed at this short residence times. The concentration profiles can be found in Appendix 6.A.

A way to decrease the height of the column is to increase the liquid hold-up per stage. Now, the liquid volume, in which the reaction takes place, is only 10% of the total volume. It is expected that with larger liquid hold-ups the total volume decreases as well as the column height. The liquid hold-up can be increased by using a tray Reactive Distillation column or a reactive Bubble Column. These will be evaluated in the next paragraphs.

Because an excess of isopropanol is applied, the product cannot be obtained in pure form at the bottom of the distillation column. The isopropanol present

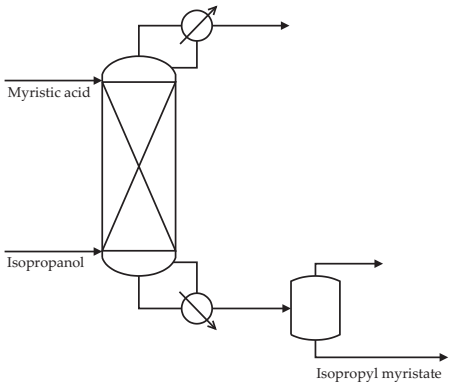


Figure 6.5: Schematic overview of the Reactive Distillation column for the production of isopropyl myristate

in the bottom stream can be easily removed through a flash. In Figure 6.5 the combination of distillation column and flash is schematically represented.

### 6.4.2 Optimisation & design of the tray Reactive Distillation column

For the tray column the outcome of the parameter optimisation will be the same as for the packed column. Only the internals have changed, which results in a different number and size of equilibrium stages. In the previous paragraph it was concluded that the vapour-liquid equilibrium does not contribute to the required liquid volume, this is mainly determined by the reaction kinetics. Therefore only the influence of the pressure on the number of stages is investigated. In Figure 6.6 the conversion versus number of stages is given for different pressures. The reboiler temperature is set to 220°C by changing the boilup-ratio. At low pressures the number of stages has to be high, and with a small number of stages the pressure has to be high. An optimal combination can be found in the circled area. In this area 99% conversion can be obtained with the lowest possible number of stages and pressure. An operating pressure of 15 bar is chosen. Higher pressures hardly have any influence on the number

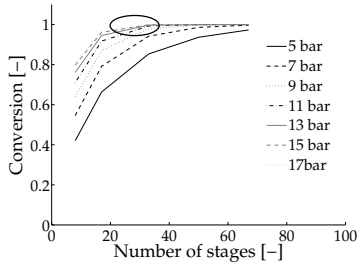


Figure 6.6: The influence of the pressure on the conversion

of stages to reach the same conversion of 99%. This is the same operating pressure as for the packed column. At a pressure of 16 bar, the average increase in conversion is 0.3%, depending of the number of stages. The same effect of thermodynamics on the conversion is seen as for the packed column. At the chosen pressure the exact number of stages to obtain 99% is determined. This results in in 22 reactive stages with an average liquid hold-up per stage of 9.57 L and a pressure of 15 bar.

In Table 6.7 an overview is given of the resulting dimensions of the conceptual design of a tray Reactive Distillation column with a temperature restriction of 220°C. The concentration profiles can be found in Appendix 6.A.

| | 220°C |
|---|---|
| Pressure [bar] | 15 |
| Reactive stages [-] | 22 |
| Column height [m] | 11 |
| Liquid hold-up per stage [L] | 9.57 |
| Total liquid hold-up [$m^3$] | 0.21 |
| Total Volume [$m^3$] | 0.54 |

Table 6.7: Results conceptual design for Reactive Distillation in a tray column

The resulting liquid volume is 40% larger compared to the packed column. In the previous paragraph it was stated that the number of equilibrium stages

does not play a role. However, at smaller values for the number of stages the number of equilibrium stages does play a role. The tray column contains a lower number of stages than the packed column (22 versus 108), therefore the required liquid volume is larger than in the packed column.

The column volume has decreased with 65% compared with the packed column. This results from the fact that the used liquid hold-up of 39% is much higher than the 10% for the packed column. The liquid hold-up can be increased even more by using a reactive Bubble Column.

### 6.4.3 Optimisation & design of the packed reactive Bubble Column

For the Bubble Column it will also be assumed that the outcome of a parameter optimisation will be the same as for the distillation column. Only the internals have changed. Therefore only the influence of the pressure on the number of stages is investigated. In Figure 6.7 the conversion versus number of stages is given for different pressures. The reboiler temperature is set to 220°C by changing the boilup-ratio. At low pressures the number of stages has to be high, and with a small number of stages the pressure has to be high. It can be seen that the pressure does not have a large influence on the number of stages as in the Reactive Distillation. For the Bubble Column the diame-

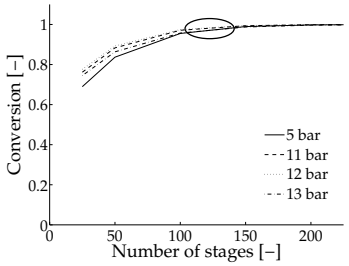


Figure 6.7: The influence of the pressure on the conversion

ter depends on the pressure: at higher pressure the diameter decreases, thus without a decreasing number of stages the volume already decreases because of the diameter. A suitable combination can be found in the circled area. In this area 99% conversion can be obtained with the lowest possible number of stages and pressure. An operating pressure of 12 bar is chosen, this is the optimal pressure: at higher pressures the conversion decreases again. This is a lower operating pressure as for the packed column. In the Bubble Column the water is not pushed out of the liquid phase to the vapour phase as described in Chapter 4, section 4.4.1. A lower driving force prevents the water from being pushed out of the liquid phase. Because of the water present in the liquid phase the backward reaction will take place and influence the conversion.

At the chosen pressure the exact number of stages to obtain 99% conversion is determined. This results in in 115 reactive stages with an average liquid hold-up per stage of 10.53 L and a pressure of 12 bar.

In Table 6.8 an overview is given of the resulting dimensions of the conceptual design for the packed Reactive Distillation column with a temperature restriction of 220°C. The concentration profiles can be found in Appendix 6.A.

| | 220°C |
|---|---|
| Pressure [bar] | 12 |
| Reactive stages [-] | 115 |
| Column height [m] | 23 |
| Liquid hold-up per stage [L] | 10.53 |
| Total liquid hold-up [$m^3$] | 1.21 |
| Total Volume [$m^3$] | 1.63 |

Table 6.8: Results conceptual design for the Bubble Column

The resulting volume is larger than the Reactive Distillation columns, although the liquid hold-up has increased enormously to 73%. The larger required total liquid hold-up can be explained by the less favourable mass transfer characteristics of the Bubble Column compared to Reactive Distillation. If kinetics were governing, the required total liquid would be equal to that of the Reactive Distillation. However the required liquid volume for the Bub-

ble Column is larger than in the Reactive Distillation column therefore mass transfer is contributing to the overall rate as well. This can be supported by the Hatta number ($Ha$) which is the ratio of the maximum possible conversion in the film to the maximum diffusional transport through the film. For higher order reactions of two components (order $n$ in component $A$ and order $b$ in component $B$), the Hatta number is defined as followed [25]:

$$Ha_A = \sqrt{\frac{\frac{2}{n+1} k_{n,m} c_{A,i,L}^{n-1} c_{B,L}^{m} D_A}{k_L^2}} \tag{6.33}$$

For the Hatta number of isopropanol (this is the component which has to be transferred from the vapour phase to the liquid phase) this can be rewritten to

$$Ha_{IPA} = \sqrt{\frac{k_1 c_{IPA,L} D_{IPA}}{k_L^2}} \tag{6.34}$$

When $Ha < 0.2$ the reaction is slow compared to the mass transfer. A large bulk liquid volume is required. When $Ha > 2$ the reaction is fast compared to the mass transfer, such that all of the reaction occurs in the film and the amount of interfacial area is controlling When $0.2 < Ha < 2$ there is a transition regime, both a large interfacial area and large bulk liquid volume are required. [25, 26] While $Ha = 0.23$ for the Bubble Column, both the kinetics and mass transfer could contribute to the overall rate.

In the Reactive Distillation process, the mass transfer was assumed ideal. Now also mass transfer should be taken into consideration which means that the overall rate is lower. Thus a longer residence time is needed to achieve the same conversion.

In the liquid composition graphs displayed in Figure 6.8 it can be seen that the isopropanol concentration in the Bubble Column is lower and the water concentration higher, compared to the Reactive Distillation column. This confirms the explanation why additional reaction volume is needed. It should be noted however that the mass transfer of the Bubble Column is based

on a single empirical correlation. Measuring the actual mass transfer for this system will give a better estimate.

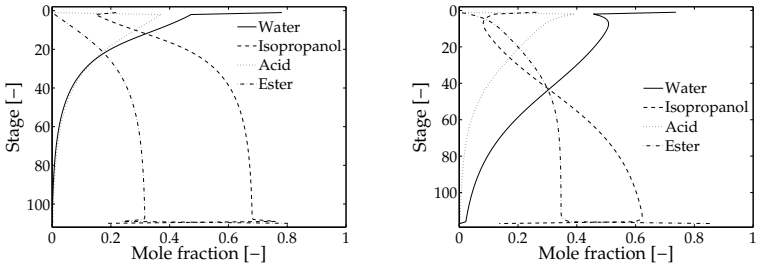


Figure 6.8: Liquid profiles in a) packed Reactive Distillation and b) Bubble Column

### 6.4.4 Batch Process

Because of equilibrium limitations, high conversions of myristic acid can be only obtained by using a large excess of alcohol. In the batch method the reactants are charged into a still pot of appropriate capacity which is fitted with an efficient fractionating column, usually of the bubble-cap or packed type. The proportions of the reactants vary with the nature of the acid and alcohol. [27] In Chapter 1 some examples of the batch production of esters made from smaller acids are discussed.

Little has been published on the production of alkyl esters of fatty acids. Zhou [1] described a semi-batch process for the synthesis of methyl oleate, which corresponds with the general description of the batch production of esters given above. The same process is assumed to be used for the production of isopropyl myristate. The process consists of a reactor and a condenser or rectifying columnn. The myristic acid is charged in the reactor in advance while the isopropanol is fed continuously in time. To prevent colouration of

isopropyl myristate the temperature should not exceed 170°C [2, 3]. The operating pressure will be around 6 bar. [28, 29] The vapour of produced water and non-consumed isopropanol is separated in the rectification column and the isopropanol is recycled back into the reactor. Because isopropanol and water form an azeotrope, part of the isopropanol will be drawn off. In order to prevent a large excess of isopropanol it is fed continuously at a slow rate, such that all added isopropanol will react immediately. This results in a very long batch time. A typical batch time of 8-12 hours is assumed. [28, 29]

Insufficient information is available to make a detailed simulation model of the batch process. Therefore a rough estimation on the required reaction volume is made, which will be compared with the required volume for the Reactive Distillation process. The estimation of the reaction volume is made based on the batch time, production capacity and the density of isopropyl myristate, assuming that the concentration of isopropanol is negligible due to the continuous feed and recycle. Depending on the batch time, the reaction volume will vary from 6 to 9 cubic metres, see Table 6.9. For the comparison the average of these batch times (ten hours) will be used.

| Batch time [hr] | Volume [$m^3$] |
|---|---|
| 8 | 6 |
| 10 | 7 |
| 12 | 9 |

Table 6.9: Required reaction volume for the batch process depending of the batch time

### 6.4.5 Comparison

In Figure 6.9 the required reaction volumes and the corresponding liquid volumes of the batch process, the packed Reactive Distillation column with a temperature restriction of 170°C and 220°C,the tray Reactive Distillation column with a temperature restriction of 220°C and the packed Bubble Column with a temperature restriction of 220°C, as discussed before, are depicted. The

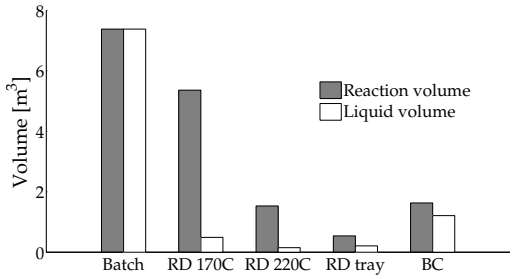


Figure 6.9: Required reaction volumes and liquid volumes in the batch process and continuous processes

total required reaction volume for the Reactive Distillation with a temperature restriction of 170°C has decreased with 27% compared to the reaction volume in the batch process. Despite this enormous decrease in volume, the height of the Reactive Distillation column is 76 metres, which is too high to realise. When the temperature restriction is 220°C instead of 170°C, the reaction volume can be decreased even more (79% in relation to the reaction volume in the batch process), and the height of the Reactive Distillation column is now realistic: 22 metres. However, first it should be investigated if higher temperatures are allowed at this short residence times.

The resulting liquid volume of the tray column is 40% larger compared to the packed column. Unlike stated before, at small number of stages the number of equilibrium stages does not play a role, therefore the required liquid volume is larger than in the packed column. The column volume had decreased with 65% compared to the packed column, and with 93% compared to the batch process. This results from the fact that the used liquid hold-up of 39% is higher than the 10% for the packed column.

It was expected that the required total volume of the Bubble Column would be smaller than the Reactive Distillation column, due to the higher hold-up. However the required reactor volume has only decreased with 78% compared to

the batch process, this is probably caused by the less favourable mass transfer characteristics of the Bubble Column.

When a temperature of 220°C is allowed in the column, the tray Reactive Distillation is the preferable process for the esterification of myristic acid isopropanol, based on the required reaction volumes.

## 6.5 Conclusion

A conceptual design for the industrial scale Reactive Distillation process (packed, tray and bubble Column) for the esterification of myristic acid with isopropanol was constructed and evaluated against the batch process.

The required reaction volume can be decreased with 27 or 79%, allowing a maximum temperature of respectively 170 and 220°C, using a packed Reactive Distillation. Using a Reactive Distillation tray column and a maximum temperature of 220°C, the required reactor volume can be decreased with 93%. Due to the less favourable mass transfer characteristics of the Bubble Column, the required reaction volume can only be decreased with 78%. When a temperature of 220°C is allowed in the column, the tray Reactive Distillation is the preferable process for the esterification of myristic acid isopropanol, based on the required reaction volumes.

The column configuration, which results in a different liquid hold-up per stage, can cause a decrease in required column volume of 67%. The maximum column temperature has a comparable influence: an increase of 50°C decreases the column volume with 71%. Thus, the column temperature and the used internals are equally important for the column volume.

## Nomenclature

$[A]$ Fatty acid concentration [mol $L^{-1}$]
$[B]$ Alcohol concentration [mol $L^{-1}$]

| | |
|---|---|
| $[E]$ | Ester concentration [mol $L^{-1}$] |
| $[W]$ | Water concentration [mol $L^{-1}$] |
| [cat] | Catalyst concentration [M] |
| $a$ | Interfacial area [$m^2$] |
| $a_e$ | Effective interfacial area [$m^{-1}$] |
| $\beta$ | Ratio of effective to toatal packing surface area [-] |
| $b$ | Weir lenght per unit bubbling area [$m^{-1}$] |
| $c$ | Concentration [mol $L^{-1}$] |
| $c$ | Number of components [-] |
| $d_b$ | Bubble diameter [m] |
| $\mathbb{E}$ | Energy transfer rate [J $s^{-1}$] |
| $\varepsilon$ | Reaction volume [$m^3$] |
| $\varepsilon_G$ | Fractional gas hold-up [-] |
| $\varepsilon_\kappa$ | Void fraction of the packing [-] |
| $\eta$ | Distance along diffusion path [-] |
| $F$ | Feed stream [mol $s^{-1}$] |
| $f$ | Component feedstream [mol $s^{-1}$] |
| $FP$ | Flow parameter [-] |
| $g$ | Gravitational constant [m $s^2$] |
| $p$ | Pitch of holes in sieve plate [m] |
| $H$ | Molar enthalpy [J $mol^{-1}$] |
| $Ha$ | Hatta number [-] |
| $H_w$ | Weir height [m] |
| $h$ | Heat transfer coefficient [W $m^{-2}$ $K^{-1}$] |
| $H_G$ | Height of a gas phase transfer unit [m] |
| $H_L$ | Height of a liquid phase transfer unit [m] |
| $H_{OG}$ | Height of an overall transfer unit [m] |
| $h_{l,bw}$ | Liquid hold-up below the weir [m] |

| | |
|---|---|
| $h_{l,ow}$ | Liquid hold-up over the weir[m] |
| $h_l$ | Liquid hold-up [m] |
| $h_l$ | Liquid hold-up per stage [$m^3$] |
| $K$ | Vapour-liquid equilibrium constant [-] |
| $k_1$ | Reaction rate constant [L $mol^{-1}$ $s^{-1}$] |
| $\kappa$ | Mass transfer coefficient [m $s^{-1}$] |
| $k_La$ | liquid side mass transfer coefficient[$s^{-1}$] |
| $L$ | Liquid flowrate [mol $s^{-1}$] |
| $\lambda$ | Stripping factor: $mV/L$ [-] |
| $m$ | Distribution coefficient [-] |
| $m$ | Slope of the equilibrium curve: $dy^*/dx$ [-] |
| $\mu$ | Chemical potential [J $mol^{-1}$] |
| $\mathbb{N}$ | Mass transfer rate [mol $s^{-1}$] |
| $n$ | Number of stages [-] |
| $p_j$ | Stage pressure [Pa] |
| $Q$ | Heat duty [J $s^{-1}$] |
| $R$ | Gas constant [J $mol^{-1}$ $K^{-1}$] |
| $Re$ | Reynolds number [-] |
| $R_{mj}$ | Reaction rate [mol $m^{-3}$ $s^{-1}$] |
| $r_E$ | Reaction rate [mol $L^{-1}$ $s^{-1}$] |
| $\rho_g$ | Vapour density [kg $m^3$] |
| $\rho_l$ | Liquid density [kg $m^3$] |
| $Sc$ | Schmidt number [-] |
| $Sh$ | Sherwood number [-] |
| $T$ | Temperature [K] |
| $u_{ge}$ | Effective gas velocity [m $s^{-1}$] |
| $u_{gs}$ | Superficial gas velocity [m $s^{-1}$] |
| $u_{Le}$ | Effective liquid velocity [m $s^{-1}$] |

| | |
|---|---|
| $u_{Ls}$ | Superficial liquid velocity [m $s^{-1}$] |
| $u_l$ | Liquid velocity [m $s^{-1}$] |
| $u_G$ | Superficial gas velocity [mm $s^{-1}$] |
| $u_g$ | Vapour velocity [m $s^{-1}$] |
| $V$ | Vapour flowrate [mol $s^{-1}$] |
| $V$ | Volume [$m^3$] |
| $V_c$ | Total column volume [$m^3$] |
| $x$ | Mole fraction in the liquid phase [-] |
| $y$ | Mole fraction in the vapour phase [-] |

### Subscripts

| | |
|---|---|
| $I$ | Referring to interface |
| $L$ | Referring to liquid phase |
| $V$ | Referring to vapour phase |
| $i$ | Component index |
| $i$ | Interface |
| $j$ | Stage index |
| $k$ | Alternative component index |
| $m$ | Reaction index |
| $t$ | Total |

### Superscripts

| | |
|---|---|
| $F$ | Referring to feed stream |
| $L$ | Referring to liquid phase |
| $V$ | Referring to vapour phase |

## References

[1] Zhou, M. *Modelisation de reacteurs d'esterification fonctionnement semi-continu et continu,* Thesis, L'institut national polytechnique de Toulouse,

1983.

[2] Bhatia, S.; Mohamed, A.; Ahmad, A.; Chin, S. *Comp. Chem. Eng.* **2007,** *31,* 1187-1198.

[3] Bock, H.; Wozny, G.; Gutsche, B. *Chem. Eng. Process.* **1997,** *36,* 101-109.

[4] Noeres, C.; Kenig, E.; Górak, A. *Chem. Eng. Process.* **2003,** *42,* 157-178.

[5] Rocha, J.; Bravo, J.; Fair, J. *Ind. Eng. Chem. Res.* **1996,** *35,* 1660-1667.

[6] J.K., K.; Hottel, H.; Sarofim, A.; Wankat, P.; Knaebel, K. Section 5: Heat and Mass Transfer. In *Perry's Chemical Engineers' Handbook*; Perry, R.; Green, D.; Maloney, J., Eds.; McGraw-Hill: 1999.

[7] Zuiderweg, F. *Chem. Eng Sc.* **1982,** *37,* 1441-1464.

[8] Taylor, R.; Krishna, R. *Chem. Eng. Sc.* **2000,** *55,* 5183-5229.

[9] Lakota, A.; Jazbec, M.; Levec, J. *Acta Chim. Slov.* **2002,** *49,* 587-604.

[10] Zehner, P.; Kraume, M. Bubble Columns. In *Ullmann's Encyclopedia of Industrial Chemistry*; John Wiley & Sons, Inc.: 2005.

[11] Sawant, S.; Pangarkar, V.; Joshi, J. *Chem. Eng. J.* **1979,** *18,* 143-149.

[12] NIST Chemistry WebBook, *http://webbook.nist.gov/* .

[13] Niranjan, K.; Pangarkar, V. *Chem. Eng. J.* **1984,** *29,* 101-111.

[14] Therning, P.; Ramuson, A. *Chem. Eng. J.* **2001,** *81,* 69-81.

[15] Therning, P.; Rasmuson, A. *Chem. Eng. J.* **2001,** *81,* 331-335.

[16] Bhatia, B.; K.D.P., B.; D., A.; G., H. *Chem. Eng. Process.* **2004,** *43,* 1371-1380.

[17] Oyevaar, M.; La Rie, T. d.; Sluijs, C. v. d.; Westerterp, K. *Chem. Eng. Process.* **1989,** *26,* 1-14.

[18] Spicka, P.; Martins, A.; Dias, M.; Lopes, J. *Chem. Eng. Sc.* **1999,** *54,* 5127-5137.

[19] Lakota, A.; Jazbec, M.; Levec, J. *Acta Chim. Slov.* **2001,** *48,* 453-468.

[20] Stichlmair, J.; Bravo, J.; Fair, J. *Gas Separation & Purification* **1989,** *3,* 19-28.

[21] Sinnott, R. *Chemical Engineering Design;* volume 6 of *Coulson & Richardson's Chemical Engineering* Butterworth Heinemann: Oxford, Third ed.; 1999.

[22] Verhoeye, L. *J. Chem. Eng. Data* **1968,** *13,* 462-467.

[23] Teodorescu, M.; Aim, K.; Wichterle, I. *J. Chem. Eng. Data* **2001,** *46,* 261-266.

[24] Hong, G.; Lee, M.; Lin, H. *Fluid Phase Equilibria* **2002,** *202,* 239-252.

[25] Brilman, D.; Heesink, A.; Hogendoorn, J.; Versteeg, G. *Chemische reactorkunde I, diktaat;* Universiteit Twente: 1999.

[26] Walas, S. Section 23: Chemical Reactors. In *Perry's Chemical Engineers' Handbook*; Perry, R.; Green, D.; Maloney, J., Eds.; McGraw-Hill: 1999.

[27] Markley, K. S. Esters and Esterification. In *Fatty acids*; Markley, K. S., Ed.; Interscience publishers, Inc., New York: 1961.

[28] Packet, D. "Email communication", 2009.

[29] Roessler, H. "Email communication", 2009.

# Appendix 6.A Concentration profiles

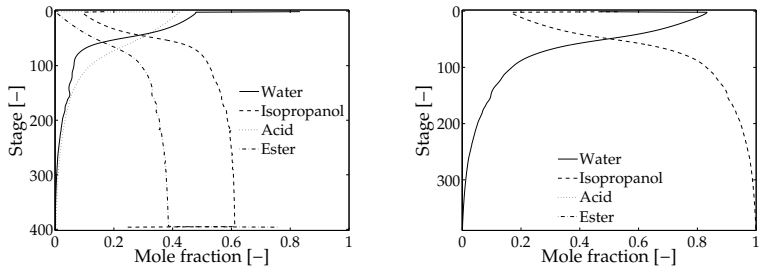


Figure 6.10: Concentration profiles of (a) liquid phase and (b) vapour phase, for the packed Reactive Distillation with a temperature restriction of 170°C

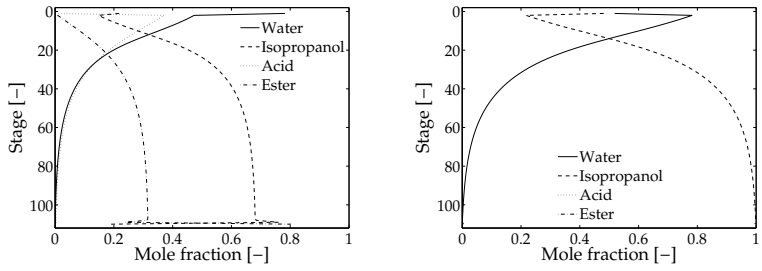


Figure 6.11: Concentration profiles of (a) liquid phase and (b) vapour phase, for the packed Reactive Distillation with a temperature restriction of 220°C

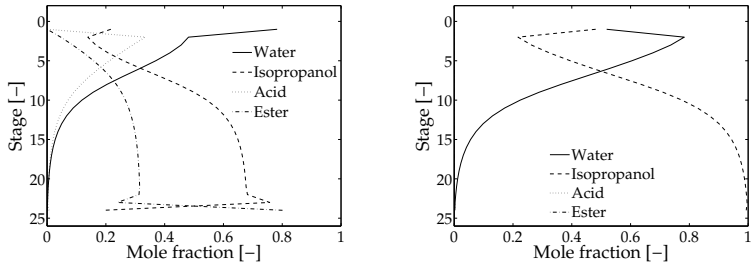


(a) (b)

Figure 6.12: Concentration profiles of (a) liquid phase and (b) vapour phase, for the tray Reactive Distillation with a temperature restriction of 220°C

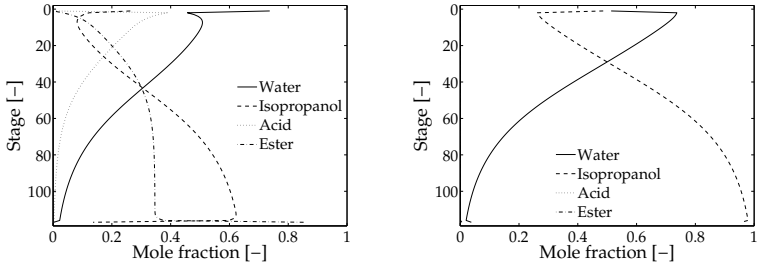


(a) (b)

Figure 6.13: Concentration profiles of (a) liquid phase and (b) vapour phase, for the reactive packed Bubble Column with a temperature restriction of 220°C

# Chapter 7

# Conclusions & Outlook

## 7.1 Conclusions

The objective of this thesis was the development of a multi-product Entrainer-based Reactive Distillation process for the synthesis of fatty acid esters using a heterogeneous catalyst, and evaluate its attractiveness compared to the current technologies.

The first step was to compile a set of selection rules to that can be used to select a suitable entrainer for Entrainer-based Reactive Distillation It was demonstrated that, due to the similarities between Entrainer-based Reactive Distillation and azeotropic distillation, the same selection rules can be applied to select a suitable entrainer. From a list of suitable entrainers for the azeotropic distillation of isopropanol and water, cyclohexane and isopropyl acetate were chosen and it was shown that both can be used as an entrainer in Entrainer-based Reactive Distillation.

In the next step a thorough evaluation of reaction kinetics had to be done. From the reaction kinetics study on the esterification of myristic acid with isopropanol with Sulphated Zirconia, Nafion SAC13 and Amberlyst 15 as catalyst, it became evident that these catalysts are not a suitable for the esterification of myristic acid with isopropanol. This was confirmed by the research

of Yalçinyuva et al. [1], in which the same reaction was investigated with Amberlyst 15 and a silica-based Degussa catalyst. As none of the investigated heterogeneous catalysts was sufficiently active for the esterification of myristic acid and isopropanol it was decided to continue with a homogeneous catalyst: *p*-toluene sulphonic acid (*p*TSA). Both the reaction with isopropanol and *n*-propanol were investigated in detail. This study showed that the reaction with *n*-propanol is considerably faster (at 373K about 3.8 times) than the reaction with isopropanol.

After the kinetics study a feasibility study was performed for the esterification of myristic acid with isopropanol and *n*-propanol. Five process configurations from conventional Reactive Distillation to Entrainer-based Reactive Distillation for the synthesis of fatty acid esters were compared. Process models for the different configurations were setup in Aspen Plus and extensive simulations were performed. This study showed convincingly that the success of Entrainer-based Reactive Distillation strongly depends on the operating conditions and reaction kinetics. Due to a combined effect of thermodynamics and kinetics the entrainer does not always improve the conversion. The amount of entrainer needed for water removal causes a decrease of the temperature in the column. This temperature decrease can have a negative influence on the conversion, because the high activation energy of the reaction cannot be overcome.

Totally unexpected and refreshing was the observation that the conventional Reactive Distillation configuration reaches the desired purity and conversion. Because of its polarity, water is pressed out of the liquid phase, in which the reaction takes place, so the reaction can reach nearly complete conversion. Since the decrease of the reaction volume due to the addition of the entrainer is rather small and the energy consumption are comparable, conventional Reactive Distillation is the preferable configuration for the esterification of myristic acid with either isopropanol or *n*-propanol.

The Aspen Plus process model for the Reactive Distillation was subsequently validated through a carefully selected set pilot plant experiments. A detailed model of the pilot plant was created for that has validity at a wide

range of operating conditions. Despite the fact that some of the experiments could not be conducted as a result of practical difficulties with the setup, the experiments correspond well with the predicted values; this makes the model very useful for the construction of a conceptual design.

Finally, the validated process model was used to construct conceptual designs for the esterification of myristic acid with isopropanol through Reactive Distillation (packed and tray column), which were evaluated against the batch process based on required reactor volumes. Also a Bubble Column was investigated, since a much larger liquid hold-up can be obtained. It was demonstrated that Reactive Distillation is an attractive process for the synthesis of isopropyl myristate, enabling a decrease in reactor volume of 84%. Due to the less favourable mass transfer characteristics of the Bubble Column, the required reactor volume can only be decreased with 78%. The column configuration, which results in a different liquid hold-up per stage, can cause a decrease in required column volume of 31%. The maximum column temperature, on the other hand, has a much larger influence: an increase of 50°C decreases the column volume with 71%. The influence of the maximum column temperature and the influence of a larger liquid hold-up per stage as a result of a different column configuration are of equal importance for the required reaction volume.

Therefore Reactive Distillation has the potential to become an economically interesting alternative, not only for fatty acid esters based on methanol and primary alcohol which is already known, but also for the production of isopropyl myristate.

## 7.2 Outlook

### 7.2.1 Heterogeneously catalysed Reactive Distillation

In this research no available heterogeneous catalyst was found that is suitable for the esterification of myristic acid with isopropanol. However, Chin et al. [2] and Bhatia et al. [3, 4] report that Reactive Distillation can be successfully

applied for the for the esterification of palmitic acid with isopropanol through Reactive Distillation with an zinc acetate catalyst supported on silica gel. They require a much smaller volume, although the reaction rate with palmitate acid is comparable to myristic acid and a heterogeneous catalyst will most likely be slower than a homogeneous catalyst. Because higher catalyst concentrations can be obtained with a heterogeneous catalysed higher reaction rates can be obtained, which result in a smaller required reaction volume.

Kiss et al. [5, 6], who worked on a research study which was part of the same project, developed a Sulphated Zirconia catalyst (UVC4) which showed high activity and selectivity for the esterification of lauric acid with a variety of primary alcohols ranging from 2-ethylhexanol to methanol. Unfortunately this particular catalyst is not commercially available, and could therefore not be supplied in sufficient quantities to be included in the present research. At a temperature of 133°C, a concentration of 0.036 M $H^+$-equivalent and a reactant ratio of 1, it shows a reaction rate of a factor four lower compared to *p*TSA. This can be seen in Figure 7.1.

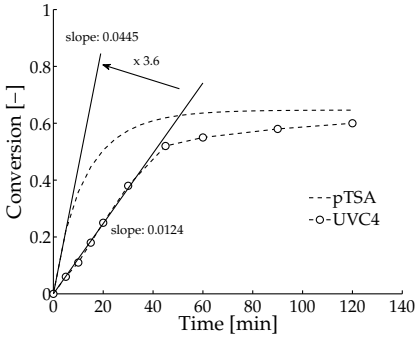


Figure 7.1: Reaction kinetics the esterification of myristic acid with isopropanol at 133°C with a reactant ratio of 1 and a H+ concentration of 0.036 M for *p*TSA and UVC4 as catalyst

Assuming a catalyst volume of 30% (catalyst volume fraction for KATAPAK SP-12 packing [7]), which was also used by Bhatia et al. [3, 4] and similar

liquid hold-ups as in the current design, the reaction rate can be 130 times higher than in the design with 0.1 M *p*TSA. For the reaction investigated by Bhatia et al. the kinetics are not available in literature. However, the reaction kinetics for the esterification of palmitic acid with isopropanol using a zinc ethanoate catalyst supported on silica gel are reported by Aafaqi et al. [8]. With those reaction kinetics the same analysis results in a reaction rate which can be 60 times higher than in the design with 0.1 M *p*TSA. When it would be possible to apply the Sulphated Zirconia catalyst developed by Kiss et al. [5, 6] in Reactive Distillation it will result in an even smaller column for the esterification of myristic acid with isopropanol, compared to the current design. Of course a more thorough study of the reaction kinetics and effects of mass transfer is necessary.

### 7.2.2 Control

Omota et al. [9, 10] found that it is possible to obtain pure fatty acid ester in a single column process, but problems may occur because the product purity is highly sensitive to changes in the reflux ratio. The optimal reflux ratio is very low, which could give control problems. Because conventional Reactive Distillation was continued is this thesis, this problem still exists. Therefore research regarding the controllability of the process is required. Another possible way to overcome the problem is to increase the reflux ratio. This will lead to a less efficient process and results in a larger required volume.

### 7.2.3 Pilot plant experiments

Validation of the model with experimental results is already shown in Chapter 5. However, not all the intended validation experiments could be performed, because of the practical difficulties to ensure no liquid level in the column and the break down of the pumps due to clogging. Therefore, it is recommended to perform more experiments in order to obtain a more stronger validation of the model before the process will be realised at industrial scale. It is advisable to adapt the equipment such that the currently experienced problems are no

longer present. Especially when a heterogeneous catalyst is applied a thorough experimental study is preferred. Heterogeneously catalysed reaction are more complex than homogeneously catalyst reactions because mass transfer within the particles and adsorption is involved.

### 7.2.4 Multi-product process

In Chapter 4 the esterification with *n*-propanol was included in the feasibility analysis. However, this was only for comparison based on the difference in reaction rates. *n*-propyl myristate is not a commercial available product and therefore not of interest. In Chapter 3 the reaction kinetics of the esterification of myristic acid with isopropanol were compared to those of the esterification of palmitic acid with isopropanol, determined by Aafaqi et al. [8]. It was shown that the reaction rate of both reaction is in the same order of magnitude. This suggest that both products can be made in same equipment. Esterifications with other alcohols will have very different reaction rates and therefore require different reaction volumes. Thus, fatty acid esters with a different alcohol are expected to be unsuitable for production in the same equipment while for fatty acid esters with a different fatty acid it is probably possible to have one plant in which multiple products can be produced. Further research on this multi-product concept is recommended.

## References

[1] Yalçinyuva, T.; Deligöz, H.; Boz, I.; Gürkaynak, M. *Int. J. Chem. Kinet.* **2008,** *40,* 136-144.

[2] Chin, S.; Ahmad, A.; Mohamed, A.; Bhatia, S. *International Journal of Chemical Reactor Engineering* **2006,** *4,* 1-17.

[3] Bhatia, S.; Ahmad, A.; Mohamed, A.; Chin, S. *Chem. Eng Sc.* **2006,** *61,* 7436-7447.

[4] Bhatia, S.; Mohamed, A.; Ahmad, A.; Chin, S. *Comp. Chem. Eng.* **2007,** *31,* 1187-1198.

[5] Kiss, A.; Dimian, A.; Rothenberg, G. *Adv. Synth. Catal.* **2006,** *348,* 75-81.

[6] Kiss, A.; Omota, F.; Dimian, A.; Rothenberg, G. *Topics in Catalysis* **2006,** *40,* 141-150.

[7] Götze, L.; Bailer, O.; Moritz, P.; Scala, C. v. *Catalysis Today* **2001,** *69,* 201-208.

[8] Aafaqi, R.; Mohamed, A.; Bhatia, S. *J. Chem. Technol. Biotechnol.* **2004,** *79,* 1127-1134.

[9] Omota, F.; Dimian, A.; Bliek, A. *Chem. Eng. Sc.* **2003,** *58,* 3159-3174.

[10] Omota, F.; Dimian, A.; Bliek, A. *Chem. Eng. Sc.* **2003,** *58,* 3175-3185.

# Dankwoord

Na ongeveer vijf jaar onderzoek is het einde van mijn promotie in zicht en kan ik terugkijken op een leuke en leerzame periode. Dit proefschrift is het tastbare resultaat en hoewel alleen mijn eigen naam op de omslag staat, had dit werk nooit gedaan kunnen worden zonder de hulp van anderen. Een aantal van hen wil ik hier bedanken voor hun bijdrage.

Allereerst een woord van dank aan André, mijn promotor; bedankt voor de mogelijkheid die je me geboden hebt om mijn promotie binnen jouw vakgroep uit te voeren en het vertrouwen dat je mij gedurende mijn promotie hebt gegeven. Mijn dagelijkse begeleiders, Norbert in Enschede en later Edwin in Eindhoven, wil ik bedanken voor alle discussies, adviezen en correcties van conferentie bijdragen, papers en natuurlijk het proefschrift.

Arthur, Ramon en Freek, als afstudeerders hebben jullie een deel van het project voor jullie rekening gekomen. Ondanks dat niet alle resultaten van jullie werk in dit proefschrift beschreven staan, hebben jullie een flinke bijdrage geleverd aan mijn onderzoek.

Bert, Alfons en Wilko bedankt voor jullie technische ondersteuning. Henny, na in Enschede geholpen te hebben met het opzetten van de analysemethode was je in Eindhoven weer parttime van de partij om de groep te ondersteunen met de installatie van de GC's en overstap op de nieuwe software. Dolf, Erik, Paul, Jan en Anton bedankt voor het realiseren van de pilot plant. Het heeft even geduurd maar uiteindelijk stond er een indrukwekkende opstelling.

Voor de financiering van dit onderzoek dank ik de Nederlandse Organisatie

voor Wetenschappelijk Onderzoek (NWO). Technologiestichting STW wil ik bedanken voor het organiseren van de halfjaarlijkse voortgangsbesprekingen. Ook wil ik de leden van de gebruikerscommissie, projectpartners en contactpersonen van STW bedanken voor de bijdrage en nuttige discussies: Hans Vreeswijk, Kees Bayense, Claudia von Scala, Johannes Gerla, Dirk Packet, Willem Dijkstra, Harald Roessler, Alexander Dimian, Gadi Rothenberg, Chris Marcelis en Monique Wiegel.

Daarnaast wil ik alle (oud)collega's van de Scheidingstechnologie groep in Enschede en de Process System Engineering groep in Eindhoven bedanken voor de fijne werksfeer, de gezelligheid tijdens de lunch en koffiepauzes, vakgroepuitjes en andere activiteiten. Paul, ook na mijn afstuderen stond je altijd voor me klaar om antwoord op mijn vragen te geven. Ferdy, van alle kamergenoten die ik in die jaren gehad heb jij het toch als langste met mij op één kantoor uitgehouden.

Natuurlijk ben ik de afgelopen jaren niet alleen maar met mijn promotieonderzoek bezig geweest. Daarnaast heb ik een leuke tijd gehad met al mijn vrienden bij onder andere de Skeuvel, Gesneuveld en ISIS en kijk ik met veel plezier terug op alle trainingen, fietsweekendjes, trainingkampen en andere activiteiten. Na de verhuizing naar Eindhoven ben ik bij La Tuniña gekomen. Jullie zorgden ervoor dat ik in no-time een sociaal leven in Eindhoven had. De repetities, optredens, feestjes en weekendjes en festivals in Spanje waren een welkome afwisseling.

Zonder nog meer namen te gaan noemen, wil ik verder graag alle vrienden, kennissen en familieleden die deze jaren hebben meegeleefd en belangstelling hebben getoond in mijn onderzoek, al was het voor hen misschien moeilijk te bevatten wat mijn onderzoek nu precies inhield, van harte bedanken.

Als laatste wil ik mijn ouders en broer bedanken; jullie zijn er altijd voor me geweest.

Marjette

# About the author

Marjette de Jong was born on the $3^{rd}$ of May 1981 in Amsterdam. After finishing secondary school (VWO) at the Hermann Wesselink College in Amstelveen in 1999, she studied Chemical Technology at the University of Twente in Enschede. Her graduation project was carried out within the Separation Technology group of prof.dr.ir. André de Haan. During this time she worked on the extrusion of oilseeds. She received her M.Sc. degree in December 2004. Following that, she has been working towards her Ph.D. degree within the same group and in the Process Systems Engineering group at the Eindhoven University of Technology, under the supervision of prof.dr.ir. André de Haan. The results of her research are contained in this thesis. From September 2009 she is working as a process engineer in the Research & Development department of Océ-Technologies B.V.

# List of publications

M.C. de Jong, A.C. Dimian, N.J.M. Kuipers, A.B. de Haan, *Entrainer selection for the synthesis of fatty acid esters by entrainer-based reactive distillation*, IChemE Symp. Ser., 152, 678-688, (2006)

M.C. de Jong, A.C Dimian, A.B. de Haan, *Entrainer-Based Reactive Distillation versus Conventional Reactive Distillation for the Synthesis of Fatty Acid Esters*, Computer-Aided Chemical Engineering, 25(18th European Symposium on Computer Aided Process Engineering, 199-204 (2008)

M.C. de Jong, R. Feijt, E. Zondervan, T.A. Nijhuis, A.B. de Haan, *Reaction kinetics of the esterification of myristic acid with isopropanol and n-propanol using p-toluene sulphonic acid as catalyst*, Appl. Catal. A, 365(1), 141-147, (2009)

M.C. de Jong, E. Zondervan, A.C. Dimian, A.B. de Haan, *Entrainer selection for the synthesis of fatty acid esters by Entrainer-based Reactive Distillation*, Chemical Engineering Research and Design, 88(1), 34-44 (2010)